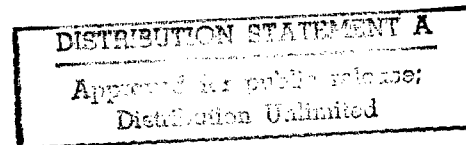




**Cultural Resources Series
Report No. CELMN/PD-RN**

**U.S. Army Corps
of Engineers
New Orleans District**



**PHASE II CULTURAL RESOURCE INVESTIGATION
OF SUBMERGED ANOMALIES, BRETON SOUND
DISPOSAL AREA, PLAQUEMINES PARISH, LOUISIANA**

September 1993

FINAL REPORT

**R. Christopher Goodwin & Associates, Inc.
5824 Plaque Street
New Orleans, LA 70123**

PREPARED FOR:

**U.S. Army Corps of Engineers
New Orleans District
P.O. Box 60267
New Orleans, LA 70160-0267**



Unclassified. Distribution is unlimited.

19980623 084

DTIC QUALITY INSPECTED 1

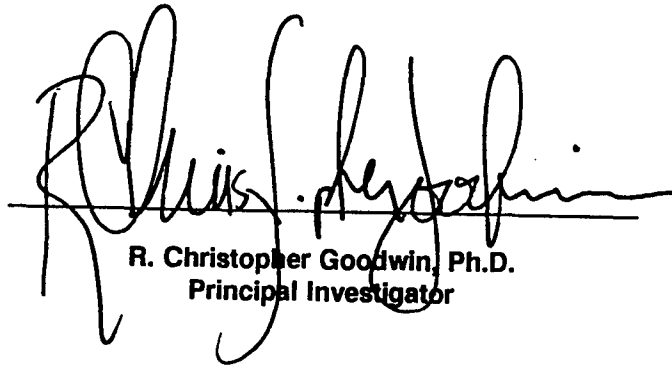
REPORT DOCUMENTATION PAGE

Form Approved
OMB No. 0704-0188

1a. REPORT SECURITY CLASSIFICATION		1b. RESTRICTIVE MARKINGS	
2a. SECURITY CLASSIFICATION AUTHORITY		3. DISTRIBUTION/AVAILABILITY OF REPORT	
2b. DECLASSIFICATION/DOWNGRADING SCHEDULE		Unclassified. Distribution is unlimited.	
4. PERFORMING ORGANIZATION REPORT NUMBER(S)		5. MONITORING ORGANIZATION REPORT NUMBER(S) COELMN/PD-93/11	
6a. NAME OF PERFORMING ORGANIZATION R. Christopher Goodwin & Associates, Inc.	6b. OFFICE SYMBOL (if applicable)	7a. NAME OF MONITORING ORGANIZATION U.S. Army Corps of Engineers New Orleans District	
6c. ADDRESS (City, State, and ZIP Code) 5824 Plauche St., New Orleans, LA 70123		7b. ADDRESS (City, State, and ZIP Code) P.O. Box 60267, New Orleans, LA 70160-0267	
8a. NAME OF FUNDING/SPONSORING ORGANIZATION U.S. Army Corps of Engineers New Orleans District	8b. OFFICE SYMBOL (if applicable) CELMN-PD-RN	9. PROCUREMENT INSTRUMENT IDENTIFICATION NUMBER DACW29-92-D-0011, Delivery Order 0003	
8c. ADDRESS (City, State and ZIP Code) P.O. Box 60267 New Orleans, LA 70160-0267		10. SOURCE OF FUNDING NUMBERS	
		PROGRAM ELEMENT NO. N/A	PROJECT NO. Civil Works Funding
		TASK NO.	WORK UNIT ACCESSION NO.
11. TITLE (Include Security Classification) PHASE II CULTURAL RESOURCE INVESTIGATION OF SUBMERGED ANOMALIES, BRETON SOUND DISPOSAL AREA, PLAQUEMINES PARISH, LOUISIANA			
12. PERSONAL AUTHOR(S) Jack Iron, Ph.D., and Paul Heinrich, M.A., A.B.D.			
13a. TYPE OF REPORT Final	13b. TIME COVERED FROM _____ TO _____	14. DATE OF REPORT (Year, Month, Day) 1993, September	15. PAGE COUNT 80
16. SUPPLEMENTARY NOTATION			
17. COSATI CODES		18. SUBJECT TERMS (Continue on reverse if necessary and identify by block number)	
FIELD	GROUP	SUB-GROUP	
05	06		
19. ABSTRACT (Continue on reverse if necessary and identify by block number)			
<p>Five clusters of magnetic anomalies were recommended for groundtruthing following Phase I remote sensing survey of the proposed Breton Sound Disposal Area, Plaquemines Parish, Louisiana. The present project concerned Phase II investigation of these clusters. Research methods involved magnetic survey of the five clusters at an interval of 15 m (50 ft), and examination of four of the clusters by divers. Search and excavation procedures were employed to locate the source of magnetic perturbation. This investigation was conducted for the U.S. Army Corps of Engineers, New Orleans District, pursuant to Delivery Order 0003 of Contract DACW 29-92-D-0011.</p> <p>Diving investigations and subsequent geophysical tests determined that the magnetic anomalies were caused by discreet areas of biological or chemical remnant magnetism associated with methane or natural gas seeps common throughout coastal Louisiana. The areas of anomalous magnetism are confined to a small zone around the gas seep and produce a magnetic signature that closely resembles that produced by a shipwreck. Recommendations were made to the New Orleans District to add sub-bottom profilers to the suite of equipment deployed on cultural resource surveys. Sub-bottom records will show gas vents as a blank area or "blow out," which, when correlated with a magnetic anomaly, will suggest that the source is geologic rather than anthropogenic.</p>			
20. DISTRIBUTION/AVAILABILITY OF ABSTRACT <input checked="" type="checkbox"/> UNCLASSIFIED/UNLIMITED <input type="checkbox"/> SAME AS RPT. <input type="checkbox"/> DTIC USERS		21. ABSTRACT SECURITY CLASSIFICATION Unclassified	
22a. NAME OF RESPONSIBLE INDIVIDUAL Joan Exnicios	22b. TELEPHONE (Include Area Code) 504-862-1760	22c. OFFICE SYMBOL CELMN-PD-RN	

**PHASE II CULTURAL RESOURCE INVESTIGATION OF
SUBMERGED ANOMALIES, BRETON SOUND DISPOSAL AREA,
PLAQUEMINES PARISH, LOUISIANA**

FINAL REPORT



**R. Christopher Goodwin, Ph.D.
Principal Investigator**

By

Jack B. Irion and Paul V. Heinrich

**R. Christopher Goodwin & Associates, Inc.
5824 Plauche Street
New Orleans, LA 70123**

September 1993

For

**U.S. Army Corps of Engineers
New Orleans District
P.O. Box 60267
New Orleans, LA 70160-0267**

**Contract No. DACW29-90-D-0011
Delivery Order No. 0003**

TABLE OF CONTENTS

	REPORT DOCUMENTATION PAGE	i
	TITLE PAGE	ii
	LIST OF FIGURES	v
	LIST OF TABLES	vii
	ACKNOWLEDGMENTS	viii
I.	DESCRIPTION OF THE PROJECT AREA	1
	Introduction	1
	Organization of the Report	1
	Natural Setting	1
	Hydrology of the Project Area	1
	Pedology of the Project Area	4
	Geology of the Project Area	6
	Unnamed Marine Complex	6
	Chandeleur Island Complex	6
	St. Bernard Delta Complex	11
	Prairie Complex	12
	Older Tertiary Strata	13
	Historical Context of the Project Area	13
	Previous Investigations	17
II.	METHODOLOGY	28
	Critique of Methodology	29
III.	RESULTS OF INVESTIGATIONS	32
	Results of Magnetic Contouring Survey	32
	Results of Diving Investigations	33
	Sources of Anomalous Magnetism	40
	Detrital Remnant Magnetization	41
	Chemical Remnant Magnetization	41
	Bacterial - Biological Remnant Magnetization	42
	Investigations into the Source of Anomalous Magnetism in Breton Sound	43
	Results of Thin Sectioning	43
	Cluster A	43
	Cluster G	44
	Discussion of Thin Sections	44
	Stable Isotope Testing	45
	Carbon	45
	Oxygen	46
	The Formation of Carbonate-Cemented Sediments in the Northern Gulf of Mexico	47
	Central Texas Inner Shelf	47
	Louisiana Continental Slope	48

Louisiana Barrier Islands	50
Alabama - Florida Shelf	51
Hypothesis	52
Summary of the Origin of Magnetic Anomalies in the Project Area	52
IV. THE ARCHEOLOGICAL SIGNIFICANCE OF CHEMICAL AND BIOLOGICAL REMNANT MAGNETISM	54
The Origin of Magnetic Anomalies in the Project Area	54
Archeological Significance	55
REFERENCES CITED	57
SCOPE OF SERVICES	Appendix A

LIST OF FIGURES

Figure 1.	A location map showing the Breton Island project area	2
Figure 2.	The Loop Current (from Ichiye et al. 1973)	3
Figure 3.	A map showing the areal distribution of sedimentary environments within the Breton Island region (from Curtis 1960:476)	5
Figure 4.	A geologic cross-section of the Chandeleur Barrier Island Chain (modified from Penland et al. 1985)	7
Figure 5.	A diagrammatic cross-section of Holocene deposits underlying shelf east of the Chandeleur Islands (constructed from data and figures by Penland et al. 1985)	8
Figure 6.	A diagram illustrating shoreline changes in the Chandeleur Barrier Island Chain between 1870 and 1978 (from Penland et al. 1985)	9
Figure 7.	A map showing the distribution of facies associated with Chandeleur Island Chain (modified from Suter et al. 1988)	10
Figure 8.	A map showing the faults, and oil and gas fields located within the Breton Island project area (modified from Bechtel [1974] and Stanfield [1981])	14
Figure 9.	Magnetic contour map of the Breton Sound Disposal Area	18
Figure 10.	Magnetic anomalies comprising Cluster A	22
Figure 11.	Magnetic anomalies comprising Cluster C	23
Figure 12.	Magnetic anomalies comprising Cluster D	24
Figure 13.	Magnetic anomalies comprising Cluster F	25
Figure 14.	Magnetic anomalies comprising Cluster G	26
Figure 15.	Acoustic anomaly at Cluster G	27
Figure 16.	Magnetic contour map of Cluster A	34
Figure 17.	Magnetic contour map of Cluster C	35
Figure 18.	Magnetic contour map of Cluster D	36
Figure 19.	Magnetic contour map of Cluster F	37

Figure 20.	Magnetic contour map of Cluster G	38
Figure 21.	Magnetic contour map showing the wreckage of a shrimp trawler in the Gulf of Mexico (from Garrison et al. 1989:II-212, Figure II-98)	39

LIST OF TABLES

Table 1.	Magnetic anomaly clusters identified in Breton Sound	19
Table 2.	Coordinates of anomalies derived from Phase I survey compared to coordinates of actual anomaly source	32

ACKNOWLEDGMENTS

The authors gratefully acknowledge the assistance of those individuals who contributed to the project. Ms. Joan Exnicios and Dr. Edwin Lyon, both of the U.S. Army Corps of Engineers, New Orleans District, ably served as Contracting Officer's Technical Representative and as Contracting Officer's Representative, respectively. Without their assistance this project would not have been possible.

Several scholars contributed their expertise and advice in the preparation of the report and in guiding our research in the right direction. Dr. Paul Aharon, on the Faculty of the Department of Geology and Geophysics at Louisiana State University, and his graduate assistant, Mr. Fu Baoshun, provided key research on the phenomenon of Biological Remnant Magnetism. Mr. Robert Floyd, a marine archeologist with Consella, Cook & Associates, Inc., in Lafayette, provided substantial knowledge from his years of experience in surveying oil fields throughout Louisiana and Texas. Mr. Thomas A. Oliver, Chief Hydrographer for Gulf Ocean Services, Inc., kindly provided information relating to the presence of anomalous magnetism in the Chandeleur Islands.

We also acknowledge the contributions of the captains of the two vessels employed during the project. Both Joe Kuljis, Captain of the *Omeco III*, and Ken Tischler, at the helm of the *TGIF*, are superbly skilled watermen whose enthusiastic assistance contributed greatly to the project.

The dive team for this project consisted of Dr. Jack Irion; David Beard, M.A.; Richard Swete, M.A.; Thomas Fenn, B.A.; David Robinson, B.A.; and John Neville, M.A. Dr. Irion, and Paul V. Heinrich, M.A., A.B.D., co-authored the report; R. Christopher Goodwin, Ph.D., provided editorial guidance. David Courington, B.A., and Shirley Rambeau, A.A., illustrated the report; Martha R. Williams, M.A., M.Ed., and David S. Robinson, B.A., edited it; and, it was produced by Kimberly S. Busby, M.A.

CHAPTER I

DESCRIPTION OF THE PROJECT AREA

Introduction

This report documents the results of Phase II testing of five clusters of submerged magnetic anomalies located within the proposed 1,600 ac (64.7 ha) Breton Sound Disposal Area in the Gulf of Mexico east of Breton Island, Plaquemines Parish, Louisiana (Figure 1) (see Irion et al. 1993 for detailed description of the U.S. Army Corps of Engineer's proposed project). These targets were selected for investigation based on recommendations made following Phase I survey of the project area in 1992 (Irion et al. 1993). The proceeding investigation had concluded that these five clusters of magnetic anomalies, designated A, C, D, F, and G, afforded the greatest potential for containing historically significant cultural remains, i.e., shipwrecks in the project area. Based on this analysis, the U.S. Army Corps of Engineers, New Orleans District, funded Phase II testing to search for and identify the source of anomalous magnetism in the five target areas.

Organization of the Report

This report is organized according to the format used in previous U.S. Army Corps of Engineers, New Orleans District, Phase II reports. The remainder of Chapter I describes the nature of the project, and presents the natural and historic context of the project area. The methods and theories applied to data-gathering during the Breton Sound Phase II project are examined on Chapter II. The results of the diving investigations are presented in Chapter III. Specific recommendations that will alter substantially the theoretical framework for detecting and analyzing magnetic anomalies off the coast of Louisiana are contained in Chapter IV. The remote sensing data acquired during Phase I are compared to those obtained during Phase II to test the efficacy of close interval magnetic survey during the testing phase. In addition, the array of remote sensing devices currently employed in underwater survey in coastal Louisiana also is examined in Chapter IV. The Scope of Services is presented in Appendix A.

Natural Setting

The proposed Breton Sound Disposal Area is located in the Gulf of Mexico. It lies in Plaquemines Parish, approximately 1.6 km (1 mi) east of Breton Island, the westernmost of the Chandeleur Island chain. The area measures 1.6 km (1 mi) wide and 4 km (2.5 mi) long. The project area is bounded by Louisiana South State Plane coordinates 2,690,588.912E/307,815.476N; 2,695,296.359E/307,905.019N; 2,695,547.466E/294,749.345N; and, 2,690,838.315E/294,659.775N. Water depths in the project area range from 2.4 to 7.6 m (8 to 25 ft).

Hydrology of the Project Area

Currents in the Gulf generally are complex and characterized by an "offshore," or open Gulf, and an "inshore," or shelf energy, regime. The open Gulf is influenced by the Loop Current (Figure 2). The shelf circulation shows strong influence from secondary flows of the Loop Current (Garrison et al. 1989:II-51). Currents along the Louisiana coast flow in a predominantly eastward direction. Longshore currents in the project area generally were light to moderate and ranged from approximately 0.5 kt to 1 kt. The

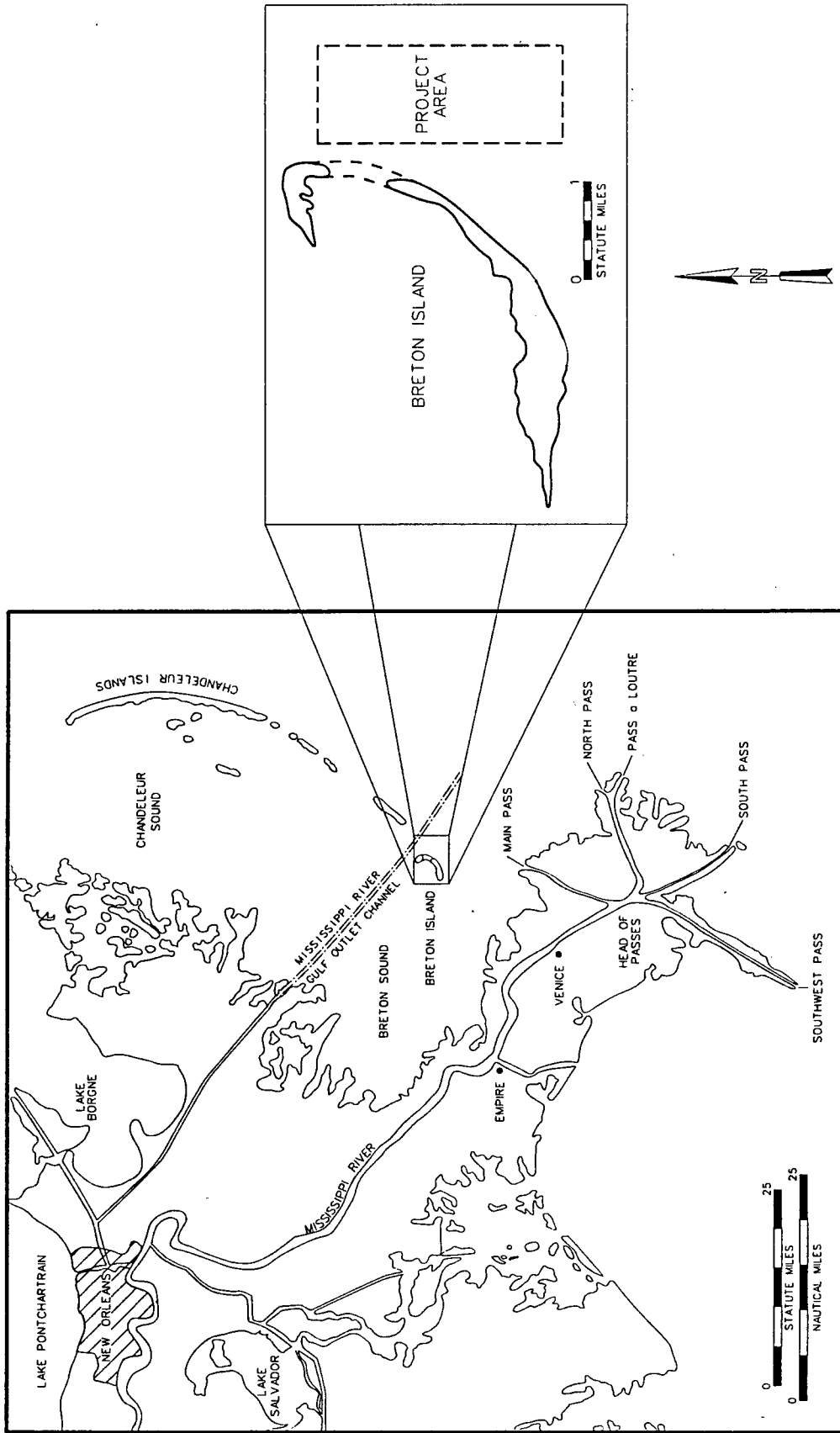


Figure 1. A location map showing the Breton Island project area.

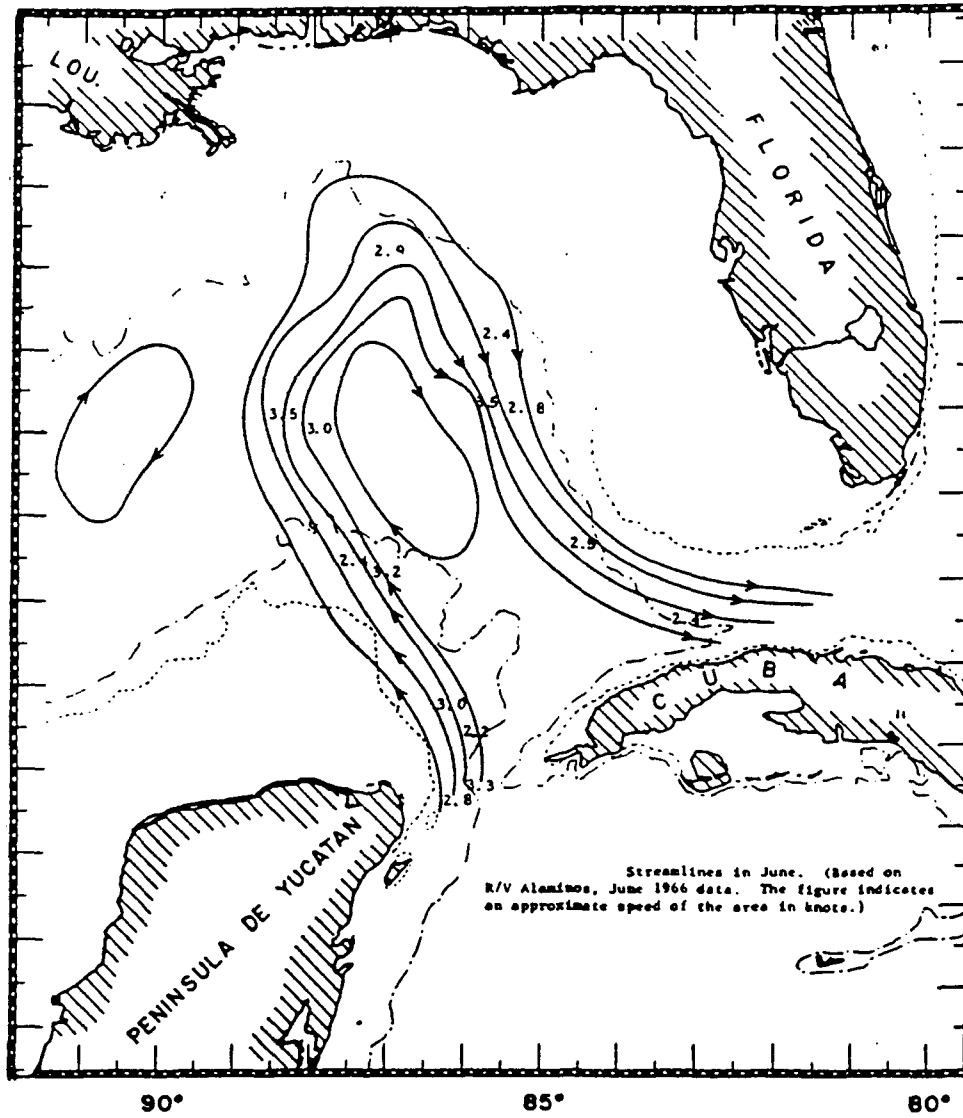


Figure 2. The Loop Current (from Ichiye et al. 1973).

strongest currents were observed in the northern part of the project area and coincided with a flood tide. The majority of the project area lay in the lee of Breton island and was unaffected by the flood tide from the Mississippi River.

Winds in the project area are dominated by easterly trades that flow from the southwest in the summer and from the northeast in winter. Waves associated with winds in the Gulf generally are 1 to 1.5 m (3 to 5 ft) in height. Cold fronts, termed "northers," often produce waves 3 to 4 m (5 to 16 ft) in height, and midwinter fronts can produce waves as high as 7 m (23 ft). Tropical storms and hurricanes can produce extreme conditions throughout the project area. Hurricane-generated waves over 30 m (100 ft) high have been calculated in the Gulf of Mexico just off the Mississippi Delta (Abel et al. 1988).

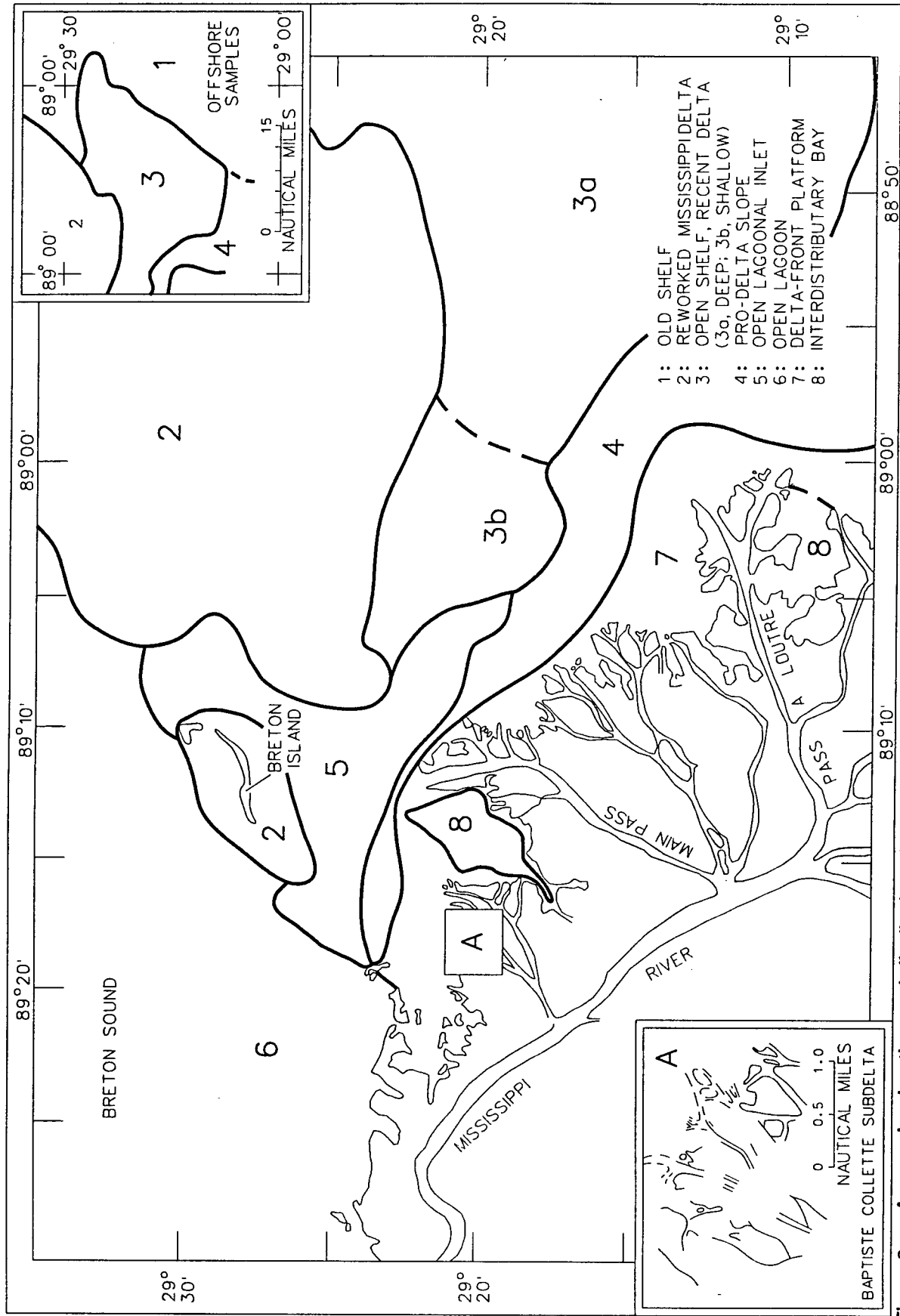
Pedology of the Project Area

Two principal sedimentary environments exist within the project area: the "open inlet lagoon" and the "reworked Mississippi delta." The majority of the project area lies within the open inlet lagoonal sedimentary environment. The southernmost portion of the project area lies in the reworked Mississippi Delta sedimentary environment (Figure 3).

The open lagoonal inlet sedimentary environment occupies two open tidal inlets that have cut into the reworked surface of the St. Bernard Delta. One inlet lies between Breton Island and the modern Mississippi Delta to the southwest, while the other lies between Breton Island and Gosier Island to the northeast. The northern tidal inlet, which starts at the strait between Breton Island and Gosier Island, turns abruptly southward, crosses in front of Breton Island, and merges with the southern tidal inlet. This inlet is characterized by strong tidal currents and by a firm bottom of either sand, silty clay, or an erosional shell lag. Between the islands, the depth of the tidal inlet, 7 to 11 m (23 to 36 ft) below mean sea level, is significantly greater than that of the adjacent shelf and sound. As it spreads seaward, the tidal inlet decreases to depths ranging from 3 to 4 m (10 to 13 ft) (Shepard 1956:Figure 5).

Surficial sediments of the open lagoonal inlet sedimentary environment found within the northern channel consist primarily of clayey silt (Shepard 1954). Its medium-grain size varies between 0.004 to 0.0625 mm (8 to 4 phi) in diameter. The percentage of sand present varies from 1 to 20 percent within the center of the inlet, to about 80 percent at the edge of the inlet. Similarly, the amount of clay varies from 30 to 50 percent within the center of the inlet, to less than 10 percent at its edge. The sediment consists primarily of detrital clastic grains with 1 to 10 percent shredded wood and a highly variable percentage of whole and fragmentary shells. Other grains often found in marine environments, such as foraminifera, carbonate grains, glauconite, and fragments of echinoids either are absent or occur in trace amounts (Shepard 1956).

The remainder of the project area lies outside of the open tidal inlet channels and consists of the reworked Mississippi Delta sedimentary environment. This former surface of the St. Bernard Delta Complex has been eroded deeply and reworked by shelf currents and waves. The surficial sediments consist of sand (Shepard 1954). The medium-grain size of these sediments ranges from 0.0625 to slightly over 0.125 mm (4 to less than 3 phi) in diameter. Typically, these sediments consist of greater than 80 percent sand, and they lack clay altogether. These sands contain an average of only 0.3 percent shredded wood and 1.0 percent fragmentary shell material; thus, they consist almost entirely of detrital clastic grains (Shepard 1956).



- 1: OLD SHELF
- 2: REWORKED MISSISSIPPIDELTA
- 3: OPEN SHELF, RECENT DELTA
(3a, DEEP; 3b, SHALLOW)
- 4: PRO-DELTA SLOPE
- 5: OPEN LAGOONAL INLET
- 6: OPEN LAGOON
- 7: DELTA-FRONT PLATFORM
- 8: INTERDISTRIBUTARY BAY

Figure 3. A map showing the areal distribution of sedimentary environments within the Breton Island region (from Curtis 1960:476).

Geology of the Project Area

The sediments that underlie the shallow shelf bottom of the project area consist of a complex assemblage of Pleistocene and Holocene deltaic, nearshore marine, and coastal sedimentary deposits. Unconformities and other discontinuities divide the Holocene deposits into three major sedimentary sequences that are informally designated as the St. Bernard, Chandeleur Island, and unnamed marine complexes. The oldest Holocene sedimentary sequence lies on a significant package of older, Late Pleistocene fluvial and deltaic sediments, i.e., the Prairie Complex.

Because of the complex heterogeneous nature of the sediments that underlie the project area, they have been defined into sedimentary sequences on the basis of regionally mappable unconformities rather than by differences in lithology. Each of these sedimentary sequences is called an alloformation, which is a mappable body of sedimentary rock or unconsolidated sediments that is defined on the basis of bounding discontinuities. A bounding discontinuity can be either an erosional unconformity or a construction surface (North American Commission on Stratigraphic Nomenclature 1983).

Within the Louisiana Shelf and adjacent Mississippi River Delta, these allostratigraphic units neither have been defined adequately nor named formally. Because they represent informal stratigraphic units, the units are termed complexes. A complex is an alloformation that has not been defined formally; it consists of a single depositional sequence that is composed of sediments deposited within different environments that are located between distinct, regionally mappable bounding discontinuities. After a complex is named and described as a formal allostratigraphic unit, the use of the term "complex" should be abandoned (Whitney J. Autin, personal communications 1992; Autin et al. 1990, 1991).

Unnamed Marine Complex. The area mapped as the reworked Mississippi Delta sedimentary environment is underlain by the Unnamed Marine Complex. This complex consists of sands and silty sands that have been eroded and continue to be eroded. Storm and tidal currents transport and deposit these sediments seaward of the barrier islands on the continental shelf. Tidal, wave, and geostrophic currents continually rework these sediments to create a blanket of scattered subaqueous bars composed of relatively clean sand that covers the continental shelf. The base of this unit is formed by a ravinement surface. It is a regionally mappable erosional unconformity formed by shoreface erosion (Nummedal and Swift 1987; Penland et al. 1985).

Chandeleur Island Complex. The Chandeleur Island Complex consists of an unconformably bounded package of lagoonal, barrier island, and tidal channel deposits (Figures 4, 5, and 6). The basal contact of this complex consists of a low-relief erosional unconformity that separates its basal lagoonal deposits from the deltaic deposits of the underlying St. Bernard Delta Complex. This unconformity has been and continues to be formed by the transgression of the inner shoreline of Breton and Chandeleur Sound over the delta plain of the St. Bernard Delta.

Seaward of Breton Island, the upper contact of the Chandeleur Island Complex is a marine erosion surface termed a ravinement surface. The continuing westward migration of the shoreface of the Chandeleur Barrier Island system is eroding the deposits of both the Chandeleur Island Complex and, eventually, the uppermost sediments of the St. Bernard Delta Complex, to form this ravinement surface. This unconformity forms the surface of this complex seaward of the barrier islands (Figure 5). The speed of this landward migration is indicated by the rapid rate at which the associated barrier islands of the Chandeleur Barrier Island System have moved landward (Figure 6) (Penland et al. 1985, 1987; Suter et al. 1988).

Typically, the basal portion of the Chandeleur Island Complex consists of 1 to 2 m (3.3 to 6.6 ft) of lagoonal sediments unconformably overlying the deltaic sediments of the St. Bernard Delta Complex (Figures 5 and 7). These basal lagoonal sediments consist of bioturbated silty clays and contain both shell

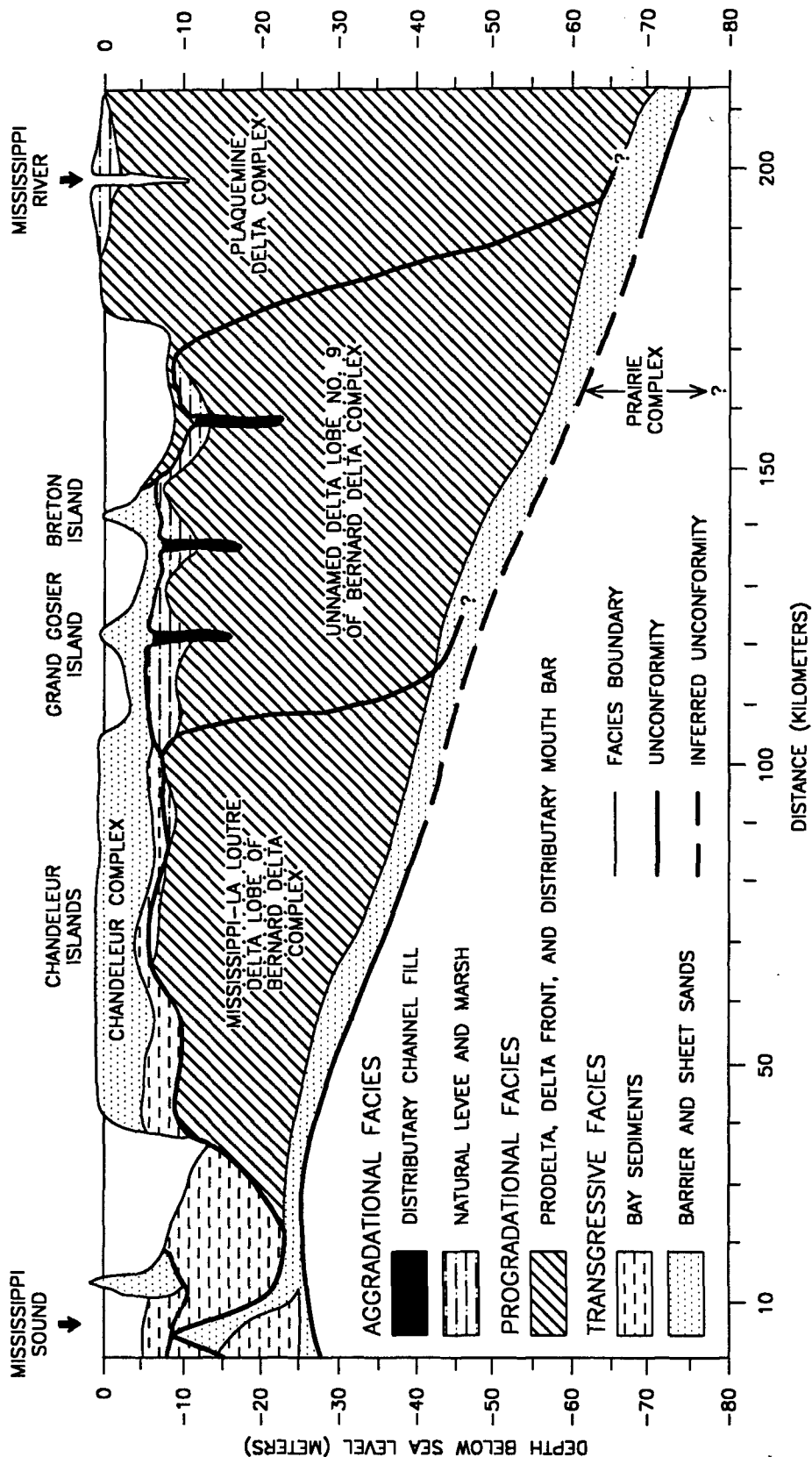


Figure 4. A geologic cross-section of the Chandeleur Barrier Island Chain (modified from Penland et al. 1985).

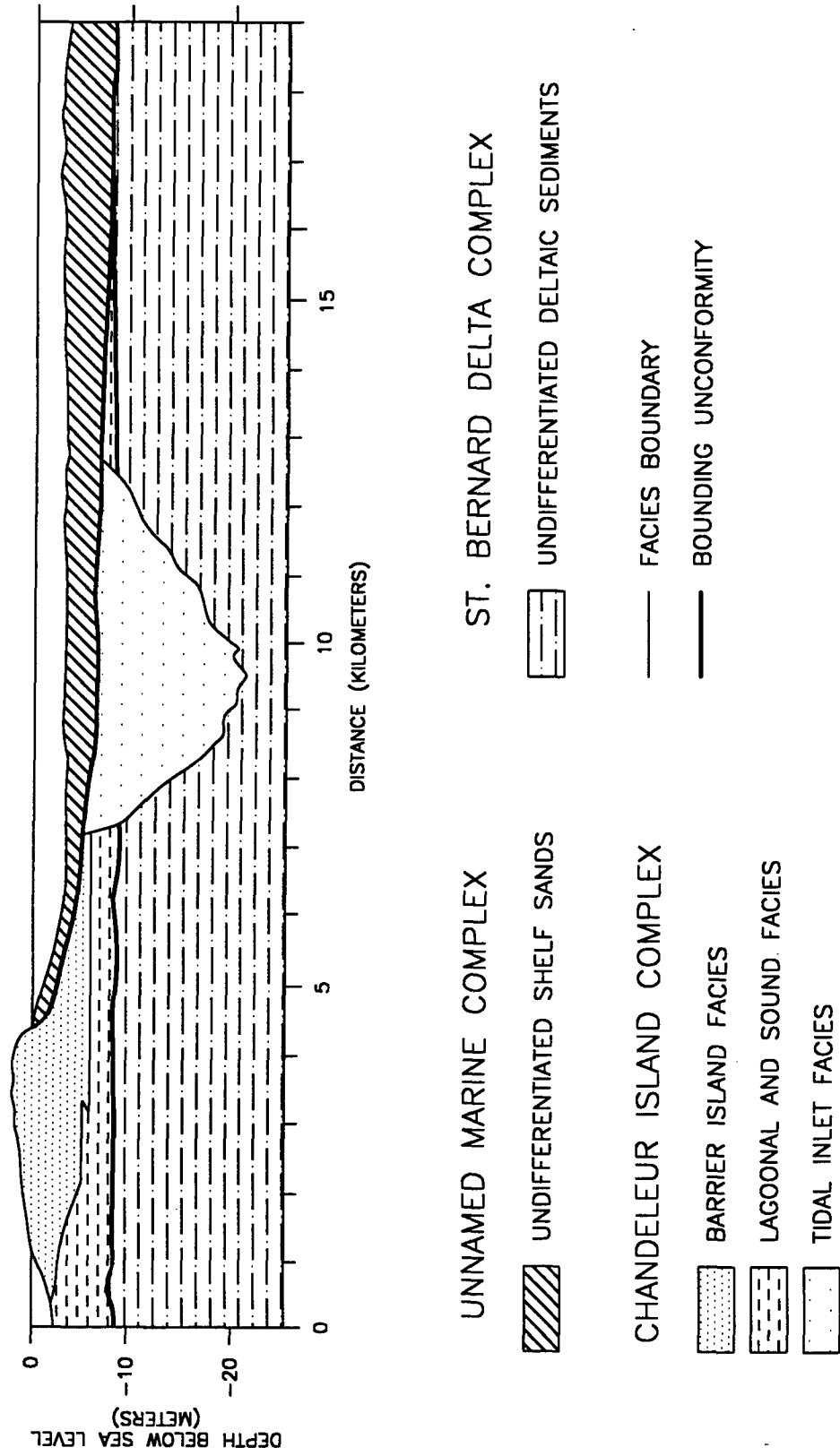


Figure 5. A diagrammatic cross-section of Holocene deposits underlying shelf east of the Chandeleur Islands (constructed from data and figures by Penland et al. 1985)

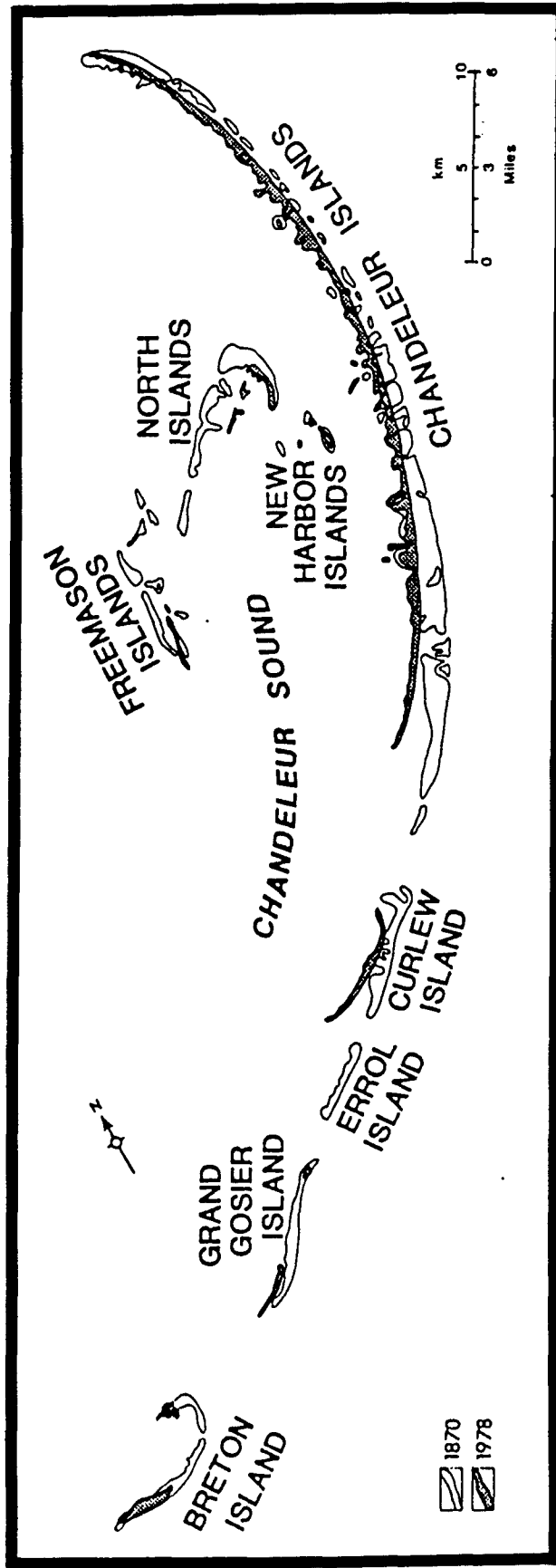


Figure 6. A diagram illustrating shoreline changes in the Chandealeur Barrier Island Chain between 1870 and 1978 (from Penland et al. 1985).

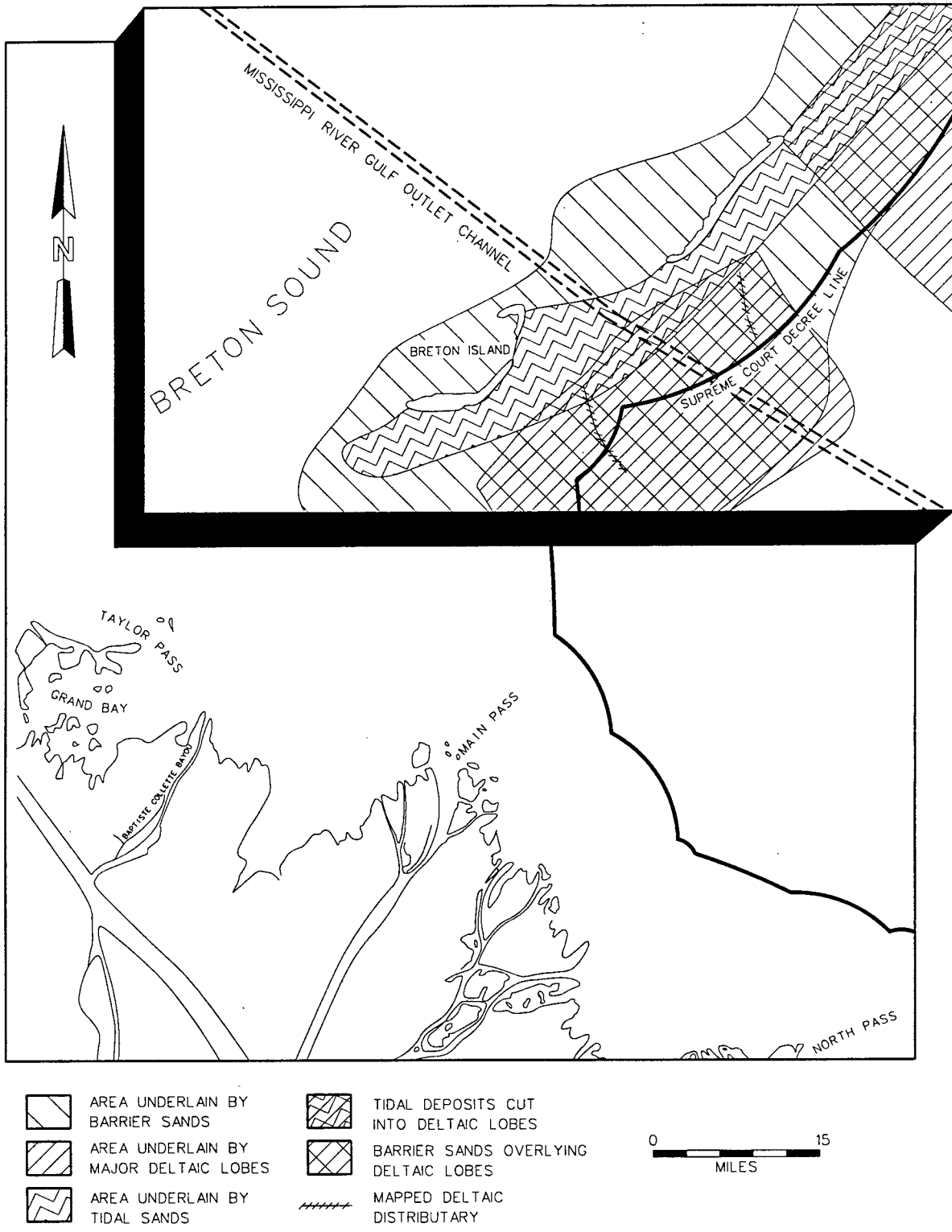


Figure 7. A map showing the distribution of facies associated with Chandeleur Island Chain (modified from Suter et al. 1988).

fragments and sand lenses. The silty clays that accumulated within the lagoon were formed behind the Chandeleur Islands as a result of the continued subsidence of the former deltaic plain. Because of the slow rates of sedimentation and high biological activity, these deposits have become highly bioturbated. The observed sand lenses found throughout the area are remnants of lag deposits formed during infrequent storms (Heerden et al. 1985:193-194).

Beneath and adjacent to the landward edge of the barrier islands, a meter or more of thinly interbedded silty clays and silty sands overlie the lagoonal silty clays. Within this unit, the coarser layers generally increase in thickness upward, with a corresponding decrease in the thickness of the finer layers. These sediments commonly are either parallel or cross-laminated and have been bioturbated to a minor degree. They represent the distal edge of washover deposits that form the leading edge of the landward-moving barrier island system (Heerden et al. 1985:194).

The barrier islands within the Chandeleur Barrier Island Chain consist primarily of silty sands (Figure 5). These sands are highly bioturbated and display very few primary sedimentary structures; they often contain organic-rich root horizons and thin clay layers. These silty sands represent washover deposits that form the core of the barrier island, and they often are overlain by an additional 1 to 1.5 m (3.3 to 4.9 ft) of clean parallel-laminated and bioturbated sands. The clean sands represent both dune and washover sediments. Periodically, hurricanes erode and wash these sands from the seaward portion and shoreface of the barrier island and transport them over the barrier island into the lagoon or onto the island. The result of this process is the landward migration of Breton Island and other islands of the Chandeleur Barrier Island chain. The landward migration of the island and its associated shoreface eventually results in the erosion of the entire barrier island-lagoonal depositional sequence. As a result, any historic or prehistoric archeological deposits associated with the subaerial sediments of these barrier islands almost certainly have been dispersed (Heerden et al. 1985:194; Penland et al. 1985).

The seaward edge of the barrier islands of the Chandeleur Barrier Island system consist of 10 to 15 m (33 to 49 ft) of sandy, tidal inlet, channel fill deposits (Figure 7). These sediments consist of upward fining, horizontally bedded to bioturbated sands that contain numerous shells, and they represent the coarse-grained fill of abandoned tidal channels. Because they are often 10 to 15 m (33 to 49 ft) thick, the basal parts of these deposits lie below the level of the ravinement surface. Hence, they commonly will constitute the only portion of the Chandeleur Island Complex to survive shoreface erosion (Penland et al. 1985, 1987).

St. Bernard Delta Complex. Underlying the deposits of the Unnamed Marine and Chandeleur Island complexes are the deltaic sediments of the St. Bernard Delta Complex. The St. Bernard Delta Complex is an allostratigraphic unit that is bounded by a lower marine erosional surface, called a "ravinement surface," cut across the Prairie Terrace, and by erosional surfaces cut to varying depths across its delta plain. Between these bounding unconformities, this complex consists of a basal layer of transgressive sediments, a middle unit of fine-grained progradational deltaic sediments, and an upper unit of aggradational, deltaic natural levee and marsh sediments. Internally, a minor unconformity formed by a brief period of nondeposition, called a "diastem," separates the deposits of the individual delta lobes within this complex. The sediments of either the Chandeleur Island Complex or the Unnamed Marine Complex unconformably overlie the St. Bernard Delta Complex (Figure 4).

Within the project area, the deltaic sediments lying between the erosional boundaries of the St. Bernard Delta Complex are approximately 45 to 50 m (148 to 164 ft) thick (Figure 4). This depositional sequence consists of a basal layer of transgressive deposits less than 5 m (16 ft) thick, which in turn is overlain by 35 to 45 m (115 to 148 ft) of progradational deposits. About 2 to 5 m (6.6 to 16 ft) of aggradational swamp and marsh deposits overlie the progradational deposits and form the surface of the St. Bernard Delta Complex (Frazier et al. 1978).

The landward movement of the shoreline over previously subaerial coastal plain formed the basal erosional unconformity of the St. Bernard Delta Complex. As the shoreline migrated landward, the beach shoreface typically cut deeply into the underlying Pleistocene sediments of the Prairie Complex. As a result, the upper meter to several meters of this coastal plain was eroded almost uniformly and was reduced to a transgressive sand lag. During the period of time that lapsed between the submergence of an area beneath the Gulf of Mexico and the influx of deltaic sediments, sediments eroded from this coastal plain were reworked into a thick transgressive sheet sand. Clayey silts and silty clays accumulated upon the basal sand lag as the water depth increased (Frazier et al. 1978).

As the St. Bernard Delta prograded into the Gulf of Mexico, a thick sequence of progradational deposits accumulated. Initially, clay was deposited from suspension to form a thick blanket of unfossiliferous, parallel-laminated, and fine-grained sediments called the "prodelta facies." As this delta prograded seaward, the accumulating prodelta facies became siltier and developed parallel and lenticular laminae of silt. As progradation continued, laminated silts and clays with thin sand layers, called the "delta front facies," accumulated as part of the St. Bernard Complex. Locally, distributaries deposited interbedded silts and silty sands that display a wide variety of sedimentary structures associated with currents and waves at their mouth. These sediments are called "distributary mouth bar facies" (Coleman 1982; Frazier et al. 1978).

Once this delta had built up to sea level, natural levee and marsh sediments accumulated upon the subaqueous progradational deposits to create a subaerial delta plain of the delta complex. The deposition of sediment by floodwaters formed low ridges, called "natural levees," that bordered the distributary channel. Through breaks in the natural levees, floodwaters built crevasse splays upon the adjacent delta plain and subdeltas; these flood episodes filled in the adjacent interdistributary bays (Coleman 1982).

The natural levee and crevasse splay deposits consist of silts, sandy silts, silty sands, and very fine sands that are characteristically small-scale, cross-laminated, and rippled with intensively bioturbated zones. These sediments generally have oxidized and contain abundant diagenetic materials such as iron sesquioxide and carbonate nodules and cements. Organic marsh deposits accumulated within the periodically flooded land away from the main distributaries (Coleman 1982).

Eventually, long-term delta lobe progradation led to the overextension of the distributary network, and to a decrease in hydraulic efficiency. The decrease in hydraulic efficiency eventually caused an upstream diversion of the trunk channel. As a result, the channel switched to a shorter, more efficient course with a steeper gradient, thus generating a new delta complex, and abandoning the St. Bernard Delta system (Fisk 1960).

Wave action started to destroy the delta lobe when the sediments needed to maintain the abandoned delta complex were diverted to building a new delta. In addition, tectonic and compactional subsidence and eustatic sea level rise caused the delta plain of the St. Bernard Delta to sink beneath the Gulf of Mexico. Initially, a landward-migrating beach formed in front of the shoreface along the edge of the eroding St. Bernard Delta. Longshore currents moved sand away from the center of the eroding headland formed by this delta lobe to create spits and barrier islands that flanked either side of it. Eventually, the subsidence submerged the delta plain of the St. Bernard Delta and created Chandeleur Sound and Breton Sound. These sounds detached the beaches from the St. Bernard Delta Plain to create the Chandeleur Barrier Island System (Penland et al. 1985, 1987; Suter et al. 1988).

Prairie Complex. As defined by Autin et al. (1991), the Prairie Complex consists of two, possibly three, depositional sequences and possible alloformations that underlie the Holocene deltaic deposits of the St. Bernard Delta Complex. Each of these depositional sequences consists of an indistinguishable and heterogeneous assemblage of deltaic, shallow marine, and strandplain deposits that vary from Sangamonian to Middle Wisconsinan in age. The Prairie Complex is the uppermost portion of some 900

m (2,950 ft) of sedimentary strata consisting of Late Quaternary fluvial, shelf phase, and nearshore strata that comprise the eastern Louisiana Shelf.

Within the project area, the upper contact of the Prairie Complex consists of a formerly exposed portion of what was once the Louisiana coastal plain. However, it now lies buried beneath younger Holocene deltaic and nearshore deposits at a depth of 50 to 60 m (164 to 197 ft) below sea level (Figure 4). In the subsurface, the top of the Prairie Complex is marked by the occurrence of a typically truncated weathering zone that developed within its uppermost sediments when this coastal plain was subaerially exposed during the Wisconsinan glaciations. This weathering zone is distinguished from the overlying Holocene deposits by a mottled orange, tan, or greenish gray color, an abrupt increase in stiffness and shear strength, and the presence of pedogenic calcareous nodules (Autin et al. 1991; Fisk and McClelland 1959; Frazier et al. 1978).

Available radiocarbon dates indicate that the former coastal plain that formed the surface of the Prairie Complex was flooded sometime after 10,000 to 9,000 radiocarbon years B.P. As a result, it could have been occupied during the initial stages of human occupation of this area. However, shoreface erosion during the Holocene submergence of the survey area by the Gulf of Mexico apparently has eroded the surface of this coastal plain deeply. This erosion probably has destroyed the majority of archeological deposits that would have been present on its surface (Fisk and McClelland 1959; Frazier et al. 1978; Nummedal and Swift 1987).

Older Tertiary Strata. The original continental shelf on which Quaternary and Pliocene sediments accumulated consists of numerous stacked Miocene period shelf-margin deltas of the ancestral Mississippi River. These shelf margin deltas consist of thick progradation wedges of deltaic strata broken by east-west trending growth faults. These faults formed contemporaneously with the deposition of the deltaic deposits. The abundant hydrocarbon traps associated with roll-over and other geologic structures created by these faults create the numerous oil and gas fields within the Breton Sound area (Curtis 1970; Winker 1982) (Figure 8).

Historical Context of the Project Area

Beginning with Lemoyne d'Iberville's first voyage to French Louisiana in 1699, many ships steered near Breton Island on their way to the mouth of the Mississippi River. Located at the southern end of the bow-shaped Chandeleur Island chain, this small sandy island occasionally has been at the center of important maritime activity. French vessels coming from such Gulf Coast ports as Mobile and Biloxi sailed close to it as they plied toward the mouth of the Mississippi River en route to New Orleans. The French also anchored warships at Breton Sound during the late eighteenth century to protect French shipping. The British similarly stationed their armada off the island in December 1814 as they prepared to assault the city of New Orleans. Rum runners anchored near the island, during the early 1920s since it lay near the three mile limit and thus beyond the jurisdiction of American Coast Guard cutters. Therefore, this small southern tip of the Chandeleur chain played a minor but insignificant role in the maritime history of the northwestern section of the Gulf of Mexico.

The French explorer, d'Iberville, was one of the first Europeans to visit Breton Island. Leaving the port of Brest in 1698, he eventually reached Mobile Bay and then relocated his three-ship fleet to Ship Island. D'Iberville then explored the coastline along the Chandeleur Islands, including Breton Island. Leaving his fleet, the Frenchman set out in small boats across "a headland of black rocks," entered the mouth of the Mississippi River, and proceeded up the river (Crouse 1954:171; McWilliams 1981:5).

In May 1699, d'Iberville initiated the second of his three voyages to French Louisiana. As he navigated small boats up the mouth of the Mississippi River, Spanish ships encountered the two French

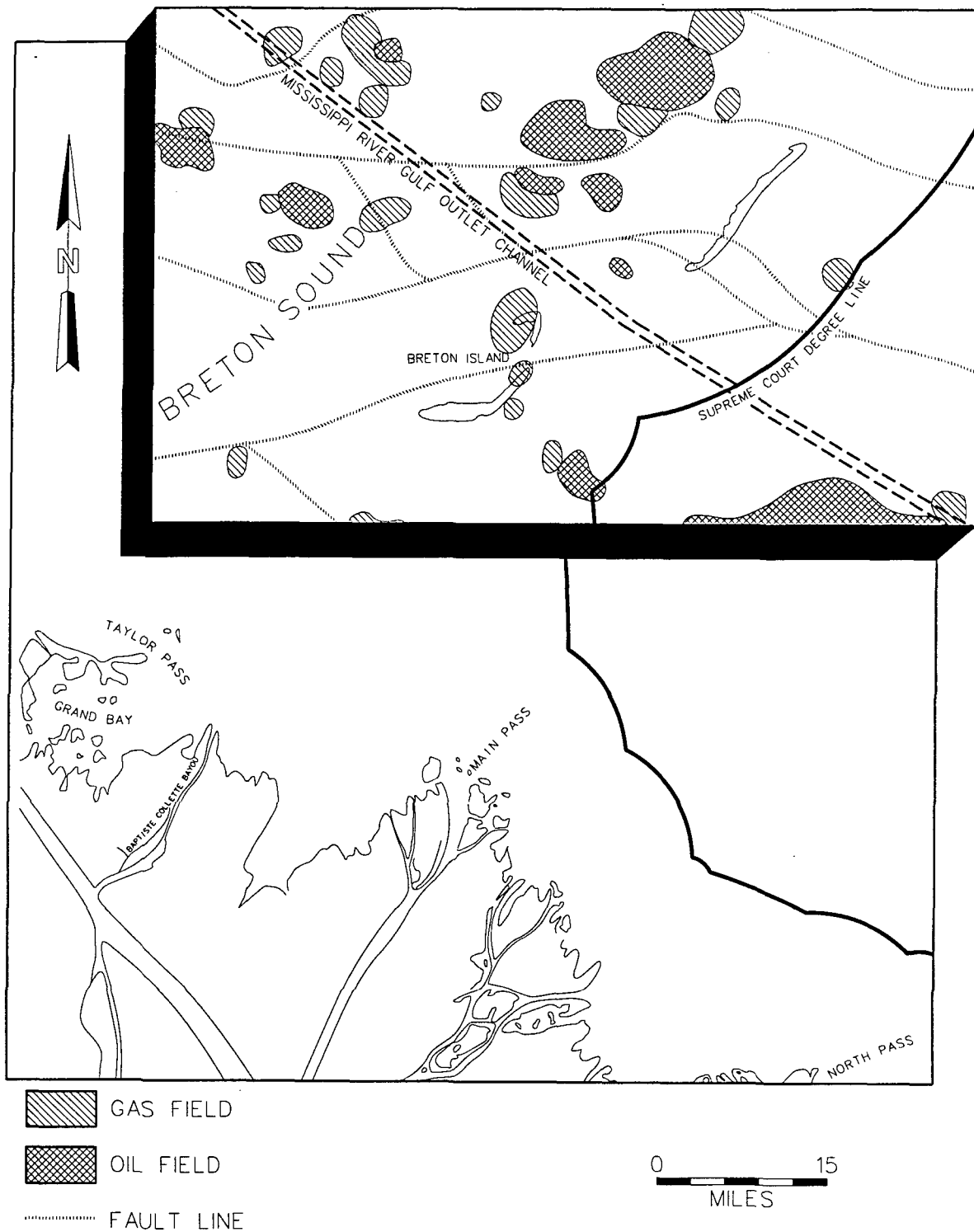


Figure 8. A map showing the faults, and oil and gas fields located within the Breton Island project area (modified from Bechtel [1974] and Stanfield [1981]).

frigates anchored at Ship Island. The Spanish vessels opted not to challenge their French counterparts and sailed away. However, one of the Spanish ships was wrecked on Chandeleur Island and lost all its cargo (McWilliams 1981:9)

Antonine Simon le Page du Pratz penned one of the earliest descriptions of Chandeleur Island. During a voyage to Louisiana in 1718, Du Pratz investigated the island which he dubbed "Candlemas Island." According to Du Pratz, the island was so flat that it was barely visible even when his ship was only one league away. He also noted that the water near the island was four fathoms deep.

Another of the few historical descriptions of Breton Island was authored by Colonel Samuel Henry Lockett, a professor of engineering at Louisiana State Seminary at Pineville, Louisiana. In 1869, Lockett initiated a topographical survey of the state. The Chandeleur Islands, he recorded, were sandy and marshy with an occasional group of pine and oak trees. He wrote that Breton Island was crooked and low, with a general northeast and southwest orientation, and was about 11 miles long. According to Lockett, there was a "good channel" between Breton and Grand Gosier islands, which lay 5 miles west (Lockett 1969:127).

Although Breton Island had a good channel in Lockett's estimation, many Gulf islands did not offer safe locations for anchorage. The frequent and violent hurricanes that arrived near the end of summer altered the shapes and shorelines of these barrier islands. One violent storm partially destroyed Ship Island in 1701, and another obstructed the channel of Massacre Island in 1717. A French missionary summed up the problem in a 1711 letter to his uncle, lamenting that "our coast changes shape at every moment; what was a muddy ridge becomes an island, and what was an island becomes a muddy ridge" (Giraud 1974:65-66). Consequently, a good, usable, and safe channel could quickly become a shallow and dangerous one.

The vast deposits of sediments at the mouth of the Mississippi River formed a virtual mud blockade that prevented all but the smallest vessels from ascending the river. Late winter and spring floodwaters inundated the waterway with even more sediment, thereby reducing the depth of water further and grounding vessels for months at a time. Some French captains ignored orders—even when accompanied by threats of violence—to proceed up the treacherous river channel. For example, Captain Le Gac of the *Dromedaire* secured a signed certificate from another captain stating that it would be easier for an elephant to go through the eye of a needle than for the *Dromedaire* to move up the river. The first sea-going ship to attempt to enter the river was an English vessel, which the French turned away in the famous English-Turn incident in 1700. It was not until 1718, when the *Neptune* entered the Mississippi River, that another ship dared to sail up the river (Lowrey 1964:233-234).

The establishment of New Orleans in 1718 soon led to an increase in water traffic between the new city and the French ports of Biloxi and Mobile. This development meant that more vessels would pass near Breton Island as they sailed between Gulf ports and the mouth of the Mississippi River. These ships carried such products as silk, tobacco, rice, indigo, sassafras, quinine, and lumber (Surrey 1916).

Though some vessels plied between Gulf ports and the mouth of the Mississippi River, many others took the shorter, safer route across the Rigolets, through Lake Pontchartrain, and down Bayou St. John to New Orleans. This way was preferable over the Mississippi River route because the sand and mud bars at the entrance of the river made navigation slow and treacherous, and because the swift river currents made heading upstream difficult. It sometimes took as long as a month for a ship to travel from the mouth of the Mississippi River to New Orleans. Despite the hazards involved in navigating the Mississippi Delta approaches, many French and Spanish vessels landed at the mouth of the river. For example, a Spanish ship arrived from Havana in 1725 and another appeared two years afterward (Giraud 1974:347). In contrast when Lake Pontchartrain overflowed it created a clear water route to the Gulf. This route easily was accessible to a substantial number of vessels, and it became the path of "ordinary communications"

between Gulf ports and New Orleans during the early eighteenth century (Giraud 1974:347; Pearson 1989:88-89; Surrey 1916:33).

During the early 1720s, the French did a considerable amount of work at the mouth of the river to make it a more usable route to New Orleans. Their efforts centered on the harbor at Balise, located at the point where vessels entered the river, where they constructed various buildings to house products from Gulf ports, such as pitch and tar from Mobile. When ships arrived at Balise, pirogues helped to lead them into the channels, and pilots took them over the bar (Giraud 1974:155-156, 347).

Both Spain and Britain stationed warships off the Chandeleur Islands, including Breton. In a 1794 military report to the Spanish government on Louisiana and western Florida, Governor Carondelet wrote that war vessels were anchored "with all safety, on Ship [Navios] Island, the Chandeleurs [Candalaria], and Breton Island" (Robertson 1911:1:320). Two decades later, during the War of 1812, the British anchored their armada off the Chandeleur Islands as they prepared to invade New Orleans. Shortly after arriving, the fleet came under attack from six American gunboats. The British returned fire and reportedly sank one of the vessels (Grummond 1962:330-332).

Many ships continued to ply the Mississippi River during most of the nineteenth century, although navigation was difficult and dangerous. The New Orleans and Ship Island Canal Company, which lobbied for a canal through the Rigolets, complained of the delays and damages to vessels entering the river. The company noted in March 1859 that there were 35 vessels waiting to egress; three were grounded on the bar; and, 17 were outside the entrance (*The New Orleans and Ship Island Canal* 1869:1-7).

Toward the close of the nineteenth century, the State of Louisiana and the Federal government finally took steps to alleviate the navigational difficulties at the mouth of the river. The city of New Orleans wanted to construct a canal from Fort St. Philip into Breton Island Sound. Benjamin Buisson, the state engineer for Louisiana, initially had formulated this plan in 1832 (Lowrey 1964:246). However, in 1875, Congress instead authorized the construction of the Eads jetties at South Pass, one of four main entrances to the river. The project, completed in 1879, gave the Mississippi River a 35-foot deep channel (Roberts 1946:274-275). Of course, the deepening of the river channel led to more traffic up the waterway and therefore to more vessels passing by Breton Island.

The initiation of Prohibition in 1920 led to the emergence of a "Rum Row" off of Breton Island and the Chandeleur Islands, as vessels loaded with alcohol assembled there just beyond the United States' three mile limit. Most of these rum ships, many of which were British, were under foreign registry, though a sizeable number were owned locally. Coming from Cuba and British Honduras, the rum boats rendezvoused at Breton Island and the Chandeleur Islands with contact or "mosquito" boats which took the alcohol through Lake Borgne, Lake Pontchartrain, or the passes at the mouth of the Mississippi River. Coast Guard cutters and customs boats initially were too slow to catch these vessels as they skirted for the American coast (Jackson 1978:277-278).

Rum runners played cat and mouse games with Coast Guard and customs vessels until about 1925. For example, in September 1925, the New Orleans *Times-Picayune* reported that patrol cutters positioned off Chandeleur Island were picketing a British schooner loaded with 9,000 cases of whiskey. According to the paper, the ship was 18 miles east-southeast of the lower end of the Chandeleurs and near the three mile limit. Later in the month, a Coast Guard vessel fired upon and sank the power vessel, *Emilia G*, in Breton Sound off Errol Island. Activity in this area soon wound down as rum runners relocated to a point off Timbalier Light that provided access through Barataria Bay and Bayou Lafourche (Jackson 1978:277-278; New Orleans *Times-Picayune* 1925).

Breton Island was often in the vortex of maritime activity in the Gulf despite being small and incompatible from a commercial standpoint. Many vessels steered near the tiny, sandy island since it lay

along the heavily traversed route from the mouth of the Mississippi River to such important Gulf Coast ports as Biloxi, Mobile, and Pensacola. Therefore, it was the location of the island, rather than its intrinsic value, that made it a significant site on the Louisiana coast.

Previous Investigations

A remote sensing survey of the Breton Sound Disposal Area was conducted by Goodwin & Associates, Inc., in 1992 (Irion et al. 1993). A total of 78 magnetic anomalies (Figure 9), ranging from low-amplitude perturbations of short duration to moderately strong and strong anomalies of significantly long duration, were recorded during this survey (Irion et al. 1993:Table 1).

Because it was not feasible economically to examine all 78 anomalies, archeologists proposed a testing strategy that utilized criteria for selecting test areas based upon the results of numerous similar investigations (Arnold 1980; Bevan 1986; Garrison, 1981, 1986; Irion 1986; Mistovich and Knight 1983; Saltus 1980; Watts 1980; Weymouth 1986).

It should be remembered that any analysis of magnetic anomalies is speculative at best - part science, part intuition, and part experience. At the 1990 meeting of the Council on Underwater Archaeology in Tucson, Arizona, researchers gathered to discuss the problem of shipwreck signature characterization. They overwhelmingly concluded that no means presently exist to discriminate confidently between shipwrecks, ferrous debris, and natural occurrences of anomalous magnetism. Faced with budget restrictions that preclude the physical examination of every anomaly, cultural resource managers therefore have sought to develop a sampling strategy that accounts for the two most prevalent characteristics: duration and spatial frequency.

In summarizing the work of previous researchers, Garrison et al. (1989:II-223) compiled the following list of magnetic and acoustic traits that are characteristic of historic shipwrecks:

1. multiple peak anomalies or spatial frequency;
2. differential amplitude anomalies;
3. areal distribution $\geq 10,000$ m²;
4. long gradients and duration;
5. axial or linear orientation of anomalies;
6. scour areas associated with anomalies;
7. a geometrically complex exposed structure associated with anomalies; and,
8. relative locational permanence.

Based upon these criteria, an analysis of the Breton Sound anomalies revealed that 58 percent of the total universe of 78 anomalies could be discounted as isolated occurrences.

The remaining 42 percent of the anomalies were grouped into seven clusters based on a model developed by Mistovich and Knight (1983:154). This model assumes a shipwreck site in a high-energy environment will yield a clustering of three or more anomalies within an area $<50,000$ m² at a survey lane spacing of 50 m (164 ft). Using this criterion, it was found that weak anomalies with durations of less than 15 seconds comprised two of the seven clusters (B and E). These also were eliminated from further consideration. The remaining five clusters, A, C, D, F, and G, were adjudged to possess some potential for containing historic shipwreck remains (Irion et al. 1993:50) (Table 1). Additional testing of these five clusters was recommended to identify the source of anomalous magnetism in each area and to determine if the potential cultural resource possessed the qualities of significance as defined by the National Register

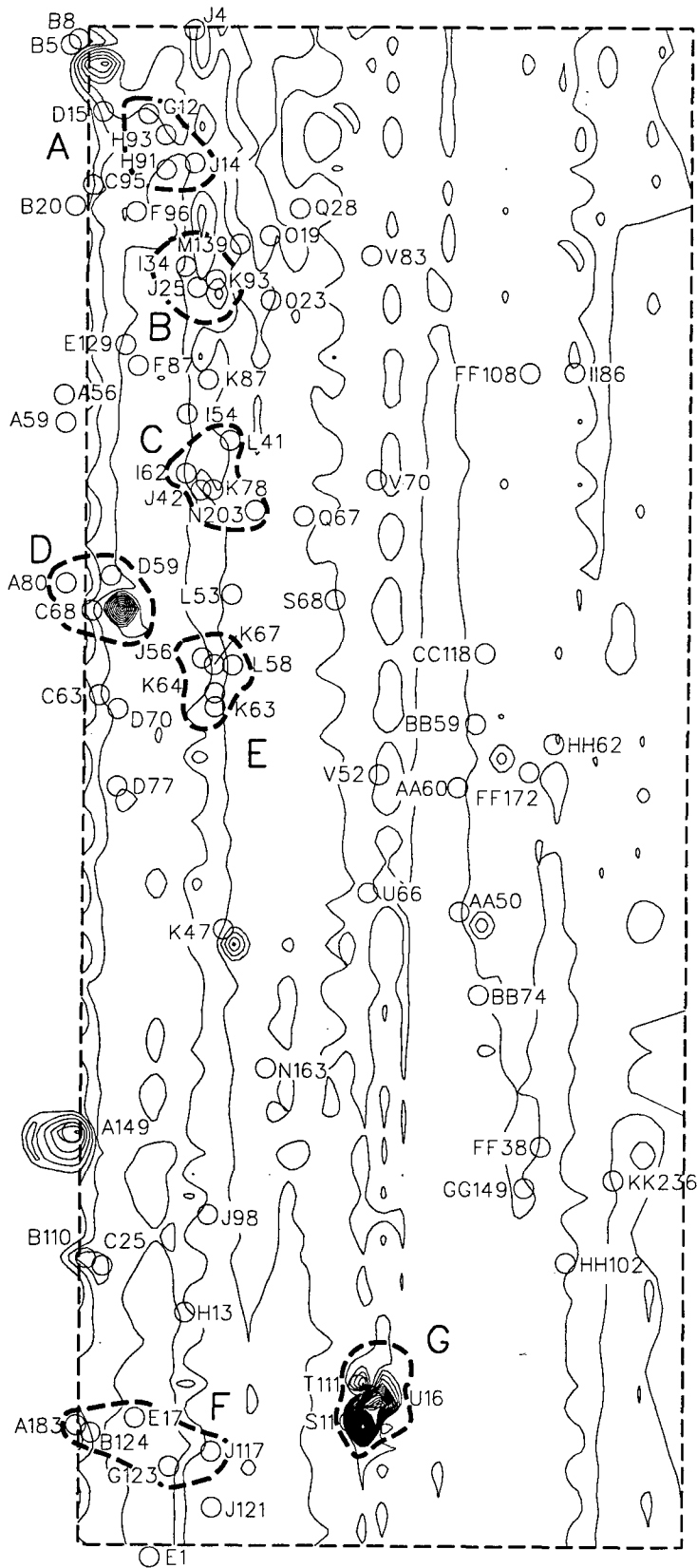


Figure 9. Magnetic contour map of the Breton Sound Disposal Area.

Table 1. Magnetic Anomaly Clusters Identified in Breton Sound.*

ANOMALY	nT	DURATION (IN SEC.)	TYPE
CLUSTER A			
G-12	61	30	Bi-polar
H-93	27	13	Negative
H-91	20	9	Negative
J-14	7	30	Multi-component
CLUSTER B			
I-34	13	11	Positive
J-25	9	11	Negative
K-93	9	15	Multi-component
CLUSTER C			
I-62	34	20	Positive
J-42	14	10	Positive
K-78	13	7	Bi-polar
L-41	16	7	Multi-component
N-203	13	5	Bi-polar
CLUSTER D			
A-80	18	9	Bi-polar
C-68	568	30	Bi-polar
D-59	20	5	Positive
CLUSTER E			
J-56	16	6	Bi-polar
K-63	13	3	Bi-polar
K-64	17	3	Bi-polar
K-67	12	7	Multi-component
L-58	15	3	Bi-polar

Table 1, continued

ANOMALY	nT	DURATION (IN SEC.)	TYPE
CLUSTER F			
A-183	11	20	Multi-component
B-124	10	6	Positive
E-17	15	35	Multi-component
G-123	15	6	Bi-polar
J-117	13	1	Positive
CLUSTER G			
T-111	1,476	100	Multi-component
U-16	436	33	Bi-polar
S-11	20	11	Bi-polar

* From Irion et al. (1993), Phase I report on the *Remote Sensing Survey of Mississippi River-Gulf Outlet, Breton Sound Disposal Area, Plaquemines Parish, Louisiana.*

of Historic Places criteria of significance (36 CFR 60.4 [a-d]). Testing consisted of a close-interval magnetic survey to identify the central area of magnetic disturbance; a physical examination of that area then was conducted.

Cluster A (Figure 10) was considered to have the most potential for producing significant cultural remains. It comprised four anomalies on three tracks, two of which were of significantly long duration; one exhibited a multicomponent signature, which usually is indicative of multiple objects. The contour plot exhibited by Cluster A was remarkably similar to that produced by small wooden-hulled vessels of the exploration or colonial periods of American history. These vessels often carried small amounts of iron and, after wrecking, their magnetic properties declined significantly as exposure to the corrosive effects of sea water metamorphosed magnetic iron to non-magnetic oxides. As a result, moderate to low amplitude anomalies (10 to 100 gammas) have been recorded over very early historic shipwreck sites, such as the 1554 wreck of the *San Esteban* in Texas (Clausen and Arnold 1975).

Five anomalies comprised Cluster C (Figure 11). Anomaly I-62 exhibited a moderately long duration of 20 seconds. The historical précis developed for the Breton Sound project area suggested that the potential presence of a small undocumented fishing craft probably would produce a magnetic reading similar to that observed at Cluster C.

Cluster D (Figure 12) contained one of the strongest perturbations recorded during survey, Anomaly C-68. With a duration of 20 seconds and an amplitude of 568 gammas, Anomaly C-68 was presumed to possess a substantial ferrous mass. The location of this anomaly was near the reported site of the 1923 loss of the yacht *Fidget* (Berman 1972:168).

Five magnetic anomalies comprised Cluster F (Figure 13). Two of the contributing anomalies, E-17 and A-183, exhibited multi-component signatures of moderately long duration (35 and 20 seconds, respectively). It was hypothesized that the cluster potentially represented a small wooden-hulled vessel that lacked massive ferrous components.

Three magnetic anomalies and an acoustic target comprised Cluster G (Figures 14 and 15). Anomaly T-111 of this cluster exhibited a complex multi-component signature of long duration (100 seconds) with a peak-to-peak amplitude of 1,476 gammas. The sonogram depicted an anomalous discontinuity of the bottom in the same location. Historical research indicated that the U.S. Coast Guard had issued Notice to Mariners No. 96 on November 25, 1971, warning of "a large piece of unidentified wreckage . . . trailing a length of wire rope" near this location. It was hypothesized that Cluster G represented the location of this wreckage (Irion et al. 1993:53).

101918	49670.0
101920	49698.5
101921	49698.0
101922	49698.5
101923	49698.0
101924	49694.5
101925	49694.5
101926	49700.5
101928	49697.0
101929	49700.0
101930	49699.0
101931	49700.0
101932	49700.0
101933	49697.0
101935	49698.5
101936	49695.0
101937	49692.0
101938	49692.0
101939	49691.5
101940	49685.5
101942	49680.0
101943	49669.5
101944	49663.5
101945	49657.0
101946	49669.0
101947	49674.5
101949	49693.5
101950	49710.0
101951	49715.0
101952	49717.5
101953	49718.5
101954	49718.0
101956	49715.0
101957	49711.5
101958	49710.0
101959	49707.0
102000	49705.0
102001	49705.0
102003	49710.5
102004	49703.5
102005	49699.0
102006	49694.5
102007	49700.0
102008	49698.5
102009	49697.5
102011	49696.0
102012	49692.0
102013	49695.0
102014	49701.0
102015	49706.0
102016	49696.0
102018	49691.5
102019	49694.5
102020	49697.5
102021	49702.5
102022	49699.0
102023	49695.5
102025	49692.5
102026	49694.0
102027	49693.5
102028	49692.5
102029	49694.0
102030	49696.5
102031	49697.0
102033	49694.5
102034	49696.5
102035	49697.0
102036	49697.0
102037	49695.0
102038	49695.5
102040	49692.0
102041	49697.5
102042	49695.0
102043	49699.0
102044	49698.5
102045	49700.0
102046	49699.5
102048	49702.0

G12

111603	49704.5
111605	49707.0
111606	49709.0
111607	49705.5
111608	49704.5
111609	49706.0
111610	49707.0
111612	49707.0
111613	49708.5
111614	49709.5
111615	49711.0
111616	49711.0
111617	49710.0
111618	49713.5
111620	49712.0
111621	49709.0
111622	49692.0
111623	49697.0
111624	49700.0
111625	49702.0
111627	49705.5
111628	49710.0
111629	49709.5
111630	49706.5
111631	49711.0
111632	49707.5
111634	49707.5
111635	49707.5
111636	49708.0
111637	49715.0
111638	49710.5
111639	49708.0
111641	49710.5
111642	49713.5
111643	49712.5
111644	49712.0
111645	49712.5
111646	49716.0
111647	49712.0
111649	49709.0
111650	49695.5
111651	49689.0
111652	49693.0
111653	49692.5
111654	49693.0
111656	49694.0
111657	49699.0
111658	49704.5
111659	49706.5
111700	49711.5
111701	49711.5
111703	49709.5
111704	49712.5
111705	49707.0
111706	49706.5
111707	49715.5
111708	49711.0
111709	49708.0
111711	49708.0
111712	49709.0
111713	49708.0
111714	49709.0
111715	49709.5
111716	49711.5
111718	49713.0
111719	49708.5
111720	49705.5
111721	49709.5
111722	49713.5
111723	49709.5
111725	49706.5
111726	49707.0
111727	49711.0
111728	49711.5
111729	49707.0
111730	49710.5

H9

Figure 10. Magnetic anomalies comprising Cluster A.

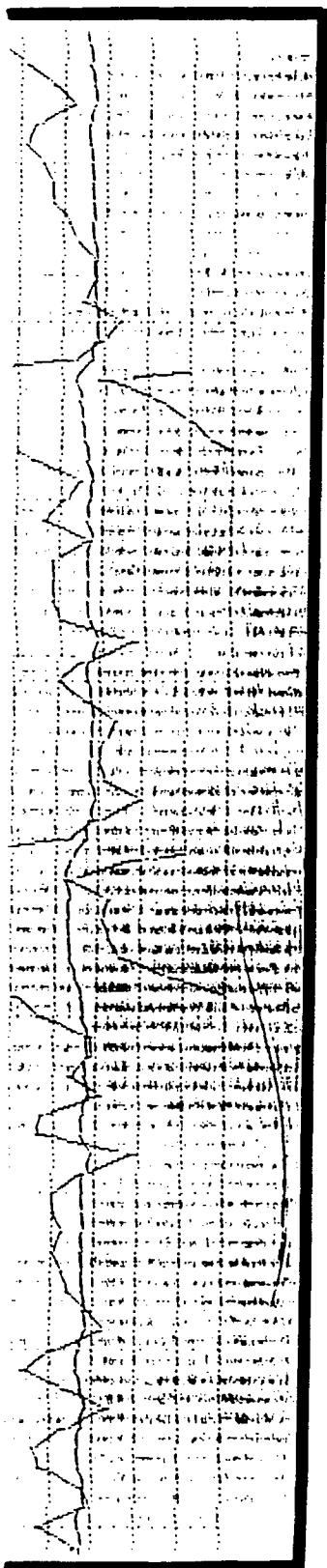
111603	49704.5	
111605	49707.0	
111606	49709.0	
111607	49705.5	
111608	49704.5	
111609	49706.0	
111610	49707.0	
111612	49707.0	
111613	49708.5	
111614	49709.5	
111615	49711.0	
111616	49711.0	
111617	49710.0	
111618	49713.5	
111620	49712.0	
111621	49709.0	
111622	49692.0	
111623	49697.0	
111624	49700.0	
111625	49702.0	
111627	49705.5	
111628	49710.0	
111629	49708.5	
111630	49706.5	
111631	49711.0	
111632	49707.5	
111634	49707.5	
111635	49707.5	
111636	49708.0	
111637	49715.0	
111638	49710.5	
111639	49708.0	
111641	49718.5	
111642	49713.5	
111643	49712.5	
111644	49712.0	
111645	49712.5	
111646	49716.0	
111647	49712.0	
111649	49709.0	
111650	49695.5	
111651	49689.0	
111652	49693.0	
111653	49692.5	
111654	49693.0	
111656	49694.0	
111657	49699.0	
111658	49704.5	
111659	49706.5	
111700	49711.5	
111701	49711.5	
111703	49709.5	
111704	49712.5	
111705	49707.0	
111706	49706.5	
111707	49715.5	
111708	49711.0	
111709	49708.0	
111711	49708.0	
111712	49709.0	
111713	49708.0	
111714	49709.0	
111715	49709.5	
111716	49711.5	
111718	49713.0	
111719	49708.5	
111720	49705.5	
111721	49709.5	
111722	49713.5	
111723	49709.5	
111725	49706.5	
111726	49707.0	
111727	49711.0	
111728	49711.5	
111729	49707.0	
111730	49710.5	

H91 & H93

112252	49710.5	
112253	49709.5	
112254	49712.5	
112255	49712.5	
112256	49708.5	
112258	49710.0	
112259	49710.5	
112300	49709.0	
112301	49713.0	
112302	49711.5	
112303	49708.5	
112304	49713.0	
112306	49713.0	
112307	49713.5	
112308	49709.5	
112309	49710.0	
112310	49711.0	
112311	49711.0	
112313	49711.5	
112314	49711.5	
112315	49712.5	
112316	49708.5	
112317	49717.0	
112318	49709.5	
112320	49714.0	
112321	49709.0	
112322	49710.0	
112323	49714.5	
112324	49707.5	
112325	49715.0	
112327	49710.0	
112328	49711.5	
112329	49714.0	
112330	49714.0	
112331	49708.0	
112332	49707.5	
112334	49715.0	
112335	49706.5	
112336	49708.5	
112337	49717.0	
112338	49710.0	
112339	49706.0	
112341	49715.0	
112342	49711.0	
112343	49706.5	
112344	49713.5	
112345	49713.0	
112346	49709.5	
112348	49711.5	
112349	49709.5	
112350	49715.5	
112351	49710.0	
112352	49709.0	
112353	49709.0	
112355	49712.5	
112356	49711.5	
112357	49709.0	
112358	49710.0	
112359	49712.5	
112400	49707.5	
112402	49709.5	
112403	49711.0	
112404	49711.5	
112405	49709.5	
112406	49709.5	
112407	49710.5	
112408	49707.0	
112410	49709.0	
112411	49710.5	
112412	49709.5	
112413	49710.5	
112414	49712.5	
112415	49709.0	
112417	49708.0	
112418	49709.5	
112419	49709.5	

J14

2

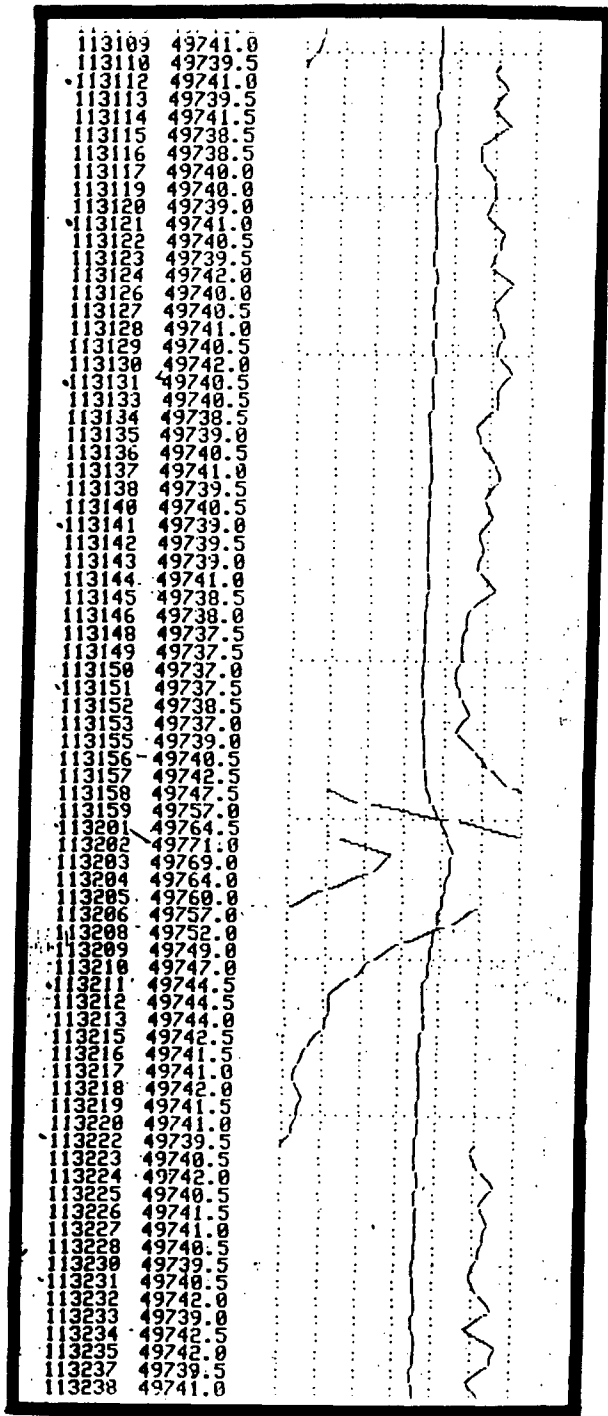


112251	49710.5
112252	49710.5
112253	49709.5
112254	49712.5
112255	49712.5
112256	49708.5
112258	49710.0
112259	49710.5
112300	49709.0
112301	49713.0
112302	49711.5
112303	49708.5
112304	49713.0
112306	49713.0
112307	49713.5
112308	49709.5
112309	49710.0
112310	49711.0
112311	49711.0
112313	49711.5
112314	49711.5
112315	49712.5
112316	49708.5
112317	49717.0
112318	49709.5
112320	49714.0
112321	49709.0
112322	49710.0
112323	49714.5
112324	49707.5
112325	49715.0
112327	49710.0
112328	49711.5
112329	49714.0
112330	49714.0
112331	49708.0
112332	49707.5
112334	49715.0
112335	49706.5
112336	49708.5
112337	49717.0
112338	49710.0
112339	49706.0
112341	49715.0
112342	49711.0
112343	49706.5
112344	49713.5
112345	49713.0
112346	49709.5
112348	49711.5
112349	49709.5
112350	49715.5
112351	49710.0
112358	49709.0
112353	49709.0
112355	49712.5
112356	49711.5
112357	49709.0
112358	49710.0
112359	49712.5
112400	49707.5
112402	49709.5
112403	49711.0
112404	49711.5
112405	49709.5
112406	49709.5
112407	49710.5
112408	49707.0
112410	49709.0
112411	49710.5
112418	49709.5
112413	49710.5
112414	49712.5
112415	49709.0
112417	49708.0
112418	49709.5
112419	49709.5
112420	49710.0

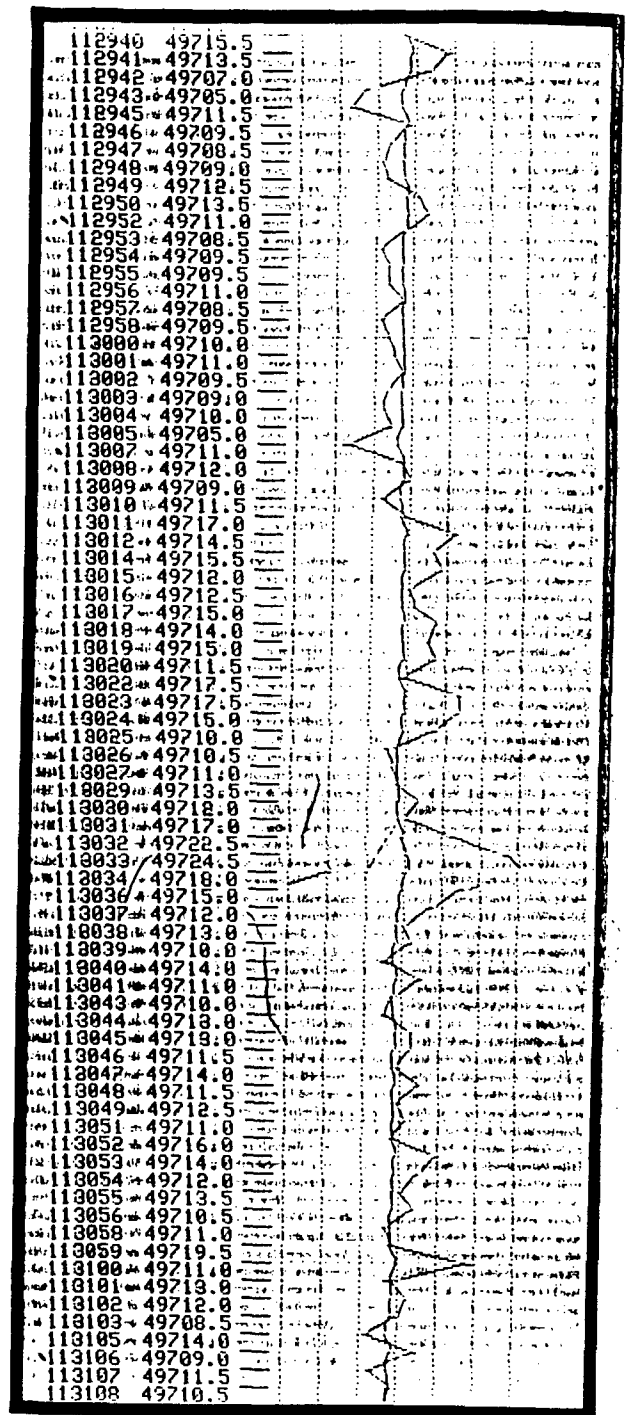
& H93

J14

3



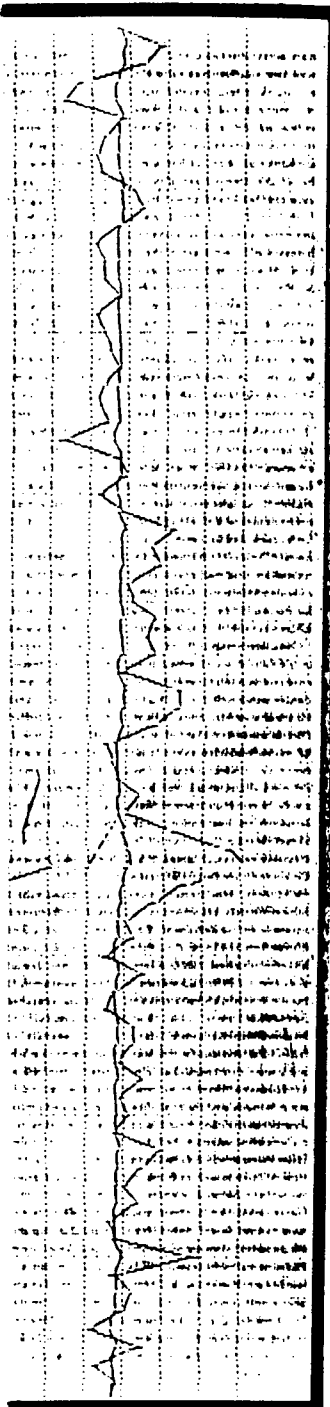
162



J42

Figure 11. Magnetic anomalies comprising Cluster C.

①



121602	49734.0
121603	49733.5
121604	49737.5
121606	49734.0
121607	49738.0
121608	49735.0
121609	49735.5
121610	49734.5
121611	49734.0
121613	49733.5
121614	49734.0
121615	49734.0
121616	49734.0
121617	49733.5
121618	49735.0
121619	49732.5
121621	49727.5
121622	49740.0
121623	49733.5
121624	49736.0
121625	49730.5
121626	49730.5
121628	49732.5
121629	49735.0
121630	49737.5
121631	49736.0
121632	49733.0
121633	49733.0
121635	49733.5
121636	49736.0
121637	49734.0
121638	49734.5
121639	49734.0
121640	49734.0
121642	49734.5
121643	49735.5
121644	49734.0
121645	49737.0
121646	49736.0
121647	49739.5
121648	49732.0
121650	49737.0
121651	49738.0
121652	49739.0
121653	49733.5
121654	49739.0
121655	49736.0
121657	49736.0
121658	49736.0
121659	49736.0
121700	49735.0
121701	49737.0
121702	49735.0
121704	49736.0
121705	49736.0
121706	49737.0
121707	49734.0
121708	49737.0
121709	49732.0
121711	49734.0
121712	49735.0
121713	49736.0
121714	49738.0
121715	49734.0
121716	49740.5
121717	49736.0
121719	49733.5
121720	49736.0
121721	49740.5
121722	49738.5
121723	49732.0
121724	49739.0
121726	49738.0
121727	49735.5
121728	49738.0
121729	49734.5
121730	49744.5

132240	49734.0
132242	49734.0
132243	49735.0
132244	49732.5
132245	49733.5
132246	49729.0
132247	49733.5
132249	49732.0
132250	49733.5
132251	49731.0
132252	49732.0
132253	49734.0
132254	49734.0
132255	49732.0
132257	49732.0
132258	49736.0
132259	49734.0
132300	49732.5
132301	49733.5
132302	49733.0
132304	49733.0
132305	49733.5
132306	49732.5
132307	49733.0
132308	49729.0
132309	49732.5
132311	49730.5
132312	49731.5
132313	49729.0
132314	49736.0
132315	49733.0
132316	49735.0
132318	49732.0
132319	49731.5
132320	49734.0
132321	49741.5
132322	49728.0
132323	49729.5
132325	49735.5
132326	49732.0
132327	49733.5
132328	49735.5
132329	49736.0
132330	49735.0
132332	49735.0
132333	49734.0
132334	49729.0
132335	49731.0
132336	49735.0
132337	49731.0
132338	49734.5
132340	49736.0
132341	49732.0
132342	49733.5
132343	49731.5
132344	49734.0
132345	49736.5
132347	49732.5
132348	49734.0
132349	49732.0
132350	49734.0
132351	49732.5
132352	49734.5
132354	49731.0
132355	49732.0
132356	49734.5
132357	49730.5
132358	49732.0
132359	49731.5
132401	49736.0
132402	49732.0
132403	49732.0
132404	49732.0
132405	49736.0
132406	49733.0
132407	49732.5
132409	49734.5
132410	49734.5

42

K78

N203

②

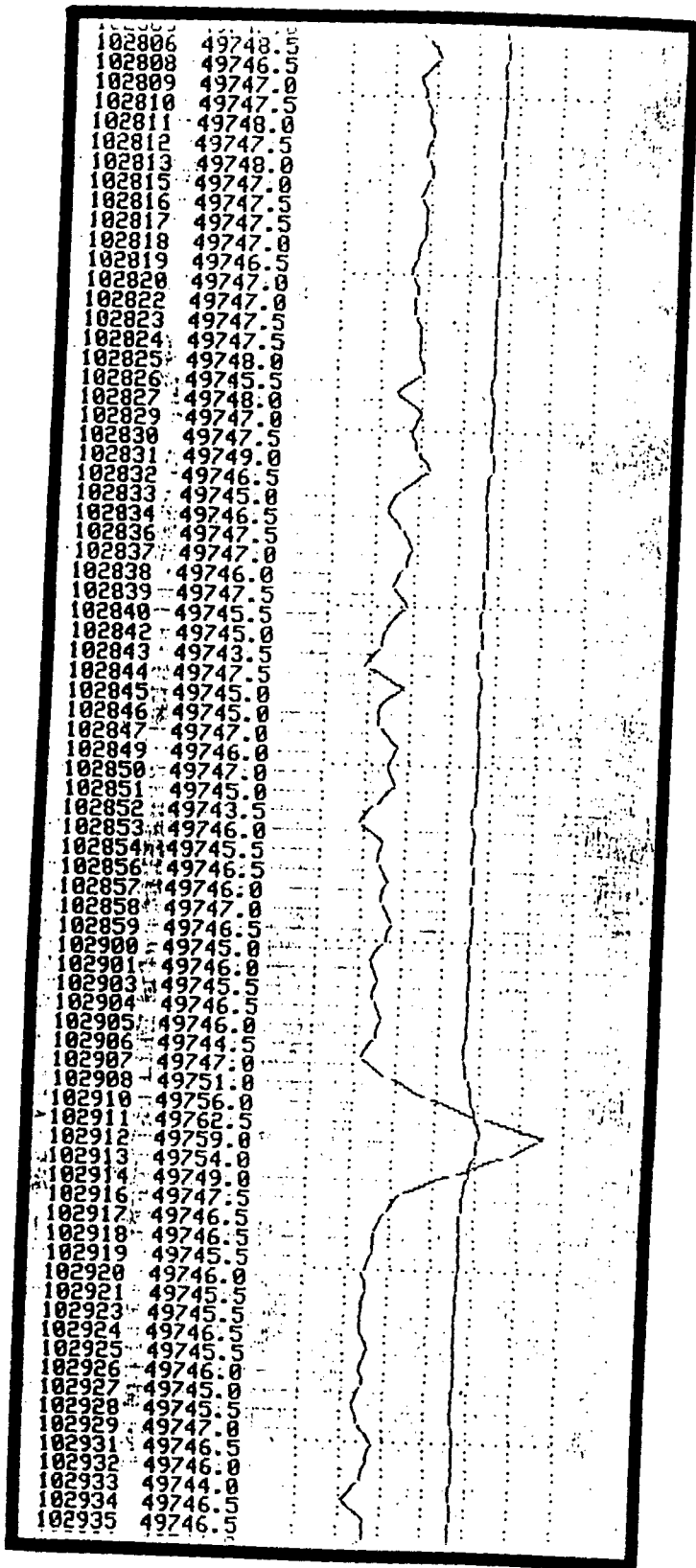
121602	49734.0	
121603	49733.5	
121604	49737.0	
121606	49734.0	
121607	49738.0	
121608	49735.0	
121609	49735.0	
121610	49734.0	
121611	49734.0	
121613	49733.0	
121614	49734.0	
121615	49734.0	
121616	49734.0	
121617	49733.5	
121618	49735.0	
121619	49732.5	
121621	49727.0	
121622	49740.0	
121623	49733.5	
121624	49736.0	
121625	49738.0	
121626	49738.5	
121628	49732.5	
121629	49735.0	
121630	49737.0	
121631	49736.0	
121632	49738.0	
121633	49733.0	
121635	49733.5	
121636	49736.0	
121637	49734.0	
121638	49734.0	
121639	49734.0	
121640	49734.0	
121642	49734.0	
121643	49735.0	
121644	49734.0	
121645	49737.0	
121646	49736.0	
121647	49739.0	
121648	49732.0	
121650	49737.0	
121651	49738.0	
121652	49739.0	
121653	49733.5	
121654	49739.0	
121655	49736.0	
121657	49736.0	
121658	49736.0	
121659	49736.0	
121700	49735.0	
121701	49737.0	
121702	49735.0	
121704	49736.0	
121705	49736.0	
121706	49737.0	
121707	49734.0	
121708	49737.0	
121709	49732.0	
121711	49734.0	
121712	49735.0	
121713	49736.0	
121714	49738.0	
121715	49734.0	
121716	49740.0	
121717	49736.0	
121719	49733.5	
121720	49736.0	
121721	49740.0	
121722	49738.0	
121723	49732.0	
121724	49739.0	
121726	49738.0	
121727	49735.0	
121728	49738.0	
121729	49734.0	
121730	49744.0	

K78

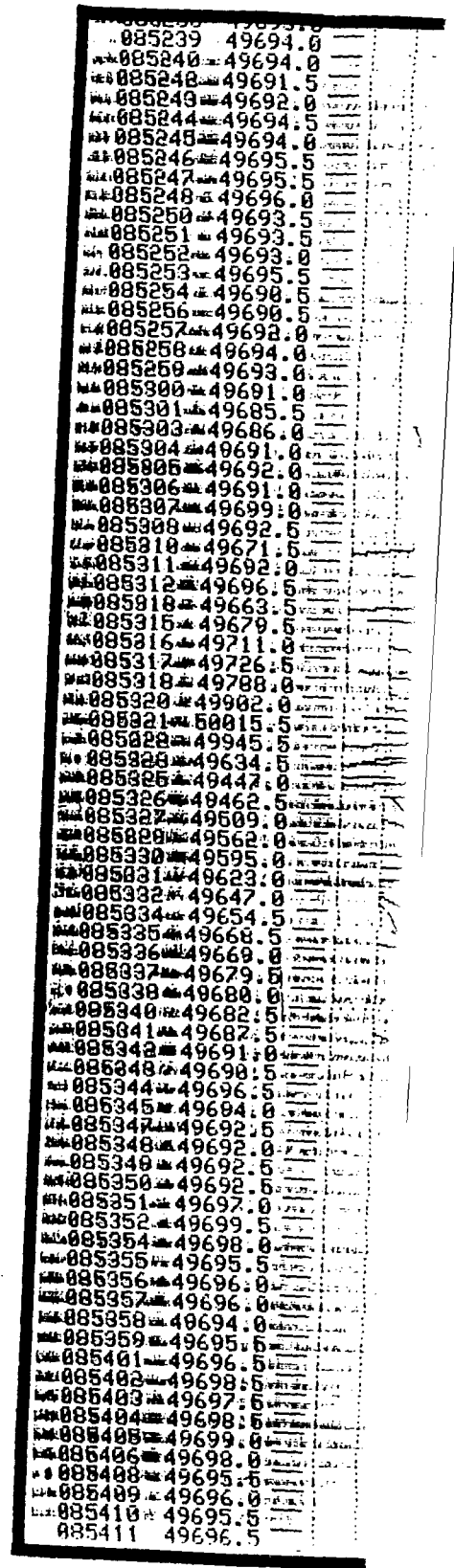
132240	49734.0	
132242	49734.0	
132243	49735.0	
132244	49732.5	
132245	49733.5	
132246	49729.0	
132247	49733.5	
132249	49732.0	
132250	49733.5	
132251	49731.0	
132252	49732.0	
132253	49734.0	
132254	49734.0	
132255	49732.0	
132257	49732.0	
132258	49736.0	
132259	49734.0	
132300	49732.5	
132301	49733.5	
132302	49733.0	
132304	49733.0	
132305	49733.0	
132306	49732.5	
132307	49733.0	
132308	49729.0	
132309	49732.5	
132311	49730.0	
132312	49731.5	
132313	49729.0	
132314	49736.0	
132315	49733.0	
132316	49735.0	
132318	49732.0	
132319	49731.5	
132320	49734.0	
132321	49741.0	
132322	49728.0	
132323	49729.0	
132325	49735.0	
132326	49732.0	
132327	49733.5	
132328	49735.5	
132329	49736.0	
132330	49735.0	
132332	49735.0	
132333	49734.0	
132334	49729.0	
132335	49731.0	
132336	49735.0	
132337	49731.0	
132338	49734.5	
132340	49736.0	
132341	49732.0	
132342	49733.5	
132343	49731.5	
132344	49734.0	
132345	49736.0	
132347	49732.0	
132348	49734.0	
132349	49732.0	
132350	49734.0	
132351	49732.5	
132352	49734.0	
132354	49731.0	
132355	49732.0	
132356	49734.5	
132357	49738.0	
132358	49732.0	
132359	49731.0	
132401	49736.0	
132402	49732.0	
132403	49732.0	
132404	49732.0	
132405	49736.0	
132406	49733.0	
132407	49732.5	
132409	49734.0	
132411	49734.0	

N203

3



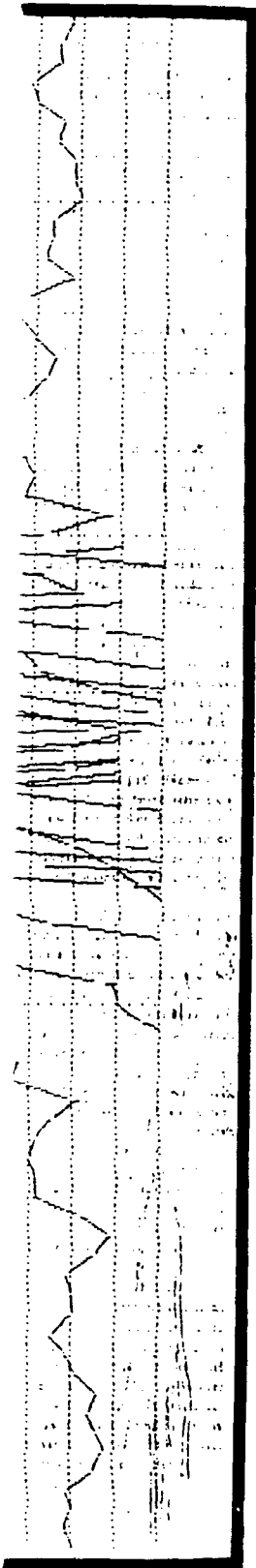
A80



C68

Figure 12. Magnetic anomalies comprising Cluster D.

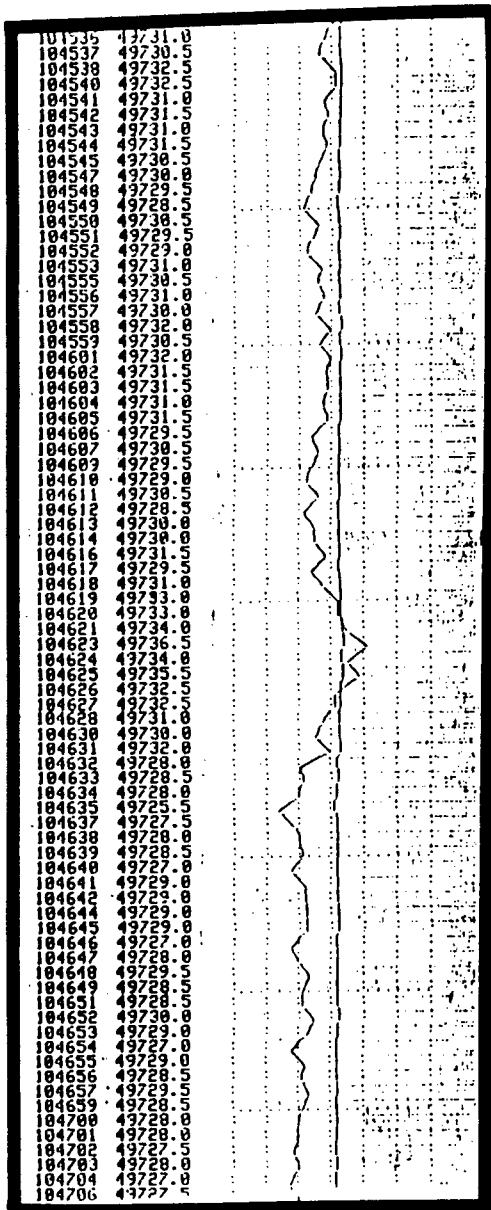
①



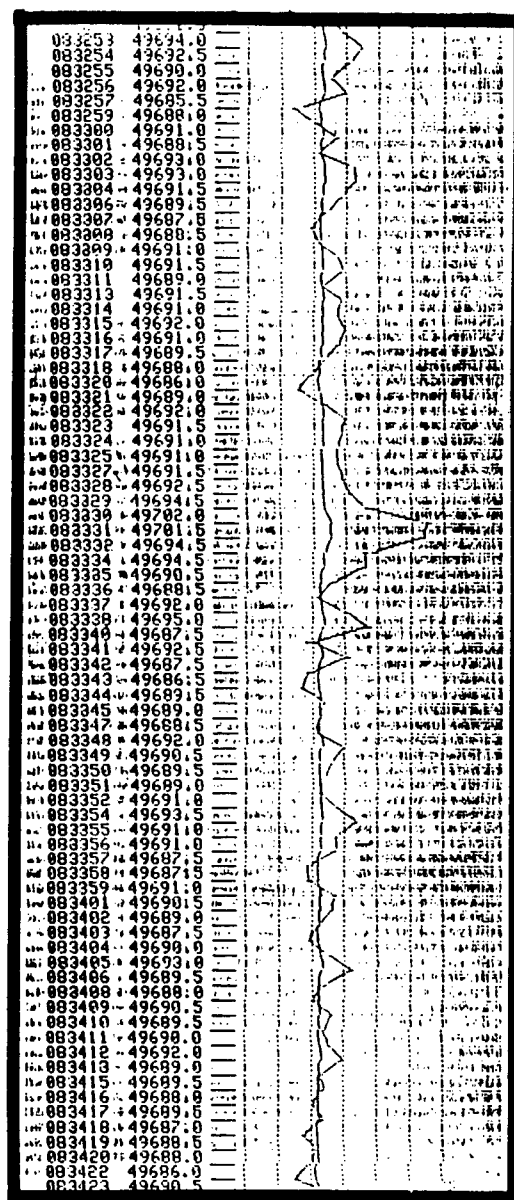
092015	49691.0	---
092016	49692.0	---
092018	49694.5	---
092019	49694.5	---
092020	49692.5	---
092021	49691.5	---
092022	49692.5	---
092023	49691.5	---
092024	49692.0	---
092026	49693.0	---
092027	49693.5	---
092028	49695.0	---
092029	49693.0	---
092030	49694.5	---
092031	49695.5	---
092033	49692.5	---
092034	49692.5	---
092035	49692.0	---
092036	49692.0	---
092037	49692.0	---
092038	49691.0	---
092040	49694.0	---
092041	49692.5	---
092042	49695.5	---
092043	49692.0	---
092044	49691.5	---
092045	49691.5	---
092046	49687.5	---
092048	49691.0	---
092049	49691.0	---
092050	49693.0	---
092051	49691.5	---
092052	49689.5	---
092053	49703.5	---
092055	49711.5	---
092056	49702.5	---
092057	49695.0	---
092058	49693.5	---
092059	49693.5	---
092101	49692.5	---
092102	49692.0	---
092103	49690.5	---
092104	49689.0	---
092105	49687.5	---
092106	49689.0	---
092108	49690.5	---
092109	49693.0	---
092110	49692.5	---
092111	49689.5	---
092112	49690.0	---
092113	49691.5	---
092114	49690.5	---
092116	49689.5	---
092117	49688.0	---
092118	49687.5	---
092119	49684.0	---
092120	49689.0	---
092121	49687.5	---
092123	49688.0	---
092124	49685.5	---
092125	49684.5	---
092126	49683.0	---
092127	49683.0	---
092128	49681.0	---
092130	49681.5	---
092131	49679.5	---
092132	49680.5	---
092133	49677.5	---
092134	49677.5	---
092135	49682.0	---
092137	49679.0	---
092138	49679.5	---
092139	49680.0	---
092140	49681.5	---
092141	49681.0	---
092142	49678.5	---
092143	49680.0	---
092145	49677.5	---

D59

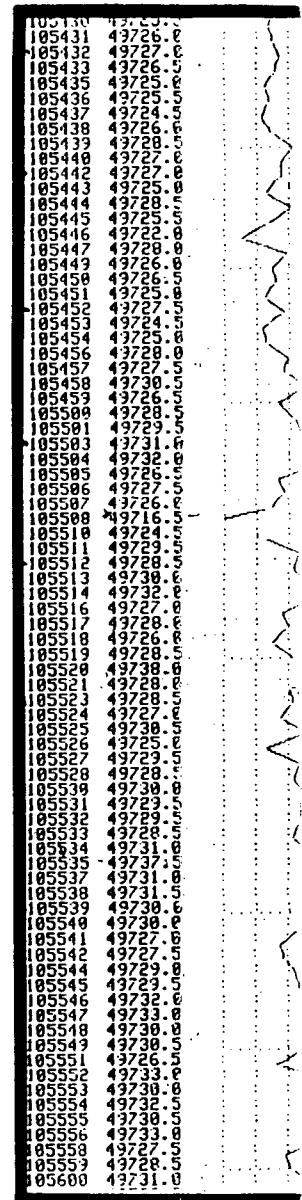
3



A183



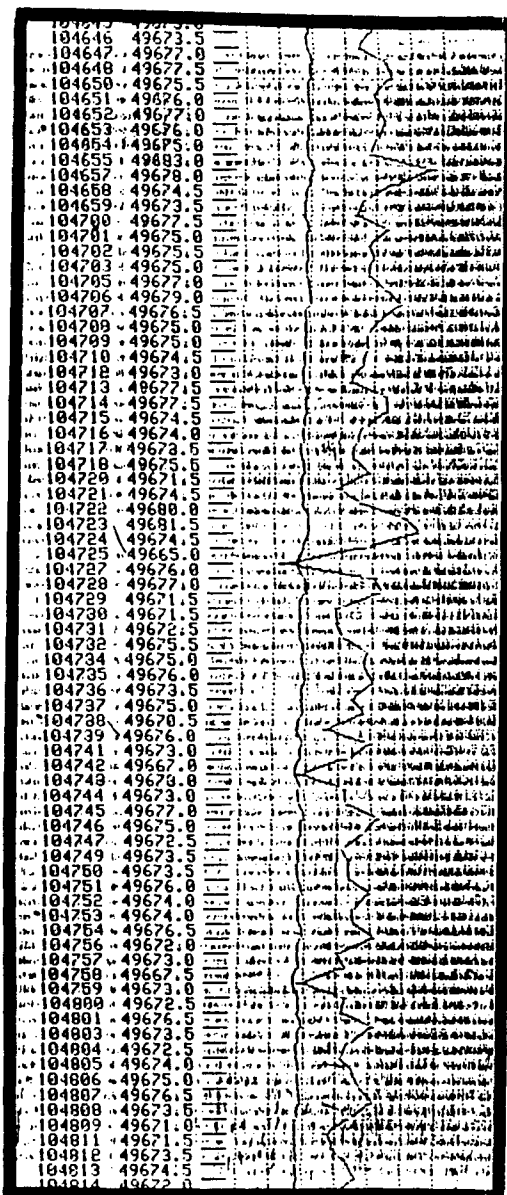
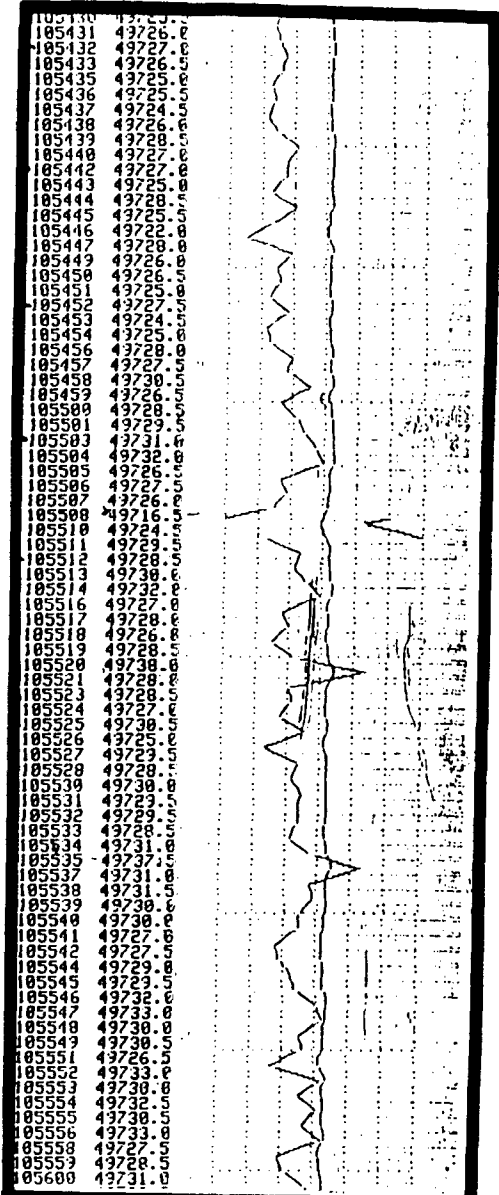
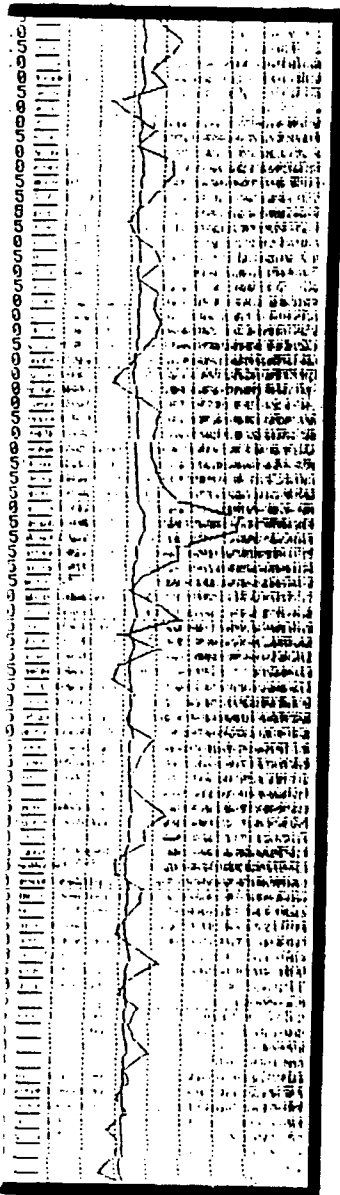
B124



E17

Figure 13. Magnetic anomalies comprising Cluster F.

0



B124

E17

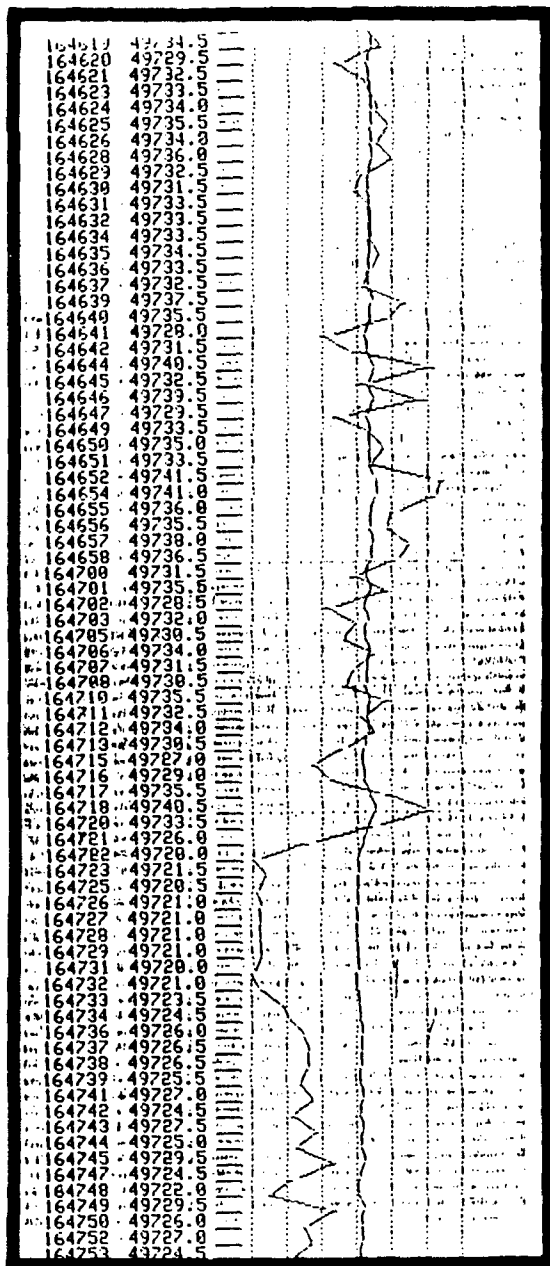
G123

104646	49673.5	
104647	49672.0	
104648	49672.5	
104650	49675.5	
104651	49676.0	
104652	49677.0	
104653	49676.0	
104654	49675.0	
104655	49683.0	
104657	49678.0	
104658	49674.5	
104659	49673.5	
104700	49677.5	
104701	49675.0	
104702	49675.5	
104703	49675.0	
104705	49677.0	
104706	49679.0	
104707	49676.5	
104709	49675.0	
104709	49675.0	
104710	49674.5	
104718	49673.0	
104713	49677.0	
104714	49677.5	
104715	49674.5	
104716	49674.0	
104717	49678.5	
104719	49675.5	
104720	49671.5	
104721	49674.5	
104722	49680.0	
104723	49681.5	
104724	49674.5	
104725	49665.0	
104727	49676.0	
104728	49677.0	
104729	49671.5	
104730	49671.5	
104731	49672.5	
104732	49675.5	
104734	49675.5	
104735	49676.0	
104736	49673.5	
104737	49675.0	
104738	49670.0	
104739	49676.0	
104741	49673.0	
104742	49667.0	
104743	49670.0	
104744	49673.0	
104745	49677.0	
104746	49675.0	
104747	49672.5	
104749	49673.5	
104750	49673.5	
104751	49676.0	
104752	49674.0	
104753	49674.0	
104754	49676.5	
104756	49672.0	
104757	49673.0	
104758	49667.5	
104759	49673.0	
104800	49672.5	
104801	49676.0	
104803	49673.0	
104804	49672.5	
104805	49674.0	
104806	49675.0	
104807	49676.5	
104808	49673.0	
104809	49671.0	
104811	49671.5	
104812	49673.5	
104813	49674.5	
104814	49672.0	

G123

114920	49705.5	
114921	49712.0	
114922	49705.5	
114923	49707.0	
114924	49706.5	
114926	49713.0	
114927	49707.0	
114928	49706.0	
114929	49702.5	
114930	49710.5	
114931	49708.5	
114933	49704.5	
114934	49703.5	
114935	49706.5	
114936	49707.5	
114937	49705.5	
114938	49705.5	
114939	49706.0	
114941	49705.5	
114942	49707.0	
114943	49704.0	
114944	49706.0	
114945	49705.5	
114946	49705.0	
114948	49706.5	
114949	49708.0	
114950	49705.0	
114951	49705.0	
114952	49708.0	
114953	49707.5	
114954	49707.0	
114956	49705.5	
114957	49706.0	
114958	49704.5	
114959	49708.5	
115000	49703.0	
115001	49708.0	
115003	49710.0	
115004	49707.0	
115005	49703.0	
115006	49706.0	
115007	49702.0	
115008	49706.0	
115010	49704.5	
115011	49706.5	
115012	49706.5	
115013	49703.5	
115014	49703.5	
115015	49716.0	
115017	49704.0	
115018	49704.5	
115019	49707.0	
115020	49706.5	
115021	49707.0	
115023	49705.0	
115023	49709.0	
115025	49705.0	
115026	49707.0	
115027	49702.0	
115028	49707.5	
115029	49704.0	
115031	49705.0	
115032	49710.0	
115033	49708.5	
115034	49706.5	
115035	49710.5	
115036	49709.0	
115037	49702.5	
115039	49704.5	
115040	49705.5	
115041	49704.5	
115042	49705.5	
115043	49705.5	
115044	49705.0	
115046	49704.0	
115047	49704.0	

J117



S11

081138	4
081139	4
081141	4
081142	4
081143	4
081144	4
081145	4
081146	4
081148	4
081149	4
081150	4
081151	4
081152	4
081154	4
081155	4
081156	4
081157	4
081158	4
081159	4
081201	4
081202	4
081203	4
081204	4
081206	4
081207	4
081208	4
081209	4
081211	4
081212	4
081213	4
081214	4
081216	4
081217	4
081218	4
081219	4
081221	4
081222	4
081223	4
081224	4
081225	4
081227	4
081228	4
081229	4
081230	4
081231	4
081233	4
081234	4
081235	4
081236	4
081237	4
081238	4
081240	4
081241	4
081242	4
081243	4
081244	4
081245	4
081247	4
081248	4
081249	4
081250	4
081252	4
081253	4
081254	4
081256	4
081257	4
081258	4
081300	4
081301	4
081302	4
081303	4
081305	4
081306	4
081307	4
081308	4
081309	4
081311	4
081312	4
081313	4
081314	4
081315	4
081316	4
081317	4
081319	4
081320	4
081321	4
081322	4
081323	4
081324	4
081326	4
081327	4
081328	4
081329	4
081330	4
081331	4
081333	4
081334	4
081335	4
081336	4

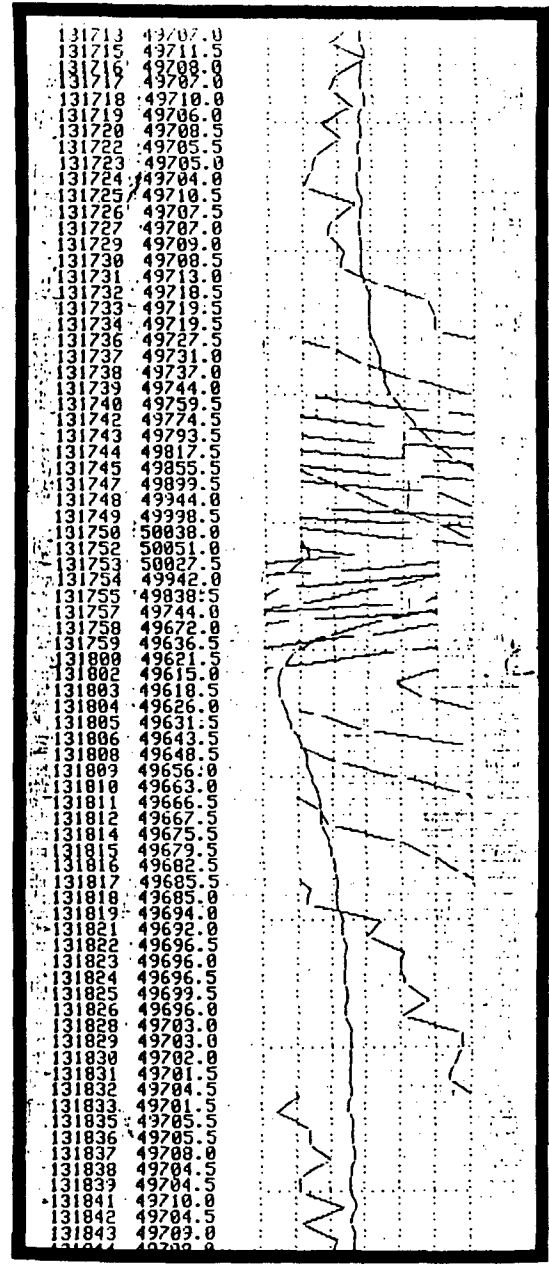
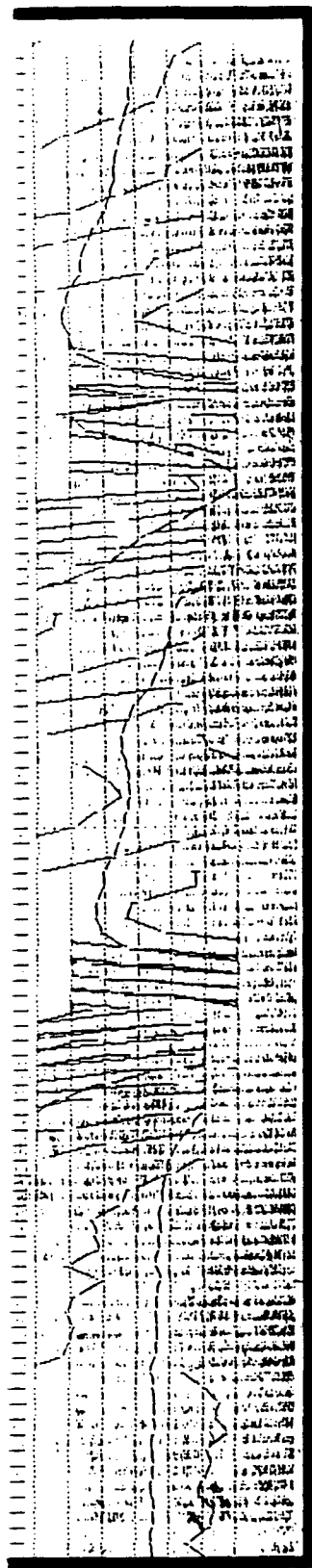
Figure 14. Magnetic anomalies comprising Cluster G.

①

081138	49717.0	
081139	49716.0	
081141	49715.0	
081142	49714.0	
081143	49709.0	
081144	49704.0	
081145	49700.0	
081146	49696.0	
081148	49695.0	
081149	49689.0	
081150	49684.0	
081151	49671.0	
081152	49662.0	
081154	49654.0	
081155	49653.0	
081156	49648.0	
081157	49636.0	
081158	49632.0	
081159	49635.0	
081201	49648.0	
081202	49691.0	
081203	49805.0	
081204	49978.0	
081206	49839.0	
081207	49859.0	
081208	49937.0	
081209	50004.0	
081211	50036.0	
081212	50035.0	
081213	50003.0	
081214	49968.0	
081215	49988.0	
081217	49988.0	
081218	49881.0	
081219	49824.0	
081221	49774.0	
081223	49762.0	
081223	49762.0	
081224	49758.0	
081225	49751.0	
081227	49743.0	
081228	49736.0	
081229	49716.0	
081230	49710.0	
081231	49699.0	
081233	49700.0	
081234	49705.0	
081235	49708.0	
081236	49710.0	
081237	49707.0	
081238	49704.0	
081240	49696.0	
081241	49689.0	
081242	49679.0	
081243	49679.0	
081244	49671.0	
081245	49670.0	
081247	49675.0	
081248	49712.0	
081249	49873.0	
081250	50309.0	
081252	50915.0	
081253	51146.0	
081254	50758.0	
081256	50365.0	
081257	50098.0	
081258	49953.0	
081300	49876.0	
081301	49825.0	
081302	49795.0	
081303	49782.0	
081305	49767.0	
081306	49759.0	
081307	49756.0	
081308	49751.0	
081309	49750.0	
081311	49746.0	
081312	49745.0	
081313	49745.0	
081314	49745.0	
081315	49748.0	
081316	49744.0	
081317	49743.0	
081319	49744.0	
081320	49744.0	
081321	49743.0	
081322	49737.0	
081323	49740.0	
081324	49742.0	
081326	49741.0	
081327	49743.0	
081328	49740.0	
081329	49741.0	
081330	49740.0	
081331	49739.0	
081333	49741.0	
081334	49741.0	
081335	49738.0	
081336	49740.0	

T111

(2)



131713 49707
 131715 49711
 131716 49708
 131717 49707
 131718 49710
 131719 49706
 131720 49708
 131722 49705
 131723 49705
 131724 49704
 131725 49710
 131726 49707
 131727 49707
 131729 49709
 131730 49708
 131731 49713
 131732 49718
 131733 49719
 131734 49719
 131736 49727
 131737 49731
 131738 49737
 131739 49744
 131740 49759
 131742 49774
 131743 49793
 131744 49817
 131745 49855
 131747 49899
 131748 49944
 131749 49998
 131750 50038
 131752 50051
 131753 50027
 131754 49942
 131755 49838
 131757 49744
 131758 49672
 131759 49636
 131800 49621
 131802 49610
 131803 49616
 131804 49626
 131805 49631
 131806 49643
 131808 49648
 131809 49656
 131810 49663
 131811 49669
 131812 49677
 131814 49679
 131817 49683
 131818 49685
 131819 49684
 131820 49685
 131821 49683
 131822 49685
 131823 49686
 131824 49686
 131825 49689
 131826 49696
 131828 49703
 131829 49703
 131830 49702
 131831 49701
 131832 49704
 131833 49701
 131835 49705
 131836 49705
 131837 49708
 131838 49704
 131839 49704
 131841 49710
 131842 49704
 131843 49703
 131844 49703

U16

111

3



Figure 15. Acoustic anomaly at Cluster G.

CHAPTER II

METHODOLOGY

The search and groundtruthing methodologies used during this project were designed to maximize personnel, equipment and time. Four steps were involved in the process of investigating the magnetic anomalies: reacquisition, contouring, refinement, and identification. The methods utilized are, for the most part, common practices for Phase II underwater archeological projects. Arnold (1982:83); Dean et al. (1992:128-144); Gearhart et al. (1990:29); Irion and Bond (1984:33); Marx (1975:123-124); Mistovich and Knight (1983:208); and Watts, (1986:109-110) all recommend variations of the methodologies employed during this project. The one major departure from common practice was the utilization of a Schonstedt GAU-20 magnetic gradiometer in place of either a magnetometer or standard metal detector for refining the locations of anomalies. The benefits of this method over the others will be discussed in a later section.

Survey and diving operations were conducted from two different vessels during the course of the project. During the first phase of the project, a 19.8 m (65 ft) long wooden-hull, live-aboard, sport fishing boat, *Omeco III*, was utilized. It provided a stable offshore work platform and saved considerable travel time because it had the capability of anchoring overnight near the project area. The vessel also was equipped with two small on-board fiberglass skiffs that could be used as chase boats and for refining the locations of anomalies. However, due to delays in the project caused by adverse weather conditions, *Omeco III* was forced to return to her home port of Biloxi to honor previous commitments.

During the second phase of the project, the *TGIF*, a 7.9 m (26 ft) fiberglass Aquasport dive charter boat based in Grand Isle, was utilized. While *TGIF* did not provide as much deck space as *Omeco III*, *TGIF*, its stern-mounted dive platform made entry and exit from the water by divers much more efficient. *TGIF* also was much more maneuverable, allowing for more rapid refinement of the locations of the anomalies. There were only two main logistical drawbacks in the use of this vessel. First, it required project personnel to find lodging onshore, necessitating approximately two hours per day of travel to and from the project area. Second, the wheelhouse of the boat in which the electronic equipment was mounted was not enclosed fully, risking the threat of having operations interrupted by rainy weather. Fortunately, this did not occur, although one additional day was lost to high winds that resulted in six- to seven-foot seas.

The reacquisition of the anomaly clusters involved a 15 m (49.2 ft) interval survey with an EG&G Geometrics Model 866 proton precession magnetometer. Positioning and trackplotting were controlled via a Magnavox MX200 Differential Global Positioning System (DGPS), supplied by Offshore Navigation, Inc. (ONI) of New Orleans. Differential GPS depends upon the mobile unit receiving pseudorange corrections from a static shore-based receiver to achieve position accuracies of <5 m. ONI maintains its own differential stations around the Gulf of Mexico; for most of the project, ONI's station on Grand Isle was used. Unfortunately, a tornado destroyed this station midway through the project, requiring ONI to transmit a signal from its headquarters in New Orleans until the station was repaired. The positioning system was interfaced with an Apple Macintosh Classic II running *Navigate* software to provide navigation control and data logging. Anomalies located during Phase I of this project first were plotted on the *Navigate* program. A survey grid with track lines spaced 15 m (49.2 ft) apart then was superimposed over the target, which was placed in the center of the grid. Guided by the navigation software, the magnetometer was towed along each lane. Since water depths in the project area did not exceed 6 m (20 ft), the sensor was towed on the surface. The data was acquired on both magnetic media and a paper printer. The data was contoured on an IBM-compatible laptop computer running the grid and topo programs of the Golden Graphics *Surfer* package. The resulting contours were analyzed to determine the most significant magnetic

perturbation within each target cluster. A position for the center of each target was derived and a buoy was placed at that location.

Once a buoy was dropped near the point of greatest magnetic deviation, a Schonstedt GAU-20 gradiometer was deployed to refine further the center of the anomaly. During the course of the project, several methods were employed for this step. The first involved extending the gradiometer sensor from the bow of a small skiff and making a series of passes around the buoy. If the gradiometer indicated that the object was away from the buoy, then a second buoy was dropped and the process was repeated until the buoy marked the strongest signal.

The second method entailed towing the gradiometer sensor within a weighted PVC sled behind the survey vessel. The sled had a buoy attached to it so that its position could be monitored from the surface. As with the previous method, a series of passes was made near the target buoy. When the strongest return signal was achieved, the survey vessel slowly backed toward the gradiometer sensor and a second buoy was dropped near the sensor.

The third method involved divers deploying the gradiometer sensor at different points away from the target buoy and then slowly pulling it toward the buoy anchor. A series of radii around the buoy was surveyed in this fashion. Upon encountering a strong signal, the diver was advised by surface personnel monitoring the gradiometer control box to investigate the area near the sensor.

The final step in the process sought to identify the source of the anomaly. Once the position of the strongest gradiometer reading was refined, divers were deployed to investigate the area. All diving was conducted using standard open-circuit SCUBA equipment with the addition of full-face EXO-26 band masks fitted with wireless diver-to-diver/surface communication units. Due to the low water temperatures, (approximately 13° C [55° F]) dry diving suits were utilized by all personnel.

The first stage of the process of sourcing the anomaly involved attaching a search line to the buoy anchor and conducting a series of visual and tactile circle searches around the buoy to determine if the source of the anomaly protruded above the sea floor. Each sweep extended the search radius by 1.5 m (5 ft) out to a distance of 15.2 m (50 ft). In the event that no-above surface features were encountered, a series of radii were surveyed with the gradiometer until the point of greatest magnetic deviation was located. All targets were probed with a small diameter 2.84 m (9 ft 4 in) stainless steel antenna. All probes were made to the length of the probe or to refusal. Refusal resulted either from a hard-packed stratum that underlay the more loosely consolidated sands, or from the source of the anomaly. More intensive probing was used to determine the horizontal extent of anomalies and their depths below surface.

The last step in identifying the source of buried anomalies was excavation. Excavations were conducted using a 10 cm (4 in) diameter hydro-induction dredge powered by 5 cm (2 in) diameter, 5 hp Honda water pump. Excavations were continued until the source of the anomaly was identified, or until the excavation became too deep for divers to work safely.

Critique of Methodology

In the past few years, a number of Phase II testing projects similar to the Breton Sound Project have been conducted, making it now possible to analyze the effectiveness of groundtruthing methods. The Breton Sound project employed what has become standardized groundtruthing methodologies for Phase II underwater archeological projects. The sole exception was the use of the magnetic gradiometer in place of a magnetometer for refining the point of highest magnetic deviation for magnetic anomalies. As will be seen by the following discussion of several similar projects, the results and success rates are similar.

One of the first major projects of this kind was conducted prior to the construction of the Tennessee-Tombigbee Waterway in Alabama and Mississippi. Larry Murphy and Alan Saltus (1981) identified a total of 21 Study Areas, each one consisting of multiple magnetic anomalies. Many anomalies were determined to require further work; these include five anomalies identified as vessels or associated vessel remains; 15 anomalies were characterized as modern debris; four could not be identified because they were buried too deeply or could not be located; and, eight were not investigated because they fell outside of project impact areas.

J. Barto Arnold III (1982) in his survey of Matagorda Bay, Texas, identified 12 magnetic anomalies as having characteristics requiring further investigation. Of these, three were the probable remains of historic shipwrecks; two were probable modern shipwrecks; two were modern debris; and, five could not be located or a source determined.

One of the more successful projects of this kind (100 percent identification of anomalies) was conducted in Mobile Bay, Alabama (Irion and Bond 1984). Of the 11 anomalies investigated, nine were identified as modern debris; one was a series of pilings associated with the Confederate obstructions in the upper bay; and, one was a brick-filled shipwreck, also part of the Confederate obstructions.

However, environmental conditions can influence the efficacy of these methodologies in the identification of anomalies. For example, Robert Gearhart et al. (1990) encountered very deep sand in their attempts to identify positively the site of the 1554 Spanish vessel, *Santa Maria de Yciar*, near Port Mansfield, Texas. These sediments prevented a positive identification of the seven anomaly clusters tested. However, two of the clusters, were believed to be associated with the wreck because of the characteristics of their magnetic signatures.

In general, the combined use of advanced magnetic detection equipment and traditional line search techniques have proven successful in locating sources of anomalous magnetism in highly turbid environments where visual search techniques are extremely limited. Magnetic detection equipment becomes even more important when one considers that the majority of shipwrecks in Louisiana waters probably show no debris above the bottom. Garrison et al. (1989:11-167) observed that of 47 significant magnetic anomalies in Texas waters, only 13 percent, or six cases, showed debris above the bottom that was detectable utilizing side-scan sonar. With no surface wreckage to aid divers in acquiring target, magnetic detection equipment becomes a requirement.

The magnetic gradiometer proved to be a useful tool for refining the locations of magnetic anomalies. The gradiometer incorporates the benefits of both a magnetometer and a hand-held metal detector. The gradiometer sensor can be towed behind a survey vessel or attached to a boom extending from the bow in shallow water, much like a magnetometer. Unlike the magnetometer, however, the gradiometer does not detect the anomaly unless it passes almost directly over it. A magnetometer begins to detect localized disturbances in the magnetic field from many meters away, resulting in a much larger field area.

The gradiometer also can be manipulated by divers on the bottom. This involves pulling or towing the gradiometer sensor in a controlled pattern around the target buoy. The divers, however, must be careful not to let the gradiometer get too close to them as any ferrous objects in their equipment will be detected. Although not as easily maneuvered as a hand-held metal detector, the gradiometer has the sensitivity to detect deeply buried ferrous metal or magnetic objects that a standard metal detector might miss.

During the present project, it was found that the gradiometer, long in use among oilfield divers to locate buried pipelines, was a useful and effective archeological tool as well. Through the combined use of this instrument deployed first from a small boat to make the initial contact and, second, carried by a diver

on the bottom to refine the position, it was possible to acquire and define the target area in a very short amount of time.

Finally, the *Navigate* program proved to be extremely accurate for relocation purposes. When a buoy was dropped on the dive site coordinates, its position was annotated on the computer screen with a special icon. As testimony to the accuracy of this program, when one buoy was inadvertently sunk and another had to be dropped, divers later reported that the buoy weights were less than 10 ft away from one another.

CHAPTER III

RESULTS OF INVESTIGATIONS

Results of Magnetic Contouring Survey

Prior to initiating diving investigations, a 50,000 m² area was re-surveyed at a 15 m (50 ft) interval at each of five target areas (A, C, D, F, and G). The methods and equipment employed in this task have been described in detail in Chapter II. The close-interval survey fulfilled one of the primary tasks of the Scope of Services and was intended to assist in site definition and target selection. However, this exercise appeared to be largely unnecessary at this stage of the investigations. Positions derived from close-interval survey only differed slightly from those reported for the clusters following Phase I survey (Table 2). The efficacy of close-interval survey has been demonstrated clearly when applied to actual historic sites (Clausen and Arnold 1975; Garrison 1986; Gearhart 1988) however, it can be argued that, while providing valuable information about the anomaly, such an exercise may be unnecessary at the Phase II level.

Table 2. Coordinates of Anomalies Derived from Phase I Survey Compared to Coordinates of Actual Anomaly Source.

CLUSTER DESIGNATION	PHASE I COORDINATES	PHASE II COORDINATES
A	29°29'31.20" N 89°09'34.80" W	29°29'31.94" N 89°09'35.58" W
C	29°29'03.60" N 89°09'30.60" W	29°29'03.68" N 89°09'32.89" W
D	29°28'53.40" N 89°09'42.60" W	29°28'52.53" N 89°09'42.00" W
G	29°27'46.29" N 89°09'17.04" W	29°27'45.62" N 89°09'16.68" W

All positions in WGS-84 geographic coordinates.

Magnetic survey at intervals of <15 m (<50 ft) has been applied to buried shipwreck sites to distinguish significant features within those sites and to analyze the extent of associated wreck scatter. The intent of close-interval survey as applied during the present study was twofold: first, to isolate the most spatially significant anomaly within a cluster for diving investigation, and, secondly, to characterize the signature of the target for the purpose of theory-building aimed at distinguishing "treasure" from trash. By conducting close-interval surveys of target anomalies, it was hoped that pattern recognition could be developed to assist resource managers in developing a strategy for deciding which anomalies must be groundtruthed and which ones can be ignored. The target clusters were selected for investigation based upon initial similarities between their characteristics of amplitude, duration, and signature and those exhibited by historic shipwrecks. It was theorized that by expanding the available data base relating to the magnetic characteristics of groundtruthed marine debris, a preliminary hypothesis concerning the magnetic patterning of submerged historic sites within the waters of the New Orleans District could be formulated. The results of this exercise were surprising.

Based on the initial analysis of the contour plots of the five clusters (Figures 16, 17, 18, 19, and 20), it was surmised that two could represent potential shipwreck sites; two clearly comprised sources; and, one could be geologic in nature. These suppositions, discussed below, illustrate the potential pitfalls of anomaly characterization based upon magnetic data alone.

Cluster A (Figure 16) was thought to possess some potential as a shipwreck site. The contour plot showed a clustering of anomalies characteristic of the debris field of a vessel containing only minimal ferrous components. The anomalies seemed to concentrate in an elongated pattern in the east-central zone of the 50,000 m² survey area. This type of clustering has been described in the literature as representing a typical shipwreck pattern (Garrison et al. 1989:II-223).

After an examination of the contour plot, Cluster C (Figure 17) did not appear to be promising as a potential cultural resource. The magnetic field within the survey area appeared to contain numerous small isolated anomalies, but it lacked any apparent focus. The signature of this cluster appeared to be geologic in nature, much as one would expect to see in a disconformity of the bottom caused by dredging. As far as could be determined, however, no activity of this type has taken place in the project area.

Cluster D (Figure 18) was displayed as a single large point source anomaly. Three other brief point source anomalies with a magnetic perturbation >100 gammas also appeared within the block. Cluster D was not characteristic of the model developed for distinguishing shipwrecks from isolated occurrences of anomalous magnetism. In the field, it was speculated that this cluster represented isolated targets lacking in the qualities of National Register significance.

Cluster F (Figure 19) consisted of several isolated monopolar anomalies. Monopolar anomalies generally are indicative of the presence of an elongated body of sufficient length that one pole is near the magnetometer sensor and the opposite pole is removed effectively to infinity (Breiner 1973:20). This type of signature has not been associated with shipwreck material. The Scope of Services called for diver investigation of Cluster F only if time allowed. Owing to adverse weather conditions in March and April, this was not possible. However, it is felt that Cluster F may be eliminated from further consideration based on the patterning of its magnetic signature, and does not represent a National Register-eligible archeological site.

Cluster G (Figure 20) appeared to resemble what has been described as the "classic" shipwreck signature. The contour of Cluster G showed a broad-based anomaly that contained several significant peaks. Lesser anomalies trailed away from the main body in an elongated shape. The contour closely resembled that of the remains of a shrimp trawler identified by Garrison et al. (1989:II-212; Figure II-98) in size, amplitude, shape, and duration (Figure 21). Based upon the magnetic signature and the presence of an anomalous acoustic disconformity (Irion et al. 1993:Figure 9), Cluster G was interpreted as the remains of steel hull wreckage reported by the Coast Guard in 1971 (Irion et al. 1993:55).

Results of Diving Investigations

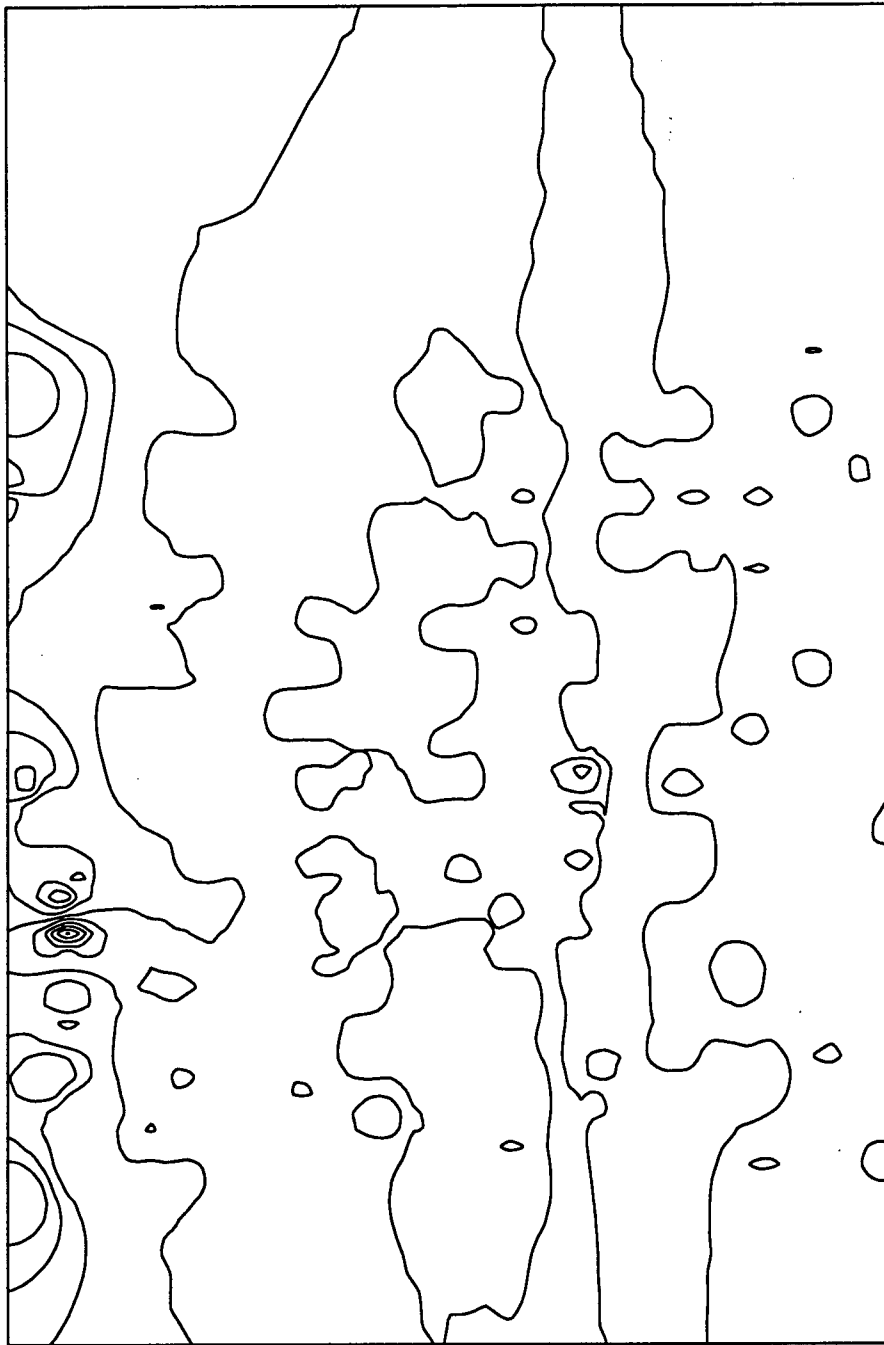
Following the close-interval resurvey of the five target anomaly clusters, two (A and G) were interpreted as potential shipwreck remains. However, the diving investigations of these targets revealed a very different source for these anomalies, which has important ramifications for all submerged cultural resource surveys in the waters of the New Orleans District.

Following the methods outlined in Chapter II, Clusters A, C, D, and G were examined using visual circle search techniques, gradiometer searches, probing, and excavation. Using the gradiometer, it was possible to refine accurately the area of magnetic moment and to concentrate probing and excavation in those areas.



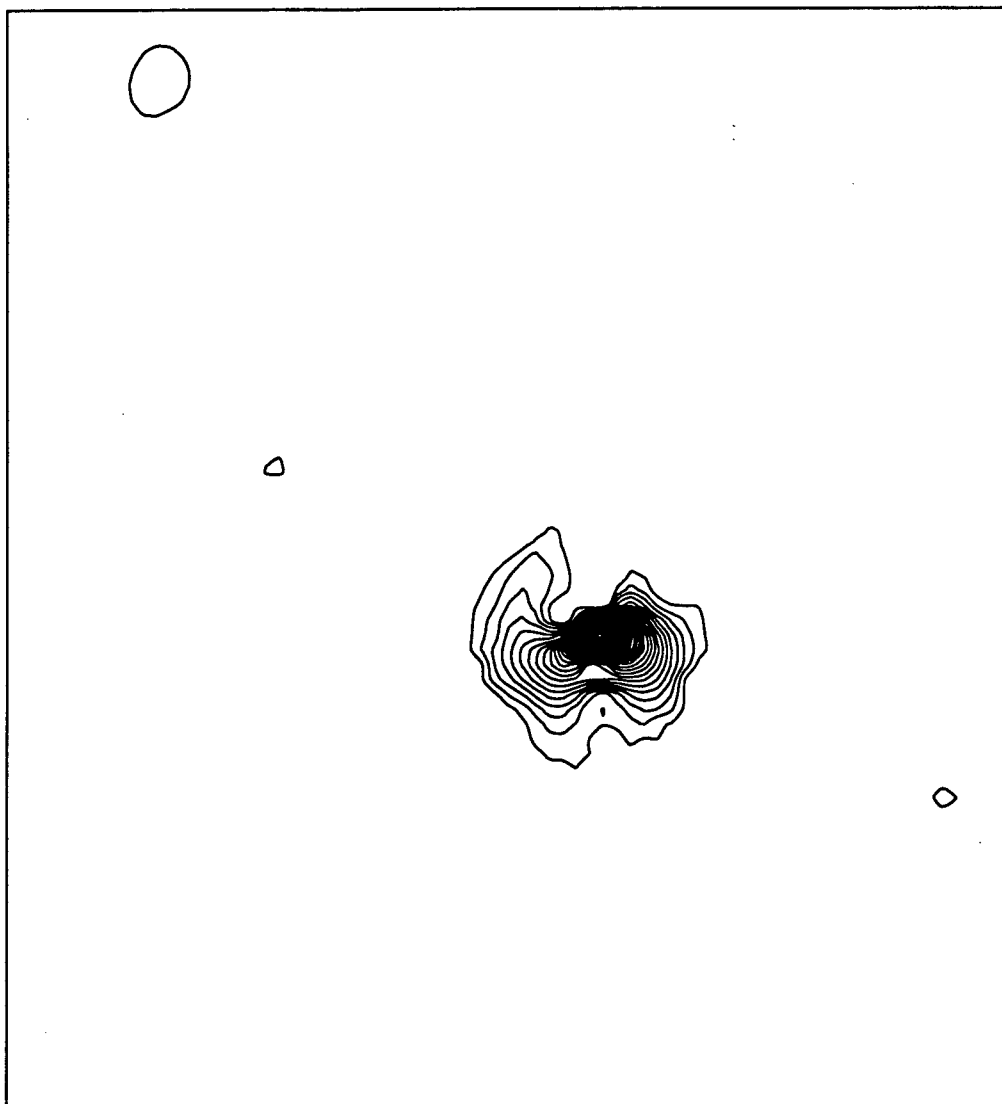
CONTOUR INTERVAL = 20 GAMMAS

Figure 16. Magnetic contour map of Cluster A.



CONTOUR INTERVAL = 10 GAMMAS

Figure 17. Magnetic contour map of Cluster C.



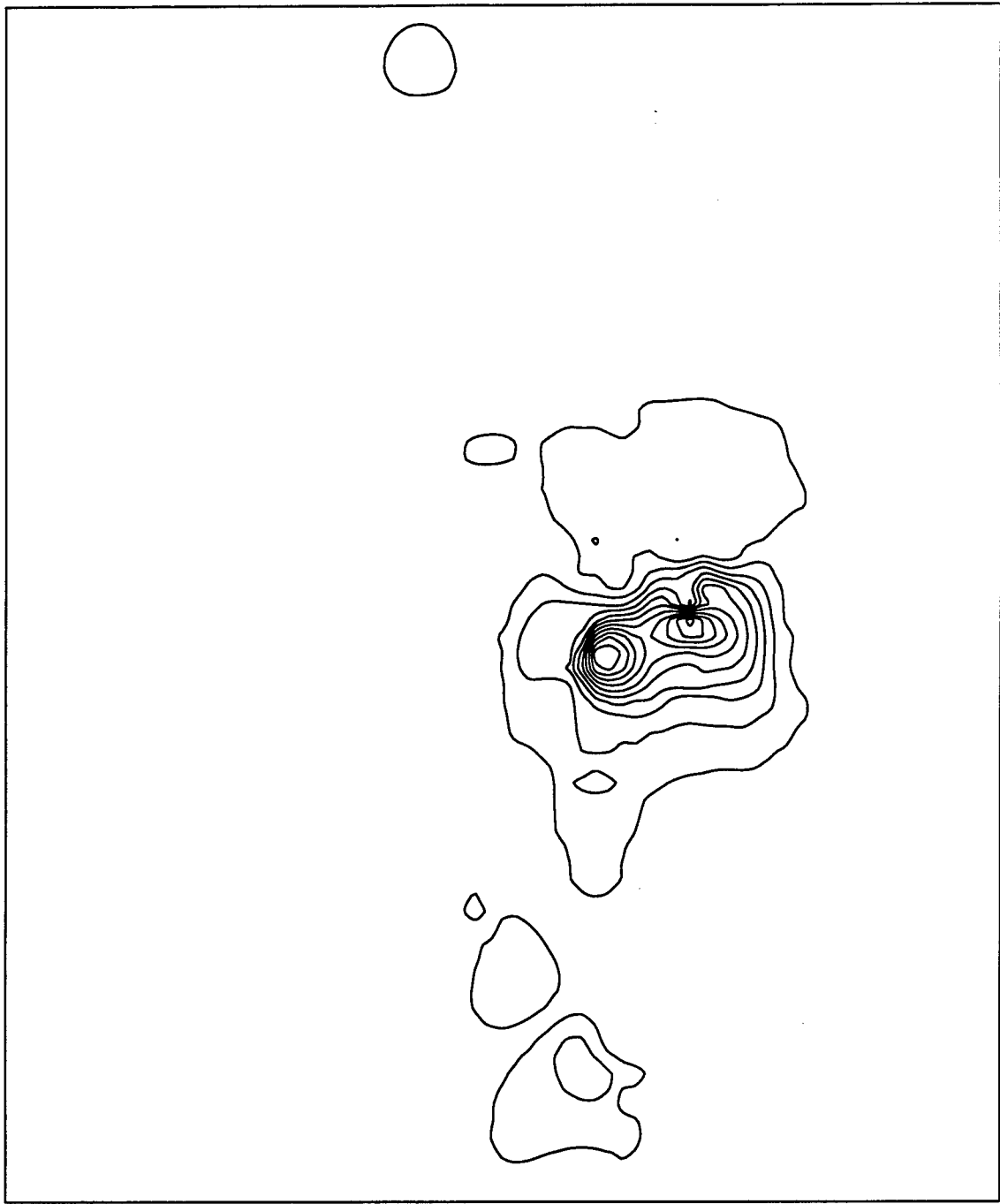
CONTOUR INTERVAL = 100 GAMMAS

Figure 18. Magnetic contour map of Cluster D.



CONTOUR INTERVAL = 10 GAMMAS

Figure 19. Magnetic contour map of Cluster F.



CONTOUR INTERVAL = 100 GAMMAS

Figure 20. Magnetic contour map of Cluster G.

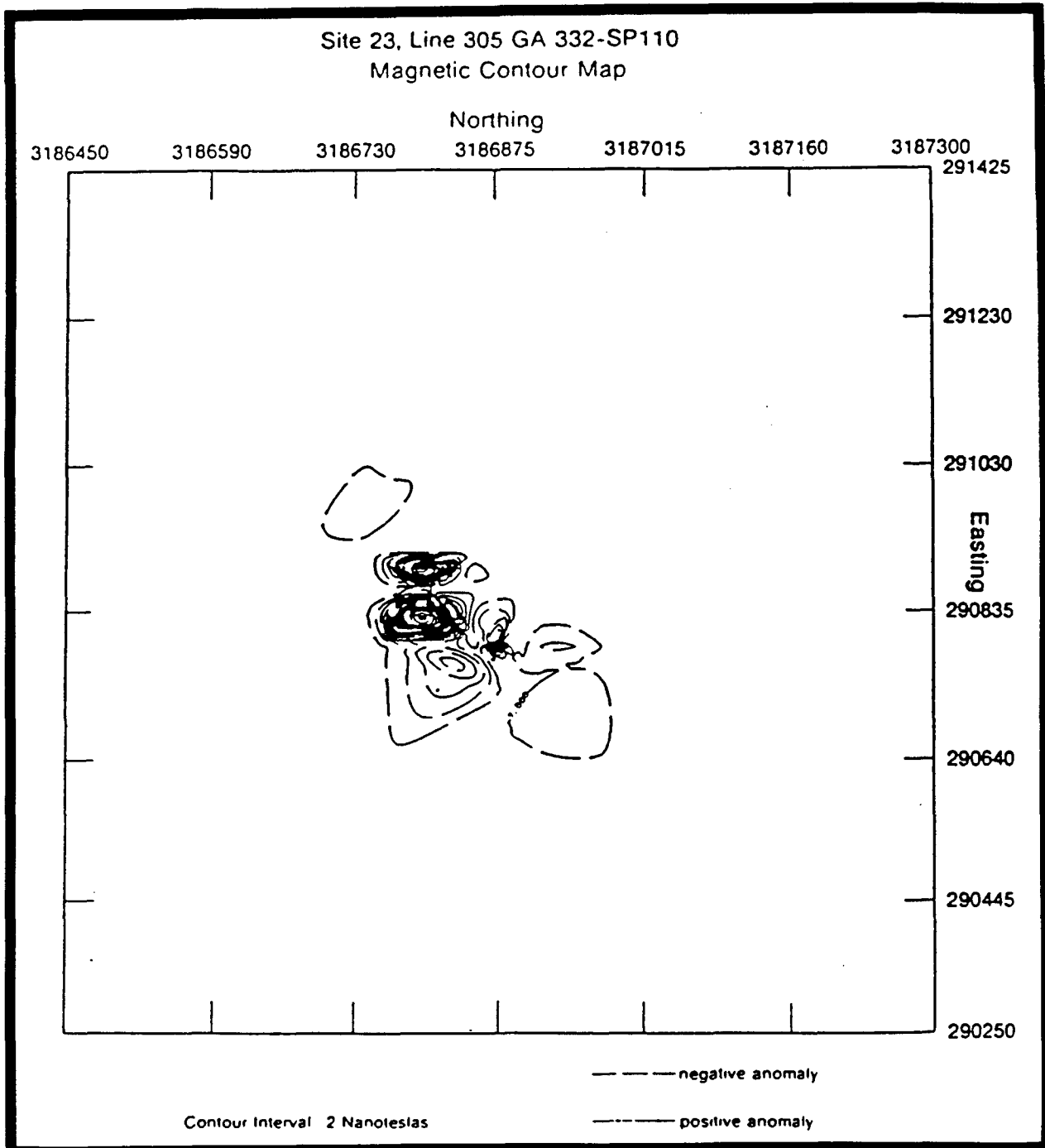


Figure 21. Magnetic contour map showing the wreckage of a shrimp trawler in the Gulf of Mexico (from Garrison et al. 1989:II-212, Figure II-98).

Cluster G was the first cluster to be examined. After the position was refined by the gradiometer, divers probed around the target area. They encountered a solid resistant surface at a depth of 1.4 m (4.5 ft). This surface appeared to extend at a consistent level over an area approximately 3 x 9 m (10 x 30 ft). Excavation of a trench to a depth of 1.8 m (6 ft) revealed that this resistant surface comprised a densely packed natural oyster shell reef. Individual oysters comprising the reef were found in growth positions, and no artifacts were encountered. The gradiometer continued to register strong readings when the sensor was placed in the trench, although no anomalous ferrous objects were encountered. No explanation was immediately apparent for the anomalous magnetism. The oyster shell certainly was not magnetic, and the only other objects encountered in the trench were large, flat platelettes of calcium-cemented sandstone. The anomalies in Cluster G do not appear to have originated from cultural materials; therefore, Cluster G does not constitute a National Register-eligible site.

When similar results were encountered during ground-truthing at Clusters A, C, and D, where submerged cultural resources were absent and only sandstone rocks were observed, it was decided to conduct an experiment to determine what effect these sand concretions had upon the gradiometer. Concretions that had been collected from Clusters A and G were brought in contact with the gradiometer sensor. In each case, the instrument registered an increase in magnetic gradient. Confident now that the sandstone concretions were related to the pockets of anomalous magnetism, it was concluded that Clusters A, C, D, and G represented natural, and not cultural, features for which consideration for National Register eligibility was unnecessary. Therefore, fieldwork ended, and research was initiated to explain this strange phenomenon.

Sources of Anomalous Magnetism

A magnetic anomaly is any mappable departure from the normal magnetic field of the earth. These measurable departures from the normal magnetic field of the earth can be caused either by natural sediments or cultural materials. A natural magnetic anomaly is caused by a body of sediment or bedrock with magnetization that is different from the magnetization of the surrounding sediment or bedrock. Geologists refer to the body of sediment or bedrock as either a "magnetic contrast" or an "anomalous magnetization;" the surrounding and differently magnetized sediment or bedrock is known as "background magnetization." Cultural magnetic anomalies are caused by the presence of ferromagnetic alloys lying upon or buried within the bottom sediments of shelf and sounds. In the Offshore Continental Shelf, the predominant cultural materials are modern ferromagnetic debris, shipwrecks, and components of the infrastructure, associated with the exploitation of natural resources such as pipelines and offshore platforms (Garrison et al. 1989; Machel and Burton 1991a).

The natural magnetization of sediments, either background or anomalous, is called the "natural remnant magnetization" (NRM) and consists of four major components. The detrital remnant magnetization component (DRM) is the magnetization associated with grains of magnetic minerals derived from the erosion of pre-existing volcanic, igneous, metamorphic, and sedimentary rocks. Chemical remnant magnetization (CRM) is the magnetization associated with authogenic minerals created by the precipitation of new mineral grains and the alteration of pre-existing grains. Bacterial-biological remnant magnetization (BRM) is the magnetization associated with magnetic minerals created by aerobic and anaerobic bacteria. Finally, viscous remnant magnetization component (VRM) is the magnetization carried by low-coercivity grains. Except for the VRM, all of these components are capable of producing magnetic contrasts within the sediments that underlie the offshore areas of Louisiana (Machel and Burton 1991a, 1991b).

Detrital Remnant Magnetization

One potential cause of magnetic contrasts within deltaic, barrier island, and marine sediments that may produce magnetic anomalies is detrital remnant magnetization (DRM). Due to its high specific gravity, the mechanical sorting of sand-size material by currents often creates concentrations of heavy, (e.g., magnetic) minerals. Within beach environments, wave action creates concentrations of heavy mineral grains of high specific gravity called "beach concentrates." Within fluvial systems, fluvial processes produce black sands composed of heavy minerals called "placers," which consist of magnetite, ilmenite, hematite, chromite, garnet, zircon, spinel, and other heavy minerals (Greensmith 1986).

However, only minor amounts of magnetic heavy minerals occur within the sand transported by the Mississippi River (Russel 1937). As a result, it is very unlikely that sediment transport processes can generate either placers or beach concentrations large enough to generate significant magnetic anomalies. Of the numerous studies of the sediments that compose the Mississippi River Delta complexes, the Chandeleur Barrier Island Complex, and the Unnamed Marine Complex, not one has reported the occurrence of either placers or beach concentrations large enough to generate magnetic anomalies like Clusters A, C, D, F, and G.

Another source of DRM is fine-grained (less than 0.1 μm in size) magnetic sediment carried in suspension by wind and water currents. This fine-grained magnetic sediment consists of various proportions of minerals such as magnetite, hematite, maghemite, or greigite. Water-borne, fine-grained magnetic sediments accumulate preferentially within natural levee sediments and, to a lesser extent, within upper point sediments because of their fine size. It will be absent from channel and lower and middle point bar sediments. The magnetic contrasts and the associated magnetic anomalies that these sediments create would be related closely to the fluvial and distributary channels in occurrence, shape, and size. Because of their fine size, these magnetic sediments can be transformed easily by diagenetic conditions either into other magnetic materials or into nonmagnetic minerals (Allen 1985; Machel and Burton 1992; Oldfield 1991, 1992).

Wind-borne, fine-grained magnetic sediments were distributed across the Louisiana Coastal Plain. As a result, they accumulated noticeably only on stable, relict geomorphic surfaces, such as the Prairie Terrace, which were exposed for long periods of time (Oldfield 1991). As these sediments accumulated, they were admixed by pedogenic processes with the soils developing within the sediments that were forming the geomorphic surface. Consequently, wind-borne magnetic sediments would become part of the regional background magnetism related to paleosols such as those present at the top of and within the Prairie Complex. Subsequent pedogenic processes very likely transformed a significant amount of this sediment into other minerals that are either magnetic or nonmagnetic (Machel and Burton 1992).

Chemical Remnant Magnetization

Four processes can create chemical remnant magnetization (CRM) and can generate positive magnetic contrasts within the fluvial-deltaic, coastal, and marine sediments that underlie the project area. These processes are pedogenesis; the formation of well-drained swamp environments; dehydration of ferric hydroxides; and, hydrocarbon seepage. Depending upon the process involved, CRM may create either regional background magnetization or magnetic anomalies of differing sizes and shapes.

Pedogenesis may create either regional background magnetization or magnetic contrasts associated with natural levee sediments. The formation of soils processes may produce abundant nodules, cements, and fine-grained sediments within subaerially exposed surfaces, e.g., the Prairie Terrace and natural levees (Machel and Burton 1992; Oldfield 1991, 1992; Schwertmann and Taylor 1977). The

production of iron oxides, such as hematite, magnetite, maghematite, and goethite, creates a CRM component that further enhances the magnetization of regional geomorphic surfaces like the Prairie Terrace and specific landforms like the subaerial natural levees of the Mississippi River and its deltaic distributaries. As previously noted, soil formation processes may produce regional background magnetization, or localized magnetic contrasts and associated magnetic anomalies within a configuration related to the shape and size of an associated channel system.

Like pedogenesis in natural levee deposits, diagenesis within the sediments of well-drained swamp environments produces significant amounts of iron oxides. Iron oxides occur as small 0.5 to 6 mm (0.002 to 0.026 in), fairly well-cemented nodules. These nodules vary in shape from irregular masses to well-rounded clasts. Iron oxides also occur as rims around plant rootlets and as disseminated cement (Coleman 1966). Depending on the mineralogy of these iron oxides, well-drained swamp deposits may form large magnetic contrasts associated with buried river valleys.

Two processes may create CRM within the sands that comprise channel fills and point bar deposits. First, fluvial systems apparently transport ferric hydroxide colloids as dilute suspensions that are absorbed on the surface of clay minerals. After deposition, ferric hydroxides spontaneously dewater to form limonite and, with complete dehydration, hematite. Secondly, the weathering of such iron-rich primary silicates as pyroxenes, amphiboles, and iron chlorites, by either soil or groundwaters, may release iron that eventually will form various iron oxides. Depending on the specific minerals formed, the formation of iron oxides may cause fluvial and distributary sands to acquire a distinct magnetic contrast (Pettijohn et al. 1987).

Hydrocarbon seeps, including biogenic methane, may create CRM produced by diagenetic pyrrhotite and magnetite. Depending on the relative amounts of magnetite, pyrrhotite, or other magnetic minerals produced and the amount of hematite destroyed, the plume of hydrocarbons may create positive, negative, or no magnetic contrast relative to the background magnetization. The type, amount, and stability of magnetic mineral or minerals created by hydrocarbon seeps depend primarily upon Eh, Ph, concentration of hydrogen sulfide, and the concentration of bicarbonate (Machel and Burton 1991a, 1991b).

Bacterial - Biological Remnant Magnetization

Several types of microbes, mainly bacterial, are known to form magnetic minerals that are deposited at their death. So-called "iron bacteria" take up iron compounds leaving iron upon their cell surfaces. This process results in the precipitation and accumulation of various types of iron oxides and hydroxides. Upon the death of the bacteria, these iron compounds are deposited in a variety of soils, lacustrine sediments, and marine deposits. A variety of anaerobic and aerobic bacteria also forms very small grains of magnetite. Upon their death, they contribute very fine-grained magnetite to soils within the shallow to deep marine and brackish to hypersaline lacustrine environments in which they lived. Certain types of these bacteria actually may produce magnetite during the oxidation of hydrocarbons in the anaerobic environment.

There are some bacteria that generate iron sulfides by generating reduced sulfur that later reacts with dissolved iron to form sulfides. Within the Gulf Coastal Plain, numerous studies, (e.g., Posey et al. [1987], Sassen [1980, 1987], Sassen et al. [1988, 1991] and others), have shown that the formation of metallic sulfides is associated with the microbial reduction of sulfate and the oxidation of thermogenic gas and crude oil. In addition, they note that the same geochemical environment that favors the formation of metallic sulfides within salt domes also supports the precipitation of ¹³C-depleted carbonate minerals. Sassen et al. (1991) imply that bacterial methane oxidation and sulfate reduction are responsible for the formation of the carbonates that comprise carbonate buildups and the metallic sulfides associated with them.

Investigations into the Source of Anomalous Magnetism in Breton Sound

Nodules of carbonate-cemented sandstone instead of historic cultural materials were found at two magnetic anomalies with signatures suggestive of historic shipwrecks. The magnetic anomalies lay along the boundary between the open lagoonal inlet and the reworked Mississippi Delta sedimentary environments. Thus, the nodules of carbonate-cemented sandstone occurred within bottom sands that had been reworked frequently by tidal, wave, and geostrophic currents. Also, they had formed within sediments that had accumulated only within the last thousand years.

Samples of these nodules were collected for analysis from two of these clusters, A and G, to determine if these nodules could be the source of the magnetic anomalies. Preliminary testing of the magnetic susceptibility of the nodules clearly demonstrated that their magnetic susceptibility was equivalent to typical carbonated-cemented sandstone, and was insufficient to produce the observed magnetic anomalies (Chad McCabe, personal communication 1993).

Additional analysis was performed to determine if the composition of these nodules could be related to the magnetic anomalies in some way. For petrographic analysis, a commercial company produced petrographic thin sections from three different nodules. During preparation, these were stained partially with Alizarin Red to identify the composition of the carbonate cement. In addition, samples from the same nodules were submitted for stable isotope analysis of the carbon and oxygen that form the carbonate cement.

Results of Thin Sectioning

Cluster A. At Cluster A, carbonated-cemented sandstone nodules were buried beneath the loose sands that comprise the local sea floor. The nodules recovered from the area of the magnetic anomaly were flat cobble-size clasts that measured approximately 0.63 to 1.9 cm (0.25 to 0.75 in) in thickness and 9.5 to 13 cm (3.75 to 5 in) in length. As defined by Folk (1980), they ranged from very bladed to very elongated in shape. Bubbles of gas were observed bleeding from the sea floor bottom within the area from which the nodules were collected.

Two samples of these nodules were collected from Cluster A. Both consist of dark gray (5Y 4/1) and very dark grayish (2.5Y 3/2), carbonate-cemented sandstone of variable hardness; one is very friable and the other well-indurated. In the friable sample, the sand fraction is well-sorted and very fine-grained; in hand specimen, neither bioclasts nor sedimentary structures could be identified. In contrast, the well-indurated sandstone nodule is well-rounded and irregular in shape, and it is has been bored by pelecypods and encrusted by bryozoa and serpulid worms. Many of the borings still contain the shells of the pelecypod that made them. The friable sandstone nodules lack any encrustations or borings. Thin Section B12-MA1 was prepared from a friable sandstone nodule, while Thin Section B12-MA2 was prepared from a well-rounded and indurated sandstone nodule.

Standard petrographic examination of both thin sections indicated that both sandstone nodules from Cluster A consist of calcite-cemented subarkose. This subarkose is composed entirely of a grain-supported framework of very fine-grained, well to moderately well-sorted sand that lacks any silt or clay matrix. Although highly variable in roundness and sphericity, the sand generally is subangular and of moderate sphericity. Thin Section B12-MA2 exhibits distinct cross laminae; similar laminae are absent in Thin Section B12-MA1.

The sandstone nodules from which Thin Sections B12-MA1 and B12-MA2 were prepared are subarkoses as defined by Folk (1980). Straight and wavy quartz are estimated to comprise about 82 to 88 percent of the sand. Potassium feldspars and plagioclase are estimated to comprise about 8 to 10 percent of the sand, and mica averages about 1 percent of the sand. Trace amounts of heavy minerals such as

zircon were observed. Opaques, apparently pyrite and altered pyrite, comprise about 2 percent of the sand in Thin Section BI2-MA1 and about 4 percent of the sand in Thin Section BI2-MA2. Rare, scattered foraminifera tests occur within Thin Section BI2-MA1. Within Thin Section BI2-MA2, the foraminifera are more abundant; unidentifiable fragments of mollusc shells also are present. In both thin sections, these bioclasts had been altered considerably by diagenesis.

Staining of the thin sections with Alizarin Red demonstrated that precipitated calcite cements the sandstone nodules. In Thin Section BI2-MA1, the calcite cement occurs as a thin, often discontinuous, lining that leaves most of the original porosity unfilled. The sandstone nodule is cemented only by very small, occasional, scattered patches of solid cement. In Thin Section BI2-MA2, the sandstone is cemented solidly by precipitated calcite so that its pore space is filled almost completely. The calcite cement has corroded many of the quartz grains and replaced both feldspar and mica grains; it is uncertain whether the calcite cement has replaced pyrite or vice versa.

Cluster G. Carbonate-cemented sandstone nodules also were found at Magnetic Anomaly G, buried beneath the loose sands that comprise the sea floor. The single nodule examined from Cluster G is a cobble-sized clast about 12.7 cm (5 in) long and 3.0 cm (1.2 in) thick. As defined by Folk (1980), it is very elongated in shape. It consists of dark gray (5Y 4/1), carbonate-cemented, indurated sandstone. Its sand fraction is well-sorted and very fine-grained. In hand specimen, no bioclasts, sedimentary structures, encrustations, or borings could be seen. Thin Section BI2-MG1 was prepared from this nodule.

Standard petrographic examination of Thin Section BI2-MG1 indicated that the sandstone nodules from Cluster G consist of calcite-cemented subarkose. This subarkose is composed entirely of a grain-supported framework of fine-grained, well-sorted sand that lacks any silt or clay matrix. Although highly variable in roundness and sphericity, the sand generally is subangular and of moderate sphericity.

The sandstone nodule from which Thin Sections BI2-MG1 was prepared is a subarkose as defined by Folk (1980). Straight and wavy quartz are estimated to comprise about 88 percent of the sand. Potassium feldspars and plagioclase are estimated to comprise about 8 to 10 percent of the sand, and mica averages about 1 percent. Trace amounts of heavy minerals such as zircon were observed. About 1 percent of the sand consists of opaques, most likely pyrite and altered pyrite. Rare bioclasts consist of highly altered foraminifera tests and unidentifiable fragments of mollusca shell.

Alizarin Red staining of the thin section demonstrated that precipitated calcite cements the sandstone nodules. In Thin Section BI2-MG1, the cement consists of a thin lining of microcrystalline calcite that leaves the majority of the original porosity unfilled. A patch of solidly cemented sandstone, in which significant filling of the intergranular porosity occurs, is present within the interior of the nodule. The calcite cement has corroded many of the quartz grains and replaced both feldspar and mica grains. Currently, it is uncertain as to whether the calcite cement has replaced pyrite or vice versa.

Discussion of Thin Sections. Four main observations support the in situ formation of these calcite-cemented sandstone nodules. First, most calcite-cemented sandstone nodules are so poorly cemented that it is unlikely that they would have survived shoreface erosion and reworking. Second, most of these nodules lack the rounding and other physical evidence of having been eroded and transported. Third, most of these nodules lack any evidence of encrusting fauna that would have formed had they been exposed at the surface for any length of time. Finally, the framework grains that compose these nodules reflect the composition of the sediments from which they were recovered. The one nodule recovered from Cluster A that is well-rounded, well-indurated, and encrusted by marine organisms simply may result from localized erosion and reworking of sediments by tidal, wave, or geostrophic currents.

The available evidence indicates that the occurrence of the calcite-cemented sandstones is restricted to small patches on the seafloor. Sedimentologists, biologists, and paleontologists such as Curtis

(1960), Heerden et al. (1985), Parker (1956), Phleger (1955), Shepard (1956), Suter and Penland (1987) and Suter et al. (1988), who have studied the sedimentology and fauna of the eastern Mississippi Delta, have sampled the sea bottoms of Breton Sound, Chandeleur Sound, and the adjacent continental shelf extensively. Despite the large number of bottom and subsurface samples taken by these researchers, none of them has reported the presence of carbonate-cemented nodules similar to those found at the Breton Sound Disposal Area. Given the intensity of sampling within the sounds and shelf of the eastern Mississippi Delta (e.g., Schroeder et al. 1988a), widespread distribution of carbonate-cemented sandstone clasts would have been detected. Therefore, the lack of previous reports concerning the presence of calcite-cemented sandstone nodules implies that they are concentrated within very small patches on the seafloor bottom.

Stable Isotope Testing

Understanding of the potential geological origins of the calcite-cemented sandstones, and of the processes by which they were formed, was enhanced by determining their specific isotopic components. This information was derived from a series of isotopic analysis of the stones, conducted by Paul Aharon of the Louisiana State University Geology Department. Results of these tests are presented below.

Carbon. Carbon (C) is one of the most abundant elements in the universe and the basis for the existence of life on earth. Consequently, it is the most important element in the biosphere, and it also occurs as a significant component within the earth's crust and mantle, the hydrosphere, and atmosphere. In its reduced form, carbon comprises organic compounds that are the basis of life, as well as crude oil, natural gas, and methane (CH₄). In its oxidized state, carbon occurs as carbon dioxide (CO₂) and bicarbonate (HCO₃⁻) in aqueous solution, and as various types of carbonate minerals within the crust of the earth. Carbon has two stable and one radioactive isotopes. The stable isotopes, ¹²C and ¹³C, respectively comprise about 98.89 percent and 1.11 percent of the nonradioactive terrestrial carbon. In addition, radioactive ¹⁴C is naturally occurring due to its formation by the interaction between ¹⁴N and cosmic rays (Faure 1986).

The stable isotopes of carbon are fractionated by a variety of natural processes. Isotope fractionation is a consequence of the fact that certain thermodynamic properties of molecules depend upon, and are sensitive to, the masses of the atoms of which they are composed. Consequently, isotopic fractionation occurs during several different types of chemical reactions and physical processes. These include: (1) isotopic exchange reactions involving the redistribution of the isotopes of an element; (2) unidirectional reactions in which reaction rates depend upon isotopic compositions; and, (3) various physical processes such as evaporation and condensation, melting and condensation, and dissolution and precipitation. As a result, the isotopic abundance of stable carbon isotopes varies by about 11 percent within the various types of organic compounds and minerals containing carbon. Because of isotopic fractionation, the relative degree of either enrichment or depletion of ¹³C relative to ¹²C within organic compounds and carbonate minerals give important clues concerning the sources of carbon and the processes that created these materials (Faure 1986).

The isotopic composition of carbon-bearing organic compounds and carbonate minerals is expressed in terms of delta notation. This notation is a measure of the degree of either enrichment or depletion of ¹³C relative to ¹²C as compared to a known standard. The parameter is defined as:

$$\delta^{13}\text{C} = \frac{[(^{13}\text{C}/^{12}\text{C})_{\text{sample}} - (^{13}\text{C}/^{12}\text{C})_{\text{standard}}]}{(^{13}\text{C}/^{12}\text{C})_{\text{standard}}} \times 10^3$$

Consequently, positive values of $\delta^{13}\text{C}$ represent enrichment of a sample in ^{13}C , whereas negative values of $\delta^{13}\text{C}$ imply depletion of a sample in ^{13}C , relative to some reference standard (Faure 1986).

Arbitrarily designated carbon-bearing compounds generally are used as reference standards for carbonate isotopes. For carbonates, the typical reference standard consists of carbon dioxide (CO_2) gas. Carbon dioxide (CO_2) gas is obtained by reacting belemnites (*Belemnitella americana*) from the Pee Dee Formation of South Carolina with 100 percent phosphoric acid at 25°C . This is the PDB (Pee Dee Belemnite) standard of the University of Chicago. Another standard, used by many to determine the relative isotopic composition of materials is the National Bureau of Standard No. 20 Reference Standard (NBS-20). This standard consists of Solenhofen Limestone from Germany (Craig 1957; Faure 1986).

Oxygen. Oxygen (O) is the most abundant element in the crust of Earth. It is an important rock-forming element for silicates, carbonates, oxides, and other minerals. It also is the principle component of water and a significant component of some organic compounds. Oxygen has three stable isotopes which are ^{16}O , ^{17}O , and ^{18}O . Their approximate abundances are $^{16}\text{O} = 99.36$ per cent, $^{17}\text{O} = 0.0375$ per cent, and $^{18}\text{O} = 0.1195$ per cent. Like the carbon isotopes, the oxygen isotopes are fractionated by specific chemical, physical, and biological processes. In Holocene carbonates, oxygen isotopes are indicative of the temperature at which minerals precipitate and the source of the water, e.g., fresh, brackish, or marine, from which they precipitate (Faure 1986).

The isotopic composition of oxide and carbonate minerals and water also is expressed in terms of delta notation. This notation is a measure of the degree of either enrichment or depletion of ^{18}O relative to ^{16}O as compared to a known standard. The parameter is defined as:

$$\frac{[(^{18}\text{O}/^{16}\text{O})_{\text{sample}} - (^{18}\text{O}/^{16}\text{O})_{\text{standard}}]}{(^{18}\text{O}/^{16}\text{O})_{\text{standard}}} \times 10^3$$

Consequently, positive values of $\delta^{18}\text{O}$ represent enrichment of a sample in ^{18}O , whereas negative values of $\delta^{18}\text{O}$ imply depletion of a sample in ^{18}O , relative to some reference standard (Faure 1986).

The reference standard used for oxygen isotopes depends upon the material analyzed. The isotopic composition of oxygen within water generally is reported in terms of differences of $^{18}\text{O}/^{16}\text{O}$ ratio relative to a standard called "SMOW," which stands for Standard Mean Ocean Water. This standard, NBS-1, consists of a large volume of distilled water distributed by the National Bureau of Standards. The oxygen isotope standard for carbonates is the PDB (Pee Dee Belemnite) standard. The PDB standard consists of carbon dioxide (CO_2) gas produced by the reaction of 100 percent phosphoric acid with Cretaceous belemnites (*Belemnitella americana*) from the Pee Dee Formation of South Carolina at 25°C . For carbonates, a sample is analyzed as carbon dioxide (CO_2) gas using mass spectrometers equipped with double collectors. Carbonate samples usually are reacted with 100 percent phosphoric acid at 25°C to produce the carbon dioxide gas. The relation between $\delta^{18}\text{OSMOW}$ and $\delta^{18}\text{OPDB}$ is given by the equation: $\delta^{18}\text{OSMOW} = (1.03086) (\delta^{18}\text{OPDB}) + 30.86$ (Faure 1986).

Preliminary analysis of the calcite-cemented sandstone nodules from the Breton Sound area suggests that they should be depleted significantly in ^{13}C , but have $\delta^{18}\text{O}$ values typical of the mean seawater for the water temperature and depth of the survey area. Unfortunately, definitive analysis of the stable isotopes of carbon and oxygen are still in progress. However, when these analyses are completed, the association of the magnetic anomalies with methane seeps will be tested firmly and the source of the methane possibly will be determined.

The Formation of Carbonate-Cemented Sediments in the Northern Gulf of Mexico

The calcite-cemented sandstones found in association with Clusters A, C, D, F, and G are atypical of siliciclastic, particularly deltaic, depositional environments (Coleman 1982). Early lithification of carbonate sediments such as oolites, intraclasts, bioclasts, pellets, and micrite, by carbonate minerals of the calcite, aragonite, and dolomite groups, is typical of and well-studied for many carbonate depositional environments. However, the early lithification of siliciclastic sediments by carbonate minerals is much rarer and less well-documented. The paucity of siliciclastics with early carbonate cements associated with the modern sea floor, such as the sandstones found in the project area, results from the facts that: (1) the pore and marine waters associated with clastic environments generally are undersaturated in respect to carbonate minerals, and (2) the sedimentation rates of clastic environments overwhelm the production of carbonate cements by precipitation and the production of carbonate by organisms (Roberts et al. 1987; Weiss and Wilkinson 1988).

Holocene carbonate-cemented siliciclastic sediments have been reported from four regions within the northern and northwestern Gulf of Mexico. Sandy limestones and carbonate-cemented shelly sandstones have been described by Weiss and Wilkinson (1988) from the Inner Shelf offshore of the Texas Gulf Coast. Carbonate-cemented sediments and nonbiologically precipitated carbonate buildups are common to the western Louisiana Continental Slope (Roberts et al. 1987). Kocurko (1984) and others have studied pebble and cobble-sized clasts of carbonate-cemented siliciclastic sediments associated with the barrier islands of South Louisiana. Schroeder et al. (1988a) described carbonate-cemented sediments on the Florida-Alabama Shelf that occur as hardbottoms consisting of carbonate buildups and extensive areas covered by rock rubble. By examining the four processes by which siliciclastic sediments form in the Northern Gulf of Mexico, it will be demonstrated that sediments in the project area are unique. The formation of these sediments can only be the result of nonbiologic carbonates.

Central Texas Inner Shelf

The carbonate-cemented sediments found within the Central Texas Inner Shelf and along the Central Texas Coast consist of pebbles and cobbles of shelly sandstones to sandy limestones, called "sandy biosparites," and shelly limestones, called "shelly biomicrites." They occur as prominent components of beach sediments along the rapidly eroding deltaic headlands of the Texas coastline, and as gravel scattered across over 3,000 square km (1160 square mi) of the adjacent Inner Shelf. This gravel covers the Inner Texas Shelf from the Rio Grande to Sabine Pass and from the modern shoreline to 15 to 20 km (49 to 66 mi) offshore (Weiss and Wilkinson 1988).

These shelly sandstones to sandy and shelly limestones occur as well-rounded, very bladed pebbles and cobbles. The gravel consists of very bladed to very elongated clasts that range in size from a few millimeters to a few centimeters in length. They typically have a maximum diameter of 20 to 40 cm (8 to 16 in) and a thickness of 1 to 10 cm (0.4 to 3.9 in). Almost all of this gravel has been bored by clams, sponges, and other marine invertebrates and encrusted by other marine invertebrates, such as barnacles, bryozoans, and oysters. Based on petrographic, trace element, and oxygen isotope data, these gravels have been classified into two distinct lithologic groups, sandy biosparites and shelly biomicrites (Weiss and Wilkinson 1988).

The sandy biosparites consist of variable proportions of quartz sand, silt, shells, and shell debris cemented by a precipitated low-magnesium calcite cement. The shells associated with the sandy biosparites consist of mixed marine estuarine to nonmarine molluscan fauna whose aragonitic shell material either has been dissolved or calcitized. Some of the micritic cement have very distinct caliche textures. Sandy biosparites have average stable isotope values of -3.11 per mil $\delta^{18}\text{O}$ (PDB) and -4.21 per mil $\delta^{13}\text{C}$ (PDB). Trace elements, stable isotopes, caliche textures, mixed and nonmarine shell fauna, and

calcitization of aragonitic shell material all argue that the cementation occurred in response to ground water movement during the subaerial exposure of the central Texas Inner Shelf during the Late Wisconsinan lowstand (Weiss and Wilkinson 1988).

The shelly biomicrites consist of well-preserved molluscan debris encased in a sandy micritic matrix. The shells associated with the shelly biomicrites consist of mixed marine estuarine to nonmarine molluscan fauna. The micritic matrix is somewhat pelleted and contains intraclasts of micrite containing greater or lesser amounts of shell debris or fine sand. The sediment is cemented by high-magnesium calcite. Shelly biomicrites have average stable isotope values of 0.01 per mil $\delta^{18}\text{O}$ (PDB) and -13.08 per mil $\delta^{13}\text{C}$ (PDB). Trace elements, stable isotopes, pelleted textures, mixed and nonmarine shell faunas, and intraclasts all argued that the shelly biomicrites consist of inner shelf shell lags formed by the erosion of Pleistocene fluvial-deltaic deposits, admixed with high-magnesium calcite mud, and cemented by ^{13}C -depleted calcite within anoxic bottom muds at some relatively shallow depth below the shelf bottom (Weiss and Wilkinson 1988). Because of the circumstances needed to create them, this type of shelly biomicrite can form only within wave-dominated continental shelves, e.g., Texas Inner Shelf, characterized by low sedimentation rates.

Neither the sandy biosparites nor the shelly biomicrites are associated with iron sulfides, iron sulfates, and magnetic minerals. The detailed petrographic analysis of these rocks by Weiss and Wilkinson (1988) contains no reference to pyrite, hematite, pyrrhotite, or any other magnetic iron-bearing mineral. Because of the surficial nature of the processes that formed these rocks, it is unlikely that they would be associated with any significant magnetic anomalies. Furthermore, such an association is unlikely because the highly rounded, bioeroded, and encrusted nature of these nodules indicates that they have been eroded and dispersed from their point of origin.

Louisiana Continental Slope

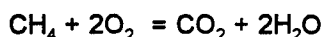
Recent research within the Louisiana Continental Slope has revealed expansive areas of carbonate-rich and frequently lithified bottom sediments, as well as enormous reeflike buildups composed of nonbiologic carbonates. The carbonate-rich sediments often are lithified sufficiently to form indurated seafloors called hardbottoms. The carbonate buildups are mounds composed of solid, nonbiologically precipitated high-magnesium calcite and dolomite. They range in relief from a few meters to over 20 m (a few feet to over 65 ft) above the adjacent bottom. Details concerning the petrography of these deposits have been published in a number of papers, e.g., Roberts et al. (1987, 1988, 1989). The shallower buildups may be capped by relict Pleistocene reefs. Carbonate buildups typically are associated with the crests and flanks of diapirs. They often form lineaments with mud vents and depressions that appear to be associated with faults (Roberts et al. 1989).

Unfortunately, specific details concerning the occurrence and petrography of the carbonate-rich sediments and associated hardgrounds are lacking in the published literature. From the Louisiana Continental Shelf, Paul Aharon (personal communication, 1993) has recovered calcite-cemented sandstones and sandstone nodules similar and identical to the ones recovered from the project area. Unfortunately, comparative data for these sandstones are lacking.

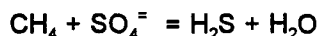
These carbonate-rich sediments and carbonate buildups are created by the seepage of either one or a combination of different types of hydrocarbons, including biogenic methane, thermogenic methane, natural gas, and crude oil. Biogenic methane is formed by the decay of woody, algal, and other botanical matter buried within sediments. Thermogenic methane is formed by the thermal degradation of organic matter at depths of hundreds of meters (Roberts et al. 1988, 1989).

The presence of hydrocarbons within sediments can cause the precipitation of carbonate cements by means of a complex process. The oxidation of methane and degradation of crude oil within these sediments increases the alkalinity of the pore fluids. The increase in alkalinity creates exceptionally high $p\text{CO}_2$ in the interstitial pore fluid of the gas-charged sediment which may subsequently result in carbonate precipitation. This process has been discussed in detail by a number of studies, namely Iversen and Jorgensen (1985); Suess and Whiticar (1989); Whiticar and Faber (1986); and, Jorgensen (1992).

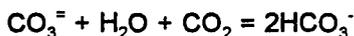
Methane oxidation is believed to occur in either the anoxic environments generated by sulfate-reducing bacteria or in oxic environments as a result of the activities of aerobic bacteria. Carbon dioxide is generated by the reaction:



The carbon dioxide, thus created, dissolves within the water to form bicarbonate ions (2HCO_3^-) that can be incorporated into the carbonate cements. Within anoxic environments, the action of reducing bacteria may cause the precipitation of carbonate cements by causing the reaction (Jorgensen 1992; Suess and Whiticar 1989; Whiticar and Faber 1986):



and then:



Through these processes, the extremely $\delta^{13}\text{C}$ depleted carbon isotopes characteristic of biogenic methane, thermogenic methane, or crude oil are inherited, in part, by the carbonate cements that their oxidation generates. As a result, methane-derived carbonates are remarkably depleted in ^{13}C . Carbonates associated with the oxidation of biogenic methane can produce carbonate cements with $\delta^{13}\text{C}$ values typically ranging from -45 to -55 per mil (PDB) and as much as -70 per mil PDB. The degradation of crude oil will produce $\delta^{13}\text{C}$ values of around -25 to -35 per mil (PDB). The $\delta^{13}\text{C}$ values for thermogenic gas will be intermediate between biogenic methane and crude oil. The actual $\delta^{13}\text{C}$ per mil values for carbonates and carbonate cements can be larger because of the admixture of contributions of bicarbonate from either methane or crude oil with bicarbonate from less ^{13}C -depleted inorganic sources within the interstitial pore water (Jorgensen 1992; Kocurko 1984; Roberts et al. 1989).

Preliminary analysis of the calcite-cemented sandstone nodules from the Breton Sound area suggests that they should be depleted significantly in ^{13}C , but should have ^{18}O per mil values typical of the mean seawater for the water temperature and depth of the survey area. Unfortunately, definitive analyses of the stable isotopes of carbon and oxygen are still in progress. When these analyses are completed, the association of the magnetic anomalies with methane seeps will be tested firmly, and the source of the methane possibly will be established.

In theory, (Machel and Burton 1991a), the same hydrocarbon seeps that form ^{13}C depleted carbonate cements and buildups have the potential to form magnetic anomalies. However, within the Gulf of Mexico almost nothing has been published concerning the association, or lack of association, between magnetic minerals and magnetic anomalies and carbonate buildups and cements associated with hydrocarbons seeps. The paucity of published research may reflect either a lack of such studies or the proprietary nature of studies that are associated with the discovery of commercial hydrocarbon deposits. However, ongoing work by Paul Aharon (personal communication 1993) and Fu Baoshun (personal communication 1993) has demonstrated that carbonate-cemented sediments and carbonate buildups associated with hydrocarbon seeps often are associated with magnetic anomalies. In addition, they have found that the carbonate-cemented sediments and carbonate buildups typically contain various iron sulfides and sulfates. Some of the samples from these deposits showed moderate magnetic susceptibility that

disappeared upon exposure to air and dehydration. This very phenomenon was observed in the samples recovered from the project area. Unfortunately, the lack of published data concerning sediments underlying surface buildups and deposits leaves the exact source of the magnetic anomalies open to question (Paul Aharon, personal communication 1993; Fu Baoshun, personal communication 1993).

Exposures of the Miocene Lucina Limestone within Italy provide revealing cross-sections of carbonate buildups formed by hydrocarbon seeps. Like the carbonate buildups in the Gulf of Mexico, these isotopically depleted carbonates contain abundant iron sulfides. These exposures exhibit the presence of concentrated accumulations of iron sulfides lying a few meters beneath the buildups (Aharon et al. 1993; Paul Aharon, personal communication 1993). Analogous accumulations of iron sulfides, e.g., pyrrhotite, underlying areas of carbonate precipitation caused by hydrocarbon seepage in the Gulf of Mexico, could produce the magnetic anomalies observed to be associated with them.

Louisiana Barrier Islands

The carbonate-cemented sediments found along the Louisiana Barrier Islands consist of crusts and sandstone nodules associated with barrier islands along the north and northwestern coast of the Gulf of Mexico. The crusts have been reported from the Chandeleur Island System, from Elmer's Island in South Louisiana, and from Mustang and Padre Islands along the Texas Coast (Kocurko 1984; Morgan and Treadwell 1954; Roberts and Whelan 1975). The nodules typically occur as a crust associated with algal mats that cover supratidal flats lying between marshes and dunes on the leeward side of barrier islands. These crusts are a thin layer of sand and silt cemented by high-magnesium calcite. Individual layers, which can form in about two months, typically are about 5 mm (0.2 in) thick. If a number of layers are superimposed on one another, the crust can be as thick as 30 mm (1.2 in). They frequently exhibit various types of sedimentary structures such as cross-lamination, root casts, and burrows, that are possessed by the sands in which they form. The cements that form the surficial crust consist of high-magnesium calcite with about 35 to 50 mole percent magnesium and minor amounts of aragonite. They have average stable isotope values of 0.80 per mil $\delta^{18}\text{O}$ (PDB) and -1.00 per mil $\delta^{13}\text{C}$ (PDB). The high magnesium content and stable isotope values indicate that evaporation and algal growth control the formation of the crusts (Kocurko 1984).

After burial, a number of changes occur within the carbonate crusts. First, the aragonite disappears, and the dolomite appears as an accessory mineral. The amount of magnesium present also drops to about 17 to 33 mole percent Mg. Finally, the crusts become depleted in ^{18}O and ^{13}C to about -0.06 per mil $\delta^{18}\text{O}$ (PDB) and -4.00 per mil $\delta^{13}\text{C}$ (PDB). These changes result from the dissolution and reprecipitation of carbonate in an environment from which the influence of active algal mat growth, the presence of decaying organic matter, and the influence of marine waters have been removed (Kocurko 1984).

The nodules consist of well-indurated calcite-cemented sandstone. Morgan and Treadwell (1954) reported that the occurrence of nodules ranged in size from small pebbles to small boulders. However, all of the nodules observed by later investigators ranged in size from pebbles to cobbles. These nodules vary greatly in shape from contorted, irregular masses and donut shaped pieces, to rounded, moderately spherical pebbles or cobbles. Typically, this type of carbonate-cemented sandstone nodule is "slab shaped" flattened parallel to the bedding of the sand bed in which it formed. These nodules exhibit small-scale cross-lamination, burrows, and root casts, and contain inclusions of clay balls, intraclasts, numerous pieces of wood, or other organic materials inherited from the original sand bed (Kocurko 1984; Roberts and Whelan 1975).

These nodules contain varying proportions of sand, silt, and shell debris cemented by calcitic micrite and microspar. The sediment cemented to form these nodules consists typically of either well-sorted fine sand, very fine sand, or silt. Less commonly, the sediment consists of poorly sorted molluscan debris

admixed with fine sand. The sandstone nodules from the Chandeleur Islands are cemented by calcite that occasionally is associated with aragonite; these nodules are depleted significantly in ^{13}C with values that range from -24.1 to -40.0 per mil $\delta^{13}\text{C}$ (NSB-20). The sandstone nodules from Elmer's Island are cemented by calcite, which is associated with minor amounts of dolomite; they have average stable isotope values of 0.60 per mil $\delta^{18}\text{O}$ (PDB) and -37.0 per mil $\delta^{13}\text{C}$ (PDB). The carbon isotope values range from -25.9 to -48.1 per mil $\delta^{13}\text{C}$ (PDB). Unfortunately, little if any information is given about the presence or absence of iron sulfides and sulfates in these rocks (Kocurko 1984; Roberts and Whelan 1975).

Stable isotopes of carbon and oxygen demonstrate uniform origin for the carbonate cements of these sandstone nodules. Their oxygen isotope values indicate that the carbonate cement precipitated in a uniform, marine pore fluid. The severely depleted carbon isotope values are characteristic of methane-derived carbonate cements. Because of the extreme depletion of ^{13}C , biogenic methane is the methane associated with the formation of these cements. The apparently uniform dispersion of carbonate nodules throughout the sediments of the Chandeleur Island Complex and other barrier islands further indicates that ubiquitous biogenic methane, not localized plumes of thermogenic methane, initiated the formation of these carbonate cements (Kocurko 1984; Roberts and Whelan 1975).

Alabama - Florida Shelf

Extensive hardbottoms composed of carbonate-cemented sediments are common on the seafloor of the continental shelf off of Alabama and northwest Florida. Three types of carbonate-cemented sediments have been identified within these hardgrounds: (1) shelly sandstone; (2) massive to nodular siderite-cemented sandstones and mudstones; and, (3) calcite-cemented calcirudite. The shelly sandstones occur as rubble fields in areas such as the Southeast Banks area and rock outcrops, and the Southwest Rock area. The siderite-cemented sandstones and mudstones occur within the rubble fields at the 17 Fathom and Southwest Rock areas (Parker et al. 1993; Schroeder 1988a, 1988b).

The rubble fields that are composed of shelly sandstones and siderite-cemented sediments consist of scattered, rounded, and abraded pieces and irregular slabs. They vary in size from small pebbles to boulders, ranging from 1 to 2 m (3 to 6 ft) in diameter. The rocks also range in color from buff to yellowish gray, dark gray, and dark brown. Many of the sandstones are well-indurated, whereas shelly sandstones and coquina are friable. These rocks are bored extensively by the bivalve *Lithophaga* and the sponge *Clinoa*. Abundant encrusting epifauna, e.g., soft corals, barnacles, bryozoa, sponges, and serpulid worms, cover the larger slabs, although the smaller, abraded rocks lack encrusting organisms (Parker et al. 1993; Schroeder et al. 1988a, 1988b).

Two rock outcrops are associated with the rubble fields at the Southwest Rock area about 17.5 km (10.5 mi) south of Dauphin Island at water depths of 20 to 22 m (66 to 72 ft). One rock outcrop measures about 7 to 9 m (23 to 30 ft) across and 1 to 1.5 m (3 to 5 ft) high; the second outcrop is about 1.5 to 3.5 m (5 to 11.5 ft) across. The rocks consist of a well-indurated, medium gray, shelly sandstone (Schroeder et al. 1988a, 1988b).

The shelly sandstones comprise submature, siliciclastic sandstones containing variable amounts of shell debris. They include a full spectrum of rock types ranging from sandy biosparites to either foraminiferal and ostracodal sandstones or quartzose sandstones. Mollusk shells, foraminifera tests, and echinoderm fragments commonly comprise the shell debris. Associated with the shelly sandstone are abraded and bored fossil shells, such as, oyster (*Crassostrea virginia*) and hardshell clam (*Mercenaria mercenaria*), characteristic of estuarine environments. The stable isotope values of these carbonate-cemented sediments range from -25 to -45 per mil $\delta^{13}\text{C}$ (PDB) (Parker et al. 1993; Schroeder et al. 1988b).

Siderite-cemented sandstone and mudstone rock rubble consist of clastic sediments cemented by siderite. These rocks are well-indurated and dark gray with a rusty-brown exterior rind. Their sedimentary structures either are lacking or indicative of intensive bioturbation. Unlike the shelly sandstones, pyrite is present as the nuclei of some of the siderite grains. The stable isotope values of these siderite-cemented sediments are about -12 per mil $\delta^{13}\text{C}$ (PDB) (Parker et al. 1993; Schroeder et al. 1988b).

Recent studies by Shroeder et al. (1988b) and Howard (1990) indicate that the carbonate- and siderite-cemented siliciclastics of the Alabama-Florida shelf are a transgressive lag derived from the destruction of Late Pleistocene and Early Holocene deposits. The highly fragmented and rounded nature of these rocks suggests that they have been reworked by shoreface erosion during the current transgression. The presence of abundant relict shells of oysters (*Crassostrea virginia*) and hardshell clams (*Mercenaria mercenaria*) demonstrates the former presence of bay, sound, or lagoon deposits associated with these rocks. The severe depletion of ^{13}C within the carbonate cements and other evidence indicates that they formed within shallow subsurface sediments heavily charged with biogenic methane (Howard 1990; Parker et al. 1993).

Hypothesis

From the comparison of the calcite-cemented sandstones nodules found in the project area with the known occurrences of carbonate-cemented siliciclastics, it is proposed that these nodules consist of local shelf sands cemented in place by calcite cements. Because they are cemented by methane-derived calcite and lack caliche-like cements, the nodules from both magnetic anomalies clearly differ in origin from the shelly sandstones to sandy limestones of the Inner Texas Coast. As previously noted, the poorly cemented, often friable nature of these nodules at both magnetic anomalies indicate that these nodules have not been reworked from older deltaic, lagoonal, or fluvial sediments as have carbonate nodules found within barrier islands of the South and Eastern Louisiana coast. The lack of primary, carbonate mud clearly differentiates these nodules from the shelly limestones that have formed in place within the Inner Texas Coast. Because of the available data and associated magnetic anomalies, it is proposed that these nodules are shallow water examples of the carbonate-cemented and carbonate-enriched sediments that have been studied extensively within the Louisiana Continental Shelf.

Summary of the Origin of Magnetic Anomalies in the Project Area

Since it was not feasible to collect core samples of sediments from the magnetic contrasts responsible for creating magnetic anomalies in the project area, an absolutely precise origin for these anomalies cannot be determined. However, because of their size, shape, and apparent association with ^{13}C -depleted carbonate-cemented sediments, it is hypothesized that the magnetic anomalies are caused by Chemical Remnant Magnetization and Bacterial-Biological Remnant Magnetization created by localized plumes of methane. Although unknown in composition, the gas that was observed to be bubbling actively from the seafloor presents additional evidence for the association of these magnetic anomalies with methane plumes generated within the sediments underlying the seafloor. If such methane seeps are present, then the most likely source for the associated magnetic anomalies would be the presence of either magnetite or pyrrhotite with minor amounts of other magnetic minerals produced within the nearsurface portion of a methane plume (Machel and Burton 1991a, 1991b).

At this time, it is unclear whether these plumes are formed by thermogenic methane escaping from oil or gas accumulations within the underlying Miocene strata, or by biogenic methane derived from the decomposition of organic matter within underlying deltaic sediments. The presence of nearby major gas fields (Figure 8) demonstrates that the Miocene strata underlying both magnetic anomalies contain thermogenic methane and natural gas. However, the presence of a major deltaic lobe underlying both

Breton Island and the magnetic anomalies also suggests that biogenic methane leaking from these deltaic sediments could be another likely cause of the hydrocarbon seeps. In either case, hundreds, if not thousands, of magnetic anomalies similar to those investigated in the project area should exist within the Louisiana Continental Shelf; theoretically, magnetic anomalies of similar origin also may occur within Lake Pontchartrain and elsewhere within the boundaries of the New Orleans District.

Presently, no regional maps exist that depict the distribution and types of magnetic anomalies on the scale of Magnetic Clusters A through G. Regional maps of magnetic anomalies within the Gulf of Mexico have been produced; however, these anomalies reflect only those magnetic contrasts related to large-scale differences between lithologic units and geologic structures within the thick wedge of Cenozoic and Mesozoic deposits and the underlying crust. The precise distribution and types of magnetic anomalies, such as those investigated in Breton Sound, presently is unknown.

According to Robert Floyd (personal communication 1993), a recognized expert on magnetic survey of the Outer Continental Shelf, hundreds of magnetic anomalies similar to those investigated in the project area occur within the Chandeleur Sound, Breton Sound, and Main Pass Lease Areas. These have been found to produce a magnetic signature that is virtually indistinguishable from that produced by an historic shipwreck. The data concerning these anomalies can be found in hazard survey reports for federal lease areas within the Louisiana Shelf. In particular, the reports concerning Chandeleur Area Blocks 9, 12, 13, 23, 42, and 43 contain detailed analyses of materials associated with similar magnetic anomalies (Robert Floyd, personal communication 1993). Unfortunately, because of their proprietary nature, permission to examine and cite any of these reports has not been obtained.

A different source of anomalous magnetism has been observed by Ted Hampton (personal communication 1993) and John Greene (personal communication 1993) within magnetic surveys from the Louisiana Continental Shelf. This type of magnetic perturbation consists either of long meandering anomalies associated with fluvial channels, or monopolar low-amplitude anomalies associated with deltaic distributary channels. These anomalies may represent CRM associated with iron oxides present within either natural levee or point bar deposits. The very common occurrence of natural gas of unspecified origin within the channel and point bar sands (Anderson and Bryant 1990; Suter 1986) implies that methane-derived magnetic minerals such as magnetite and pyrrhotite also may have formed within these channels and may be responsible for these anomalies.

CHAPTER IV

THE ARCHEOLOGICAL SIGNIFICANCE OF CHEMICAL AND BIOLOGICAL REMNANT MAGNETISM

The Origin of Magnetic Anomalies in the Project Area

Since it was not possible to collect core samples of sediments from the magnetic contrast responsible for creating magnetic anomalies in the project area, an absolutely precise origin for these anomalies cannot be determined. However, their size, shape, and apparent association with ¹³C-depleted carbonate-cemented sediments suggest that these magnetic anomalies were caused by Chemical Remnant Magnetization (CRM) and Bacterial-Biological Magnetization (BRM) created by localized plumes of methane. Although unknown in composition, gas actively bubbling from the seafloor presents additional evidence of these associations. If such seeps are present, then the most likely source for these magnetic anomalies would be the presence of either magnetite or pyrrhotite with minor amounts of other magnetic minerals produced within the nearsurface portion of the methane plume (Machel and Burton 1991a, 1991b).

At this time, it is unclear whether these plumes are formed by thermogenic methane escaping from oil or gas accumulations within the underlying Miocene strata, or are formed by biogenic methane derived from the decomposition of organic matter within the underlying deltaic sediments. The presence of nearby gas fields (Figure 8) demonstrates that the Miocene strata underlying the magnetic anomalies contain thermogenic methane and natural gas. However, the presence of a major deltaic lobe underlying Breton Island and the project area implies that biogenic methane leaking from these deltaic sediments also could be the cause of the hydrocarbon seeps. In either case, hundreds, if not thousands, of magnetic anomalies similar to those investigated in the project area should exist within the Louisiana Continental Shelf. Theoretically, magnetic anomalies of similar origin also may occur within Lake Pontchartrain and elsewhere within the boundaries of the New Orleans District.

Regional mapping of the distribution and types of magnetic anomalies, on the scale of Magnetic Clusters A through G, is lacking at this time. Regional maps of magnetic anomalies within the Gulf of Mexico have been produced; however, these maps reflect only magnetic contrasts related to large-scale differences between lithologic units and geologic structures within the thick wedge of Cenozoic and Mesozoic deposits and the underlying crust. The precise distribution and types of magnetic anomalies, such as those investigated in Breton Sound, presently is unknown.

According to Robert Floyd (personal communication 1993), a recognized expert on magnetic survey of the Outer Continental Shelf, hundreds of magnetic anomalies similar to those investigated in the project area occur within the Chandeleur Sound, Breton Sound, and Main Pass Lease areas. These have been found to produce a magnetic signature that is virtually indistinguishable from that produced by an historic shipwreck. The data concerning these anomalies can be found in hazard survey reports for federal lease areas within the Louisiana Shelf. In particular, the reports concerning Chandeleur Area Blocks 9, 12, 13, 23, 42, and 43 contain detailed analyses of materials associated with similar magnetic anomalies (Robert Floyd, personal communication 1993). Unfortunately, because of their proprietary nature, permission to examine and cite any of these reports has not been obtained.

A different source of anomalous magnetism has been observed by Ted Hampton (personal communication 1993) and John Greene (personal communication 1993) within magnetic surveys from the Louisiana Continental Shelf. This type of magnetic perturbation consists of either long meandering anomalies associated with fluvial channels or monopolar, low amplitude anomalies associated with deltaic

distributary channels. These anomalies may represent CRM associated with iron oxides present within either natural levee or point bar deposits. The very common occurrence of natural gas of unspecified origin within the channel and point bar sands, e.g., Anderson and Bryant (1990) and Suter (1987), implies that methane-derived magnetic minerals, such as magnetite and pyrrhotite, also may have formed within these channels and might be responsible for these anomalies.

Archeological Significance

The available evidence indicates that Magnetic Clusters A, C, D, F, and G are caused by localized natural magnetic contrasts within the seafloor bottom. The presence of friable calcite-cemented sandstone associated with these anomalies strongly implies that the magnetic contrasts were associated with plumes of methane or natural gas seeping from the underlying sediments. Without further tests involving core sampling, it is not clear precisely whether the methane is thermogenic or biogenic in origin. Within the sandy sediments of the near surface seafloor, microbial oxidation of the methane produces a geochemical environment rich in bicarbonate and reprecipitated calcite. Magnetic minerals, such as magnetic and pyrrhotite, formed by chemical and biological processes related to the methane seep a few meters below the surface, have created most of the magnetic anomalies recorded during Phase I survey. These formations have created pockets of anomalous localized magnetism that closely mimic the localized magnetic perturbations of historic shipwrecks in amplitude, duration, type, and extent.

If the magnetic anomalies comprising Clusters A, C, D, F, and G are related to hydrocarbon seeps, two criteria might be used to differentiate natural magnetic anomalies from those produced by shipwrecks. First, either subbottom profiler, minisparker, or high frequency seismic data might be used to detect the presence of gas seeps associated with these types of magnetic anomalies. For example, bubble plumes rising from seafloor seeps show up as strong backscattering regions in these types of data. Typically, the seismic record from any of these techniques should show gas-charged sediments associated with this type of magnetic natural anomaly as acoustic wipeout zones and zones of acoustic turbidity, also called "chaotic facies." These techniques also may show gas-charged sediments as velocity pull-downs or as multiple reservations called "ringing" on their records (Andersen and Bryant 1990). Diver investigations performed at the Phase I level also could help to characterize the bottom conditions and ascertain the presence of carbonate sandstone in suspected areas.

It will be difficult to predict the distribution of these magnetic anomalies. Thermogenic methane, natural gas, and biogenic methane underlie almost the entire Louisiana Continental Shelf (Andersen and Bryant 1990). Also, although general rules about the association between hydrocarbon seeps and either geomorphic or geologic features, such as faults, can be generated, such rules will fail to predict the location of many seeps because of insufficient data concerning many of the factors governing their location.

Since it is virtually impossible to predict the occurrence of pockets of anomalous magnetism resulting from chemical and biological remnant magnetism, it is recommended to the New Orleans District that two changes be made in the methods employed to survey for submerged cultural resources within the District. First, it is recommended that continuous seismic profiling records be obtained of the upper 10 to 15 m (32.8 to 49.2 ft) of the sub-bottom materials. The system should offer the ability to produce very high resolution records without transducer ringing that commonly acts to obscure the first 4.5 to 9 m (15 to 30 ft) of conventional pinger-type sub-bottom profiling records.

Secondly, characterization of bottom conditions should be made at selected anomalies that appear to possess significant duration to determine the potential presence of carbonate-cemented sandstone. The presence of this material coincides with the presence of methane seeps.

The mere presence of naturally occurring pockets of anomalous magnetization does not obviate the need for diver groundtruthing. While it is hoped that implementation of the recommendations discussed above will help to eliminate some non-anthropogenic anomalies from further consideration, no means of remote sensing offers a panacea to the cultural resource manager. The troubling fact remains that a shipwreck could well occur in the same area as methane seeps and contribute its anomalous magnetism to that occurring naturally.

REFERENCES CITED

- Abel, C. E., B. A. Tracy, C. L. Vincent, and R. E. Jensen
1988 *Hurricane Hindcast Methodology and Wave Statistics for Atlantic and Gulf Hurricanes from 1956-1975*. U.S. Army Corps of Engineers, Washington, D.C.
- Aharon, Paul, C. Terzi, F. R. Lucchi, G. B. Vai, and M. Taviani
1993 Fossil Record of Hydrocarbon and Fluid Venting Imprinted in the Miocene-Age Lucina Limestones of the Northern Appennines, Italy. *Abstracts With Program of the Annual Convention of the American Association of Petroleum Geologists New Orleans, April 25-28, 1993*, p. 67, American Association of Petroleum Geologists, Tulsa.
- Allen, J. R. L.
1985 *Principles of Physical Sedimentology*. Allen & Unwin, Boston.
- Anderson, Aubrey L., William R. Bryant
1990 Gassy Sediment Occurrence and Properties: Northern Gulf of Mexico. *Geo-Marine Letters* 10:209-220.
- Arnold, J. Barto, III
1980 Concerning Underwater Remote Sensing Surveys, Anomalies, and Groundtruthing. Paper presented at the Eleventh Conference on Underwater Archaeology, Albuquerque, New Mexico, January 8-11.

1982 *A Matagorda Bay Magnetometer Survey & Site Test Excavation Project*. Texas Antiquities Committee Publication No. 9, Austin.
- Autin, Whitney J., Scott F. Burns, Bobby J. Miller, Roger T. Saucier, and John I. Snead
1991 Quaternary Geology of the Lower Mississippi River Valley. In *Quaternary Nonglacial Geology, Conterminous U.S.*, edited by R. B. Morrison, pp. 20-56, *The Geology of North America*, Vol. K-2. Geological Society of America, Boulder.
- Autin, Whitney J., John I. Snead, Roger T. Saucier, Scott F. Burns, and Bobby J. Miller
1990 Current Approach to Quaternary Research in the Lower Mississippi Valley. In *Field Guide to the Mississippi Alluvial Valley Northeast Arkansas and Southeast Missouri*, Friends of the Pleistocene South-Central Cell 1990, edited by M. J. Guccione and E. M. Rutledge, pp. 23-45, University of Arkansas, Fayetteville.
- Berman, Bruce D.
1973 *Encyclopedia of American Shipwrecks*. The Mariners Press, Boston.
- Bevan, B. W.
1986 Geophysical Search Techniques for Distinguishing Shipwrecks from Trash. *Proceedings of the Seventh Annual Gulf of Mexico Information Transfer Meeting*, U.S. Department of the Interior. Minerals Management Service. OCS Regional Office. New Orleans.

- Breiner, S.
1973 *Applications Manual for Portable Magnetometers*. Geometrics, Sunnyvale, California.
- Clausen, Carl J. and J. Barto Arnold III
1975 The Magnetometer and Underwater Archaeology: Magnetic Delineation of Individual Shipwreck Sites; A New Control Technique. *International Journal of Nautical Archaeology* 5(2):159-169.
- Coleman, James M.
1966 Ecological Changes in a Massive Fresh-water Clay Sequence. *Transactions of the Gulf Coast Association of Geological Societies* 16:159-174.

1982 *Deltas - Processes of Deposition and Models for Exploration*. International Human Resources Development Corporation, Boston.
- Craig, H.
1957 Isotopic Standards for Carbon and Oxygen and Corrections for Mass Spectrographic Analysis of Carbon Dioxide. *Geochimica et Cosmochimica Acta* 12:133-149.
- Crouse, Nellis M.
1954 *Lemoyne d'Iberville: Soldier of New France*. Cornell University Press, Ithaca.
- Curtis, Doris M.
1960 Relationship of Environmental Energy Levels and Ostracod Biofacies in the East Mississippi Delta Area. *Bulletin of the American Association of Petroleum Geologists* 44:471-494.

1970 Miocene Deltaic Sedimentation, Louisiana Gulf Coast. In *Deltaic Sedimentation Modern and Ancient*, edited by James P. Morgan, pp. 293-308. SEPM Special Publication No. 15, The Society for Sedimentary Geology, Tulsa.
- Dean, M., B. Ferrari, I. Oxley, M. Redknap, and K. Watson
1992 *Archaeology Underwater: The NAS Guide to Principles and Practice*. Nautical Archaeology Society, Cambridge.
- Faure, Gunter
1986 *Principles of Isotope Geology*. John Wiley and Sons, Inc., New York.
- Fisk, Harold N.
1960 Recent Mississippi River Sedimentation and Peat Accumulation. In *Congres Pour L'avancement des Etudes de Stratigraphie et de Geologie du Carbonifere, 4th Heerlen*, edited by Van Aelst, pp. 189-199. *Compte Rendu*, Maastricht, Netherlands.
- Fisk, Harold N., and B. McClelland
1959 Geology of Continental Shelf of Louisiana: Its Influences on Offshore Foundation Design. *Geological Society of America Bulletin* 70:1369-1394.
- Folk, Robert L.
1980 *Petrology of Sedimentary Rocks*. Hemphill Publishing Company, Austin.
- Frazier, David E., Alex Osanik, and W. C. Elsik
1978 Environments of Peat Accumulation - Coastal Louisiana. In *Gulf Coast Lignite Conference: Geology, Utilization, and Environmental Aspects*, edited by W. R. Icasier, pp. 5-20. Bureau of Economic Geology Report of Investigations No. 90, University of Texas, Austin.

Garrison, Ervan G.

1981 *Riverine Archeology, Shipwrecks and Blackwater Techniques: Mapping and Site Characterization*. Paper presented at the Second International Conference for Archeological Exploration of Inland Waters. Zurich.

1986 An Analytical Consideration of Three Interpretive Parameters: Amplitude, Signature and Duration. *Proceedings of the Seventh Annual Gulf of Mexico Information Transfer Meeting*, U.S. Department of the Interior, Minerals Management Service, OCS Regional Office. New Orleans.

Garrison, Ervan G., C. P. Giammona, F. J. Kelly, A. R. Tripp, and G. A. Wolff

1989 *Historic Shipwrecks and Magnetic Anomalies of the Northern Gulf of Mexico*, 3 Vols. Report submitted to U.S. Dept. of the Interior, Minerals Management Service, by Texas A&M Research Foundation, College Station.

Gearhart, Robert L., II

1988 *Cultural Resources Magnetometer Survey and Testing, Great Highway/Ocean Beach Seawall Project, San Francisco, California*. Espey, Huston & Associates, Inc., Austin.

Gearhart, Robert L., II, J. C. Neville, S. D. Hoyt and C. L. Bond

1990 *Ground Truthing Anomalies, Port Mansfield Entrance Channel, Willacy County, Texas*. Report prepared for U.S. Army Corps of Engineers, Galveston District, by Espey, Huston & Associates, Inc., Austin.

Giraud, Marcel

1974 *A History of French Louisiana, Vol. 1, The Reign of Louis 14th*. Louisiana State University Press, Baton Rouge.

Greensmith, J. T.

1986 *Petrology of Sedimentary Rocks*. George Allen & Unwin, Boston.

Grummond, Jane Lucas de (ed).

1962 "Platter of Glory," *Louisiana History*, Vol. 3, (4).

Heerden, Ivor Li. van, Shea Penland, and Ron Boyd

1985 A Transgressive Stratigraphic Sequence from the Central Chandeleur Islands, Louisiana. In *Transgressive Depositional Environments of the Mississippi Delta Plain: A Guide to the Barrier Islands, Beaches, and Shoals in Louisiana*, edited by S. Penland and R. Boyd, pp. 189-201. Louisiana Geological Survey Guidebook Series No. 3, Baton Rouge.

Howard, R. O.

1990 *Petrology of Hardbottom Rocks, Mississippi-Alabama-Florida Continental Shelf*. Unpublished M.S. thesis, Department of Geology, University of Alabama, Tuscaloosa.

Irion, Jack B.

1986 *Underwater Archaeological Investigations, Mobile Bay Ship Channel, Mobile Harbor, Alabama*. Report to the U.S. Army Corps of Engineers, Mobile District, by Espey, Huston & Associates, Inc., Austin.

- Irion, Jack B. and Clell L. Bond
 1984 *Identification and Evaluation of Submerged Anomalies, Mobile Harbor, Alabama*. Report prepared for U.S. Army Corps of Engineers, Mobile District, by Espey, Huston & Associates, Inc., Austin.
- Irion, Jack B., P. Morrison, P. V. Heinrich, and D. Kostandarithes
 1993 *Remote Sensing Survey of Mississippi River-Gulf Outlet, Breton Sound Disposal Area, Plaquemines Parish, Louisiana*. Report submitted to U.S. Army Corps of Engineers, New Orleans District, by R. Christopher Goodwin & Associates, Inc., New Orleans.
- Iversen, N., and Niels O. Jorgensen
 1985 Anaerobic Methane Oxidation Rates at the Sulphate-methane Transition in Marine Sediments from Kattegat and Skagerrak (Denmark). *Limnology and Oceanography* 30:944-953.
- Jackson, Joy J.
 1978 "Prohibition in New Orleans: The Unlikeliest Crusade," *Louisiana History*, Vol. 19, (3).
- Jorgensen, Niels O.
 1992 Methane-derived Carbonate Cementation of Marine Sediments from Kattegat, Denmark: Geochemical and Geological Evidence. *Marine Geology* 103:1-13.
- Kocurko, M. John
 1984 Interaction of Organic Matter and Crystallization of High Magnesium Calcite, South Louisiana. In *Roles of Organic Matter in Sediment Diagenesis*, edited by D. L. Gautier, pp. 13-21, SEPM Special Publication No. 38, The Society for Sedimentary Geology, Tulsa.
- Lockett, Samuel H.
 1969 *Louisiana As It Is*. Louisiana State University Press, Baton Rouge.
- Lowrey, Walter M.
 1964 "The Engineers and the Mississippi" *Louisiana History*, Vol. 5, (3).
- Machel, H. G., and E. A. Burton
 1991a Chemical and Microbial Processes Causing Anomalous Magnetization in Environments Affected by Hydrocarbon Seepage. *Geophysics* 56:598-605.
 1991b Causes and Spatial Distribution of Anomalous Magnetization in Hydrocarbon Seepage Environments. *American Association of Petroleum Geologists Bulletin* 75:1864-1876.
 1992 Comment on "Sediment Magnetism: Soil Erosion, Bushfires, or Bacteria?" *Geology* 7:670-671.
- Marx, Robert F.
 1975 *The Underwater Dig: An Introduction to Marine Archaeology*. Henry Z. Walck, New York.
- McWilliams, Richebourg G. (trans. & ed.)
 1981 *Iberville's Gulf Journals*. University of Alabama Press, University, Alabama.
- Mistovich, Timothy S. and Vernon K. Knight, Jr.
 1983 *Cultural Resources Survey of Mobile Harbor, Alabama*. Report submitted to the U.S. Army Corps of Engineers, Mobile District, by OSM Archaeological Consultants, Inc., Moundville, Alabama.

Morgan, James P., and Robert C. Treadwell

1954 Cemented Sandstone Slabs of the Chandeleur Islands, Louisiana. *Journal of Sedimentary Petrology* 24:71-75.

Murphy, Larry and Allen R. Saltus

1981 *Phase II Identification and Evaluation of Submerged Cultural Resources in the Tombigbee River Multi-Resource District, Alabama and Mississippi*. Report of Investigations No. 17, Office of Archaeological Research, The University of Alabama, Moundville.

New Orleans and Ship Island Canal

1869 J. H. Duyckinck & Stationer, New York.

New Orleans Times-Picayune

1925 Times-Picayune Publishing Company, New Orleans.

North American Commission on Stratigraphic Nomenclature

1983 North American Stratigraphic Code. *American Association of Petroleum Geologists Bulletin* 67:841-875.

Nummedal, Dag, and Donald J. P. Swift

1987 Transgressive Stratigraphy at Sequence-bounding Unconformities: Some Principles Derived from Holocene and Cretaceous Examples. In *Sea-Level Fluctuations and Coastal Evolution*, edited by Dag Nummedal, Orrin H. Pilkey, and James D. Howard, p. 241-260. SEPM Special Publication No. 41., Society for Sedimentary Geology, Tulsa.

Oldfield, Frank

1991 Sediment Magnetism: Soil Erosion, Bushfires, or Bacteria? *Geology* 12:1155-1156.

1992 Reply on "Sediment Magnetism: Soil Erosion, Bushfires, or Bacteria?" *Geology* 7:671.

Parker, Robert H.

1956 Macro-invertebrate Assemblages as Indicators of Sedimentary Environments in East Mississippi Delta Region. *Bulletin of the American Association of Petroleum Geologists* 40:295-376.

Parker, Steven J., Albert W. Shultz, and William W. Schroeder

1993 Sediment Characteristics and Seafloor Topography of a Palimpsest Shelf, Mississippi-Alabama Continental Shelf. In *Quaternary Coasts of the United States; Marine and Lacustrine Systems*, p. 243-251. SEPM Special Publication No. 48, Society for Sedimentary Geology, Tulsa.

Pearson, Charles E., George J. Castille, Donald Davis, Thomas E. Redard, and Allen R. Saltus

1989 *A History of Waterborne Commerce and Transportation within U.S. Army Corps of Engineers New Orleans District and an Inventory of Known Underwater Cultural Resources*. Report by Coastal Environment, Inc. for Contract No. DACW 29-77-D-0272, U.S. Army Corps of Engineers, New Orleans District.

Penland, Shea, John R. Suter, and Ron Boyd

1985 Barrier Islands Arc along Abandoned Mississippi River Deltas. *Marine Geology* 63:197-233.

Penland, Shea, John R. Suter, and Randolph A. McBride

1987 Delta Plain Development and Sea Level History in the Terrebonne Parish Region, Louisiana. In *Coastal Sediments*, pp. 1689-1705. American Society of Civil Engineers, New York.

- Pettijohn, F. J., P. E. Potter, and R. Siever
1987 *Sand and Sandstone*. Springer-Verlag, New York.
- Phleger, Fred B.
1955 Ecology of Foraminifera in Southeastern Mississippi Delta Area. *Bulletin of the American Association of Petroleum Geologists* 39:712-752.
- Posey, H. H., P. E. Price, and J. R. Kyle
1987 Mixed Carbonate Sources for Calcite Cap Rocks of Gulf Coast Salt Domes. In *Dynamical Geology of Salt and Related Structures*, edited by I. Lerche and J. J. O'Brien, p. 593-630. Academic Press, New York.
- Roberts, Harry H., Roger Sassen, and Paul Aharon
1987 Carbonates of the Louisiana Continental Slope. *Proceedings of the 19th Annual Offshore Technology Conference* 2:373-382.
- Roberts, Harry H., Roger Sassen, and Paul Aharon
1988 Petroleum-derived Authogenic Carbonates of the Louisiana Continental Slope. *Oceans '88 Proceedings* 1:101-105.
- Roberts, Harry H., Roger Sassen, Robert Carney, and Paul Aharon
1989 ¹³C-depleted Authogenic Carbonate Buildups from Hydrocarbon Seeps, Louisiana Continental Slope. *Transactions of the Gulf Coast Association of Geological Societies* 39:523-530.
- Roberts, Harry H., and Thomas Whelan
1975 Methane-derived Carbonate Cements in Barrier and Beach Sands of a Subtropical Delta Complex. *Geochimica et Cosmochimica Acta* 39:1085-1089.
- Roberts, W. Adolphe
1946 *Lake Pontchartrain*. The Bobbs-Merrill Co., Indianapolis.
- Robertson, James Alexander
1911 *Louisiana under the Rule of Spain, France, and the United States, 1785-1807*. 2 Vols. Arthur H. Clarke Co., Cleveland.
- Russel, R. D.
1937 Mineral Composition of Mississippi River Sands. *Geological Society of America Bulletin* 48:1307-1348.
- Saltus, Allen R.
1980 Response to a Problematic Approach to Resolution of Unidentified Magnetic Anomalies. *Proceedings of the Seventh Annual Gulf of Mexico Information Transfer Meeting*, U.S. Department of the Interior. Minerals Management Service, OCS Regional Office. New Orleans.
- Sassen, Roger
1980 Biodegradation of Crude Oil and Mineral Deposition in a Shallow Gulf Coast Salt Dome. *Organic Geochemistry* 2:153-166.
1987 Organic Geochemistry of Salt Dome Cap Rocks, Gulf Coast Salt Basin. In *Dynamical Geology of Salt and Related Structures*, edited by I. Lerche and J. J. O'Brien, p. 631-649. Academic Press, New York.

- Sassen, Roger, E. W. Chin, and Chade McCabe
 1988 Recent Hydrocarbon Alteration, Sulphate Reduction and Formation of Elemental Sulfur and Metal Sulfides in Salt Dome Cap Rock. *Chemical Geology* 74:57-66.
- Sassen, Roger, Penny Grayson, Gary Cole, Harry H. Roberts, and Paul Aharon
 1991 Hydrocarbon Seepage and Salt-dome Related Carbonate Reservoir Rocks of the U. S. Gulf Coast. *Transactions of the Gulf Coast Association of Geological Societies* 41:570-589.
- Schroeder, William W., M. R. Dardeau, J. J. Dindo, P. Fleischer, K. L. Heck, and Albert W. Shultz
 1988a Geological and Biological Aspects of Hardbottom Environments on the L'MAFLA Shelf, Northern Gulf of Mexico. *Oceans '88 Proceedings* 1:17-21.
- Schroeder, William W., Albert W. Shultz, and John J. Dindo
 1988b Inner-shelf Hardbottom Areas, Northeastern Gulf of Mexico. *Transactions of the Gulf Coast Association of Geological Societies* 38:535-541.
- Schwertmann, U., and R. M. Taylor
 1977 Iron Oxides. In *Minerals in Soil Environments*, edited by J. B. Dixon, p. 145-180. Soil Science Society of America, Madison.
- Shepard, Francis P.
 1954 Nomenclature Based Upon Sand-Silt-Clay Ratios. *Journal of Sedimentary Petrology* 38:1792-1802.
- 1956 Marginal Sediments of the Mississippi Delta. *Bulletin of the American Association of Petroleum Geologists* 40:2537-2623.
- Suess, E., and M. J. Whiticar
 1989 Methane-derived CO₂ in Pore Fluids Expelled from the Oregon Subduction Zone. *Palaeogeography, Palaeoclimatology, Palaeoecology* 71:119-136.
- Surrey, N. M. Miller
 1916 The Commerce of Louisiana During the French Regime, 1699 - 1763. In *Studies in History, Economics, and Public Law*, 71(1). Columbia University Press, New York.
- Suter, John R.
 1986 Ancient Fluvial Systems and Holocene Deposits, Southwestern Louisiana Continental Shelf. In *Late Quaternary Facies and Structure, Northern Gulf of Mexico*, edited by H. L. Berryhill, p. 88-129. AAPG Study in Geology No. 23., American Association of Petroleum Geologists, Tulsa.
- Suter, John R., Henry L. Berryhill, and Shea Penland
 1987 Late Quaternary Sea-level Fluctuations and Depositional Sequences, Southwest Louisiana Continental Shelf. In *Sea-Level Fluctuations and Coastal Evolution*, edited by S. Nummedal, O. H. Pilkey and J. D. Howard, p. 199-222. SEPM Special Publication No. 41, The Society for Sedimentary Geology, Tulsa.
- Suter, John R., and Shea Penland
 1987 *Preliminary Assessment of the Sand and Aggregate Resources of Three Areas of the Louisiana Inner Continental Shelf: Timbalier Islands, Chandeleur Islands, and Trinity Shoal*. Louisiana Geological Survey Open File Series 87-04, 87 pp.

- Suter, John R., Shea Penland, S. J. Williams, and Jack L. Kindinger
1988 Transgressive Evolution of the Chandeleur Islands, Louisiana. *Transactions of the Gulf Coast Association of Geological Societies* 38:315-322.
- Watts, Gordon P., Jr.
1980 *Submerged Cultural Resource Survey and Assessment of the Mark Clark Expressway, Wando River Corridor, Charleston and Berkeley Counties, South Carolina.* Tidewater Atlantic Research, Wilmington, North Carolina.

1986 *A Cultural Resource Reconnaissance of Charleston Harbor at Charleston, South Carolina.* Report prepared for U.S. Army Corps of Engineers, Charleston District, by Tidewater Atlantic Research, Washington, North Carolina.
- Weiss, Christopher P., and Bruce H. Wilkinson
1988 Holocene Cementation Along the Central Texas Coast. *Journal of Sedimentary Petrology* 58:468-478.
- Weymouth, J. W.
1986 Geophysical Methods of Archaeological Site Surveying, in *Advances in Archaeological Method and Theory*, edited by Michael Schiffer. Vol. 9, pp 311-395. Academic Press, New York.
- Winker, Charles D.
1982 Cenozoic Shelf Margins, Northwestern Gulf of Mexico. *Transactions of the Gulf Coast Association of Geological Societies* 38:427-448.
- Whiticar, M. J., and E. Faber
1986 Methane Oxidation in Sediment and Water Column Environments-Isotopic Evidence. *Organic Geochemistry* 10:759-768.

PERSONAL COMMUNICATIONS

Paul Aharon 1993

Whitney J. Autin 1992

Fu Baoshun 1993

Robert Floyd 1993

John Greene 1993

Ted Hampton 1993

Chad McCabe 1993

APPENDIX A
SCOPE OF SERVICES

8 February 1993

REVISED SCOPE OF SERVICES
CONTRACT DACW29-D-0011
Delivery Order 03

**Investigation of Anomalies located within the Breton Sound Disposal Area,
Plaquemines Parish, Louisiana.**

1. Introduction. The Breton Sound Disposal Area is located at Mile 0.0 to -2.5 just south of the Mississippi River Gulf Outlet (MRGO). The proposed COE project calls for the construction of a pilot berm consisting of material routinely dredged from the Mississippi River Gulf Outlet. This pilot berm will be constructed on the right descending side of the channel, southeast of Breton Island. A submerged cultural resources survey was conducted of the area selected for the berm in 1992. Five anomaly clusters were located which may have the potential to be significant resources. This investigation consists of testing four of the anomalies in the impact area to determine if any are significant historic properties (Anomaly Clusters A, C, D, and G).

2. Study Area. The study area consists of four anomaly clusters located within the area selected for berm construction. The fifth anomaly cluster will be evaluated if possible, within the time allotted for this project.(see attached map).

3. Background Information. The study area was surveyed by Goodwin and Associates in 1992. Approximately 1,850 acres were surveyed using a EG&G 260 sidescan sonar, a Geometrics G866 proton precession magnetometer, an Odom Echotrack survey fathometer and a real time positioning system consisting of a Magnavox MX200 differential GPS receiver, a Micronet terrestrial MF data link, and a Macintosh computer with Navigate software. The complete equipment array was deployed over the project area at track intervals of 600 feet for collecting acoustic data and at 150 ft. intervals for magnetic data (as was specified in the scope of services). A total of 79 magnetic anomalies were located of which a portion were attributed to the same magnetic event on adjacent lines. Additional investigations were recommended at five anomaly clusters A, C, D, F, and G. The State Historic Preservation Officer concurs with the recommendation to further investigate these four anomalies.

4. General Nature of the Work. The study consists of relocating the four anomaly clusters and exposing, delineating, and recording the most aerially significant magnetic target associated with each anomaly cluster to determine significance for the National Register. Each contributing anomaly in the cluster need not be tested based on the theory that any significant shipwreck would produce a single wreck focus with a scattering of associated debris. Testing of the focus should be sufficient to determine significance.

5. Study Requirements. The study will be conducted utilizing current professional standards and guidelines including, but not limited to:

*the National Register Bulletin 15 entitled, "How to Apply the National Register Criteria for Evaluation";

*the Secretary of the Interior's Standards and Guidelines for Archeology and Historic Preservation as published in the Federal Register on September 29, 1983;

*the Louisiana Division of Archeology's Comprehensive Archeological Plan dated October 1, 1983 and the Cultural Resources Code of Louisiana, dated June 1980;

*the Advisory Council on Historic Preservation's regulation 36 CFR Part 800 entitled, "Protection of Historic Properties."

The study will be conducted in two phases: investigation of anomaly clusters and data analysis report preparation.

A. Phase 1. Investigation of Anomaly Clusters. Phase 1 will begin with relocating the four anomaly clusters A, C, D and G. Once located each cluster will be subjected to a close interval magnetic survey. The focus of the cluster will be examined to determine the nature of the anomaly. The search grid will include the 50,000 square meters to define the cluster (224 m to a side). Survey tracks will be spaced 15 m. apart. A magnetic contour plot of the survey area will be produced in the field to further define the area exhibiting the highest magnetic reading. The results of the contour plot will then be used to guide underwater subsurface testing at the area. Previous work on shipwrecks has indicated that the focus normally represents the greatest concentration of submerged wreckage.

The only anomaly cluster to produce an acoustic reading, anomaly cluster G, will be examined primarily by diving on the objects. A Marine gradiometer will be used to further define the area of anomalies A, C, and F with the greatest magnetic reading which then will be the focus for diving, probing, and excavation.

Investigations at buried anomaly clusters will attempt to delineate, expose, record and identify the nature of the anomaly. The targets will be characterized as much as possible in the time allotted but may not be identified positively. Either an eight foot solid steel probe or an 15 ft hollow core hydraulic probe will be utilized to determine if the anomaly can be uncovered by standard excavation techniques. If an anomaly cluster is covered with 3 feet or less of overburden, a small test trench will be excavated using a hydraulic dredge. Each anomaly cluster will be examined and evaluated for its potential historical significance.

In the event that the anomaly cluster is buried with more sediment than is practical to utilize hand excavation techniques, then other mechanical means will be employed, such as prop washes.

The fifth anomaly cluster, Anomaly Cluster F, which was recommended for testing in the

survey report will be investigated if possible, within the time allotted for this phase. The full time allotted (including travel and possible weather days) will be utilized to examine to examine this anomaly cluster.

At a minimum, a measured map incorporating horizontal and vertical controls should be made of each potentially significant site. This will be accompanied by measured drawings of significant features that may contribute to a determination of significance. If visibility permits, all anomaly clusters will be photographed. Two copies of a brief management summary which presents the results of the fieldwork will be submitted to the COR within 6 weeks after delivery order award. The management summary will include a brief description of each anomaly located during the survey and recommendations for further work if necessary.

B. Phase 2: Data Analysis and Report Preparation. All data will be analyzed using currently acceptable scientific methodology. The data analyses and report presentation will include as a minimum:

- (1) post-plots of survey transects, data points and bathymetry;
- (2) same as above with magnetic data included;
- (3) plan views of all potentially significant anomalies showing transects, data points, and contours;
- (4) correlation of magnetic, sonar, and fathometer data, where appropriate.

The interpretation of identified magnetic anomalies will rely on expectations of the character (i.e. signature) of shipwreck magnetics derived from the available literature. The potential for each anomaly cluster to contribute to archeological or historical knowledge will be assessed. Thus, the Contractor will classify each anomaly as either eligible for inclusion in the National Register, or not eligible. The Contractor shall fully support his recommendations regarding site significance. The report will include a summary table listing all anomalies, the assessment of potential significance, and recommendations for further work.

If determined necessary by the COR, the final report will not include detailed site location descriptions, state plane or UTM coordinates. The decision on whether to remove such data from the final report will be based upon the results of the survey. If removed from the final report, such data will be provided in a separate appendix. The analyses will be fully documented. Methodologies and assumptions employed will be explained and justified. Inferential statements and conclusions will be supported by statistics where possible. Additional requirements for the draft report are contained in Section 6 of this Scope of Services.

6. Reports:

Management Summary Two copies of a brief management summary will be submitted to the COR within 6 weeks after delivery order award.

Draft and Final Reports (Phase 1-3). Eight copies of the draft report integrating all phases of this investigation will be submitted to the COR for review and comment within 9 weeks after work item award. As an appendix to the draft report, the Contractor shall

submit the state site forms. The written report shall follow the format set forth in MIL-STD-847A with the following exceptions:

- (1) separate, soft, durable, wrap-around covers will be used instead of self covers;
- (2) page size shall be 8-1/2 x 11 inches with 1-inch margins;
- (3) the reference format of American Antiquity will be used. Spelling shall be in accordance with the U.S. Government Printing Office Style Manual dated January 1973.

The COR will provide all review comments to the Contractor within 6 weeks after receipt of the draft reports (15 weeks after work item award). Upon receipt of the review comments on the draft report, the Contractor shall incorporate or resolve all comments and submit one preliminary copy of the final report to the COR within 3 weeks (18 weeks after work item award). Upon approval of the preliminary final report by the COR, the Contractor will submit 30 copies and one reproducible master copy of the final report to the COR within 22 weeks after work item award. The Contractor will also provide computer disk(s) of the text of the final report in Microsoft Word or other format acceptable to the COR.

7. Weather Contingencies. The potential for weather-related delays during the investigation necessitates provision of weather contingency days in the delivery order. Two weather contingency days have been added to the fieldwork. The Contractor assumes the risk for any additional costs associated with weather delays in excess of two days. If the Contractor experiences unusual weather conditions, he will be allowed additional time on the delivery schedule but no cost adjustment.